

NEW BIS(AMIDATE)TITANIUM-BIS(AMIDO) COMPLEXES
AS HYDROAMINATION PRECATALYSTS:
SYNTHETIC AND MECHANISTIC INVESTIGATIONS

By

CHUNYU LI

B. Sc., Nankai University, 1995

M. Sc., Shanghai Institute of Materia Medica, Chinese Academy of Sciences, 1998

A THESIS SUBMITTED IN PARTIAL FULFILMENT OF
THE REQUIREMENTS FOR THE DEGREE OF

MASTER OF SCIENCE

In

THE FACULTY OF GRADUATE STUDIES

(Department of Chemistry)

We accept this thesis as conforming to the required standard

THE UNIVERSITY OF BRITISH COLUMBIA

November, 2003

© Chunyu Li, 2003

In presenting this thesis in partial fulfilment of the requirements for an advanced degree at the University of British Columbia, I agree that the Library shall make it freely available for reference and study. I further agree that permission for extensive copying of this thesis for scholarly purposes may be granted by the head of my department or by his or her representatives. It is understood that copying or publication of this thesis for financial gain shall not be allowed without my written permission.

Department of Chemistry

The University of British Columbia
Vancouver, Canada

Date 28-11-2003

Abstract

This thesis focuses on the exploration of a new titanium complex for the hydroamination of alkynes/alkenes. A new pentafluoro amide proligand, [HN-C₄H₉CO(C₆F₅)] **5**, and two related bis(amidate)titanium-bis(amido) complexes (**8** and **9**) were designed, prepared and fully characterized by multinuclear NMR spectroscopy, mass spectrometry, elemental analysis and X-ray crystallography.

Both intramolecular and intermolecular hydroamination of alkynes were investigated using the bis(amidate)titanium-bis(amido) complexes as catalysts. Preliminary results were obtained from NMR tube scale reaction monitored by ¹H NMR spectroscopy using an internal standard. Larger scale intermolecular hydroamination reactions followed by LAH/THF reduction were carried out to give corresponding isolated amines in yields comparable to that of the NMR tube scale reaction. Hydroamination of alkenes using these precatalysts was unsuccessful. Compared with other reported titanium complexes, our precatalysts demonstrated better or comparable hydroamination reactivity.

Based on literature reports, a mechanism was proposed for the bis(amidate)titanium complex-catalyzed hydroamination which was further verified by preparation of catalytically active intermediates. Stoichiometric reactions of precatalysts with bulky primary amines indicated formation of a titanium imido complex, the active species for hydroamination. Titanium imido complexes or pyridine-trapped imido complexes were isolated and characterized by multinuclear NMR spectroscopy and mass spectrometry. In one case a pyridine-trapped imido complex shows higher reactivity than the corresponding bis(amidate) precatalyst. However, the stoichiometric reaction between precatalysts and less bulky amines form titanium imido dimers, explaining

the poor yield of the hydroamination reaction when a less sterically hindered primary amine was employed.

Table of Contents

Abstract.....	ii
Table of Contents.....	iv
List of Figures.....	vi
List of Tables.....	vii
List of abbreviations.....	viii
Acknowledgements.....	x
Chapter 1. Introduction.....	1
1.1 Background.....	1
1.2 Reference.....	8
Chapter 2. Preparation of Amidate Ligand and Titanium Complexes.....	11
2.1 Introduction.....	11
2.2 Proligand Design and Synthesis.....	12
2.3 Metal Complex Preparation.....	15
2.4 Conclusion.....	19
2.5 Experimental Procedures.....	20
2.6 References.....	24
Chapter 3. Catalytic Hydroamination.....	26
3.1 Introduction.....	26
3.2 Results and Discussion: Intramolecular Hydroamination.....	36
3.3 Intermolecular Hydroamination of Terminal Alkynes with Primary Amines	39
3.4 Intermolecular Hydroamination of Internal Alkynes with Primary Amines.....	45
3.5 Conclusion.....	46
3.6 Experimental.....	47
3.7 References.....	54
Chapter 4. Mechanistic Investigations.....	56

4.1 Introduction.....	56
4.2 Hydroamination Mechanistic Investigations of Titanium Amidate Complexes as Hydroamination Catalysts.....	61
4.2.1 Proposed Mechanism.....	61
4.2.2 Reaction Between Titanium Complex 8 or 9 with Hindered Primary Amines.....	63
4.2.3 Reaction of Titanium Complex 8 or 9 with Less Sterically Hindered Amines.	69
4.2.4 Cycloaddition of Titanium Imido Complexes to Alkynes.....	71
4.3 Conclusion.....	72
4.4 Experimental.....	72
4.5 References.....	76
Chapter 5. Summary.....	78
Appendix	
I. Crystal Structure Data: Experimental details of proligand 5.....	81
II. Crystal Structure Data: Experimental details of titanium complex 8.....	85

List of Figures

Figure 1-1 Mono- and bicyclic alkaloids prepared by hydroamination.....	4
Figure 2-1 Titanium complexes for hydroamination.....	12
Figure 2-2 ORTEP plot of the structure of N- <i>t</i> -butylperfluorophenylamide.....	15
Figure 2-3 Possible isomers for titanium complex $[\text{NO}]_2\text{Ti}(\text{NR}_2)_2$	17
Figure 2-4 ORTEP plot of the structure of $[\text{NO}]_2\text{Ti}(\text{NR}_2)_2$ 8	18
Figure 3-1 Pyridine-trapped imido complex.....	31
Figure 3-2 Ti complexes for hydroamination.....	33
Figure 3-3 Amidate titanium complexes for hydroamination.....	36
Figure 3-4 Hydroamination transition state of 5-membered ring substrate.....	38
Figure 3-5 Isolated amine after LAH/THF reduction.....	44
Figure 3-6 Internal alkyne substrates.....	45
Figure 4-1 Influence of the substituents on the relative stabilities of CpTi complexes.....	58
Figure 4-2 Non-Cp based Ti complexes.....	60
Figure 4-3 Bis(sulfonamide) titanium complex.....	61
Figure 4-4 ^1H NMR Spectrum of the Stoichiometric Reaction between 8 and 2,6- Dimethylaniline.....	64
Figure 4-5 Pyridine stabilized Ti imido complex.....	65
Figure 4-6 ORTEP plot of the structure of Ti imido complex 49	67
Figure 4-7 Structures of 48 , 49 , 50 , 51	68
Figure 4-8 Chemical shift for methyl group of the 2,6-dimethylaniline moiety (imido).....	69

List of Tables

Table 2-1 Important bond lengths (Å), bond angles and dihedral angles (deg) for 5	14
Table 2-2 Important bond length (Å) and bond angles (deg) for 8	18
Table 2-3 NMR data for Compound 5 , 8 and 9	20
Table 3-1 Comparison of Hydroamination of aminoalkynes/alleneamines.....	38
Table 3-2 Hydroamination of terminal alkynes with primary amines.....	40
Table 3-3 Results of Hydroamination followed by LAH/THF reduction.....	45
Table 4-1 Summary of NMR spectroscopic data for 10 and 48	65
Table 4-2 Summary of NMR Spectroscopic data of 48 , 49 , 50 , 51	68

List of Symbols and Abbreviations

Å	angstroms, (10^{-10} m)
Anal	analytical
anti-M	anti-Markovnikov
Ar	aryl or 2,6-dimethylaniline
br	broad
Bu	butyl
°C	degrees Celsius
Calcd.	calculated
Cat.	catalyst
cod	1,5-cyclooctadiene
Cp	cyclopentadienyl
Cp*	pentamethylcyclopentadienyl
d	day or doublet (NMR) or deuterated
deg	degree
DFT	Density Functional Theory
DMF	N, N-dimethylformamide
dmpm	dimethyldipyrrolylmethane
dpma	dipyrrolyl- α -methyl-methylamine
EI	electronic ionization
Equiv	equivalent
Et	ethyl
g	gram
GC	gas chromatography
<i>i</i>	<i>iso</i>
h	hours
HR	high resolution
IR	infrared
J	coupling constant (Hz)
mg	milligram
mL	millilitre
LAH	lithium aluminium hydride
Ln	lanthanide
LR	low resolution
M	molar (mol L^{-1}) or Markovnikov
m	multiplet
Me	methyl
min	minute
mmol	millimole
MS	mass spectrometry
NMR	nuclear magnetic resonance
NO	amidate ligand
<i>p</i>	para
Ph	phenyl
ppm	parts per million
Pr	propyl
py	pyridine
quant.	quantative

r.t.	room temperature
S	entropy
s	singlet (NMR)
T	temperature
t	triplet
<i>t</i>	tertiary
THF	tetrahydrofuran
Ts	tosylate
VT	variable temperature
w	wide (IR)
α	Alpha
γ	Gamma
ϵ	Epsilon
δ	Delta (chemical shift)

Acknowledgements

This thesis is finished under the support and instruction of Dr. Laurel Schafer. I hope to express my appreciations for her help and encouragements during my study and research.

Thanks for the Schafer group's help during my research and thesis writing.

Thanks UBC chemistry department staff (NMR facilities, Analytical Services, X-ray services, glass blower.....).

Thanks for all friends' help during my stay at UBC.

Thanks for my family's understanding and support.

Chapter 1 Introduction

1.1 Background

The catalytic synthesis of organic molecules from inexpensive and readily available starting materials is important for both research and chemical industries. Catalytic reactions involving unsaturated hydrocarbons to form carbon-carbon or carbon-hydrogen bonds are well-known.¹ However, apart from the oxidation of carbon-carbon double bonds (C-O bond formation), other catalytic carbon-heteroatom bond forming reactions are less common.² Yet the catalytic construction of C-N bonds from N-H bond addition across a C-C multiple bond to give amines or imines is an area of recent intense investigation.³

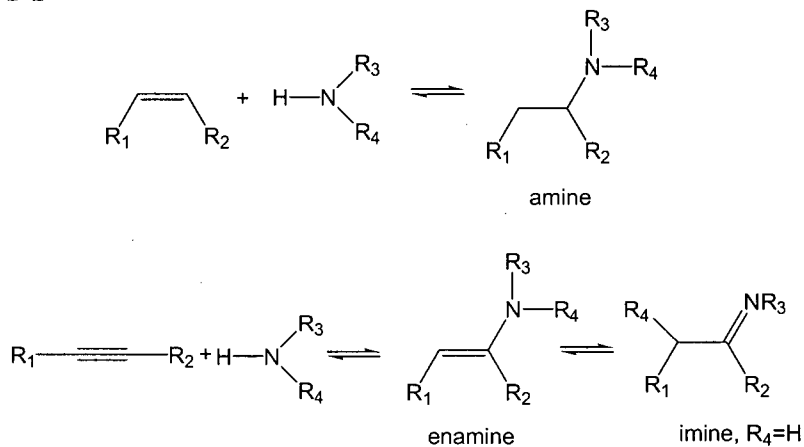
Amines and their derivatives are of great importance in many fields of chemistry, such as natural product total synthesis, the pharmaceutical industry, as well the preparation of fine and bulk chemicals. Typically amines are produced from alcohols with a solid-acid catalyst by elimination of water.⁴ Meanwhile, the alcohols used for these reactions are often produced from alkenes. Clearly, the direct preparation of amines by addition of N-H bond across a C-C multiple bond is an important synthetic challenge.

Known aminations of olefins often require stoichiometric use of transition metals to activate the alkenes.⁵ Furthermore, most of the present enantioselective syntheses of amines use classical stoichiometric reactions with chiral auxiliaries or utilize enantiomerically pure starting material.⁶ Thus new methods for the synthesis of amines are of fundamental importance.

Hydroamination of alkenes or alkynes, which results in the addition of an N-H bond across a C-C multiple bond, offers an attractive route for the efficient synthesis of nitrogen-containing molecules. This transformation can also be regarded as

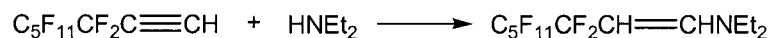
alkylation of primary/secondary amines with alkenes or alkynes.^{3b} In this manner alkylated amines, enamines and imines can be prepared (Scheme 1-1). This approach eliminates the need for alcohol or other isolated intermediates, thereby resulting in cost saving and the added advantage of no side products. Furthermore, the reaction proceeds with 100% atom efficiency.

Scheme 1-1



While the hydroamination reaction was initially reported in the 1950's, it has been limited by its lack of generality.⁷ Amines will undergo direct nucleophilic addition to a carbon-carbon triple bond if the π -system is electron-deficient (such as perfluoroalkynes) or activated by neighboring functional groups (i.e. COR, COOR, CCH) (Scheme 1-2).⁷ The π -bond of alkenes is less reactive but once again additions can proceed if the double bond is activated by neighboring groups such as a carbonyl or nitrile group. However, unactivated carbon-carbon multiple bonds exhibit considerable inertness towards amines and the hydroamination of even activated alkyne/alkene often requires harsh conditions.

Scheme 1-2



A thermodynamic evaluation of the balanced equations indicates that the hydroamination reaction of alkene or alkyne is only slightly exothermic or

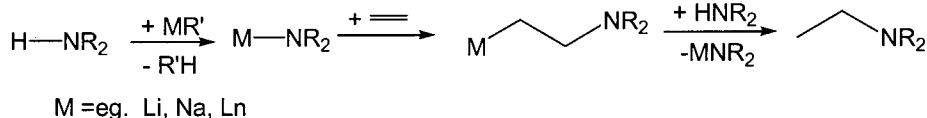
approaching thermoneutral.⁸ The energy barrier for this transformation originates from the nucleophilic attack of the amine nitrogen bearing the lone pair on the electron-rich nonactivated multiple bonds resulting in electrostatic repulsion. A [2+2] cycloaddition of N-H to the alkene would be an orbital symmetry-forbidden process and there is an unfavorable high-energy difference between the π and σ orbitals involved, also contributing to the energy barrier. However, increasing reaction temperature to overcome this barrier results the equilibrium shifting toward the starting materials because of the highly negative entropy of the reaction.

An alternative approach for this transformation is to overcome the energy barrier by employing metal-mediated (stoichiometric or catalytic) hydroamination of alkynes /alkenes. Various synthetic approaches for amination of olefins have been developed.⁹ The fact that mercury and thallium compounds can be used as reagents or catalysts for the hydroamination of alkynes has been known for more than 20 years.¹⁰ The employed reaction conditions are mild and various remote functional groups are tolerated. However, the high toxicity of the employed mercury or thallium limits the wide application of this approach.

Active research in this field has demonstrated a few catalytic routes for the hydroamination of alkenes/alkynes that involve either carbon carbon multiple bond activation or amine activation. Recent research efforts have spanned the periodic table with examples from alkali metals, lanthanide, actinide to early and late transition metals.^{3,11}

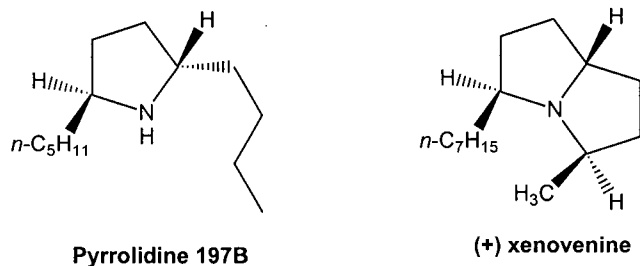
Strong bases or highly electropositive metals like alkali, alkali earth or the lanthanide group elements can deprotonate amines to give more nucleophilic amides (amine activation), which can add to certain substrates (Scheme 1-3).¹²

Scheme 1-3

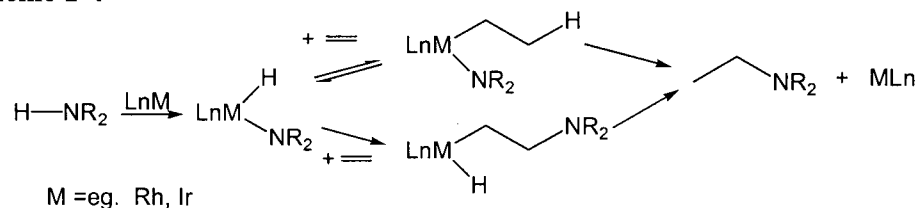
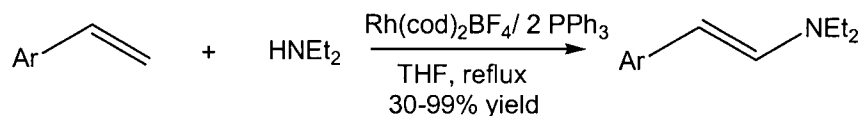


T. J. Marks *et al.* achieved both the intramolecular and the intermolecular hydroamination of alkenes/alkynes catalyzed by lanthanide complexes.¹³ The intramolecular hydroamination/cyclization of aminoalkenes, aminoalkynes, aminoallenes and conjugated amidodienes represents a valuable new tool for regio- and stereoselective construction of mono- and bicyclic alkaloid compounds such as pyrrolidine 197B and (+) xenovenine (Figure 1-1).¹³ The catalytic efficacy of the organolanthanide center is highly sensitive to the electronic and steric characteristics of both the substrate and the catalyst.¹³

Figure 1-1 Mono- and bicyclic alkaloids prepared via hydroamination

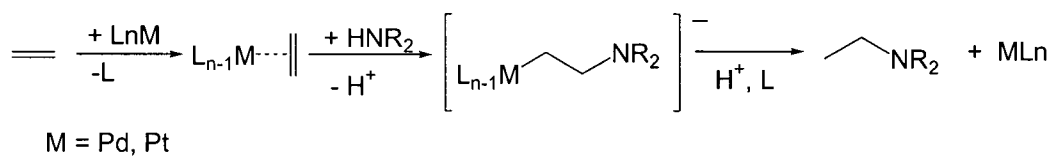


Alternatively, amines can be activated by oxidative addition to a transition metal, which allows insertion of the alkene into the M-N or M-H bond, thereby promoting the hydroamination catalytically (Scheme 1-4).¹⁴ M. Beller and co-workers demonstrated for the first time the possibility of oxidative aminations with anti-Markovnikov regioselectivity in the presence of 2.5 to 10 mol% [Rh(cod)₂]BF₄ and 2 equivalents of PBr₃. Various secondary amines were found to react with styrene under these conditions to give the oxidative amination product (Scheme 1-5).¹⁵

Scheme 1-4**Scheme 1-5**

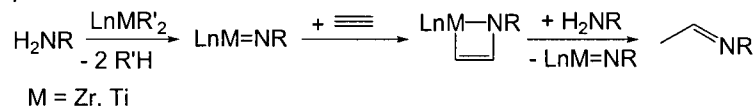
Ar = Ph, 4-Me-C₆H₄, 4-MeO-C₆H₄, 3,4-(MeO)₂-C₆H₄, biphenyl

C-C multiple bonds can also be activated towards hydroamination by late transition metals. The nucleophilic attack of amines on the unsaturated C-C bond is facilitated by coordination of the olefin/alkyne to an electrophilic transition metal center. Protonolysis of the resulting 2-aminoalkylmetal complex leads to the hydroamination product (Scheme 1-6).¹⁶ Several research groups have reported hydroamination of alkenes catalyzed by late transition metal complexes. Nickel, in the presence of phosphines and protic acid, was shown to catalyze the hydroamination of norbornadiene with morpholine or piperidine.¹⁷ A. Togni *et al.* reported the first enantioselective intermolecular alkene hydroamination as well as its intramolecular variant.¹⁸ J. F. Hartwig *et al.* developed hydroamination of vinylarenes using aniline substrates catalyzed by phosphine-ligated palladium triflates.¹⁹ However, most known hydroaminations of alkenes are only limited to activated olefins.

Scheme 1-6

Group 4 early transition metal complexes can activate primary amines by converting them to imido $M=NR$ complexes, thereby enabling the reaction of C-C triple bonds with the M-N bond (Scheme 1-7).²⁰ Compared with other known metal complexes as hydroamination precatalysts, group 4 metal complexes are noteworthy for their low toxicity, low cost and high activity.

Scheme 1-7



In the 1990's Bergman reported the first group 4 metal catalyzed hydroamination of alkynes as well as a proposed mechanism.^{20e} These pioneering investigations resulted in the development of more efficient and general hydroamination catalysts. Further investigations in the Doye group indicated that titanium complexes have higher activity than the corresponding zirconium complexes. Significant progress has been made since Doye *et al.* discovered that Cp_2TiMe_2 , **1**, a commercially available complex, is an efficient hydroamination catalyst.²¹ Thus so far, most reported titanium complexes for hydroamination are Cp-based derivatives such as Cp^*TiMe_2 , $\text{Cp}(\text{NHAr})(\text{py})\text{Ti}=\text{NAr}$ and $\text{Cp}_2\text{Ti}(\text{alkyne})$.^{11a} They each have varied hydroamination activities and selectivities that are significantly affected by the employed substrates. Generally alkynes/allenes can be used for intermolecular hydroamination while aminoalkynes/aminoallenes can be used for intramolecular hydroamination. Corresponding reactions employing alkenes remain to be developed. Thermodynamic considerations suggest that hydroamination of alkynes can be realized more easily than that of alkenes. However, the obtained knowledge for alkyne hydroamination should be the basis for future hydroamination of alkenes.

Considering the challenges associated with the modification of Cp and Cp-based ligands, further improvement beyond the scope already reported in the literature is

limited. Recent efforts have been made in the development of titanium complexes with non-Cp containing ancillary ligand systems. For example, Odom *et al.* applied titanium tetrakis(amido) complexes,²² Richeson reported the use of a guanidinate-supported titanium imide,²³ and Bergman *et al.* have developed titanium complexes bearing sulfonamidate ligands.²⁴ All these complexes have been shown to be active hydroamination precatalysts. Most recently, L. Ackermann reported a TiCl₄-catalyzed intermolecular hydroamination reaction.²⁵

Despite the considerable effort that has been expended in the search for new methodologies for the hydroamination of alkenes/alkynes, general solutions for the problem have been elusive. In general, the hydroamination of unsymmetrical alkenes or alkynes can lead to two regioisomeric products: Markovnikov and anti-Markovnikov products. Control of this regiochemistry is also an important synthetic challenge. Consequently, the further investigation of this important reaction remains an area of intense investigation.

Our group is interested in the development of novel N, O chelating amidate ligands for early transition metals, and lanthanides. To this end, we have identified organic amides as a desirable class of proligands suitable for titanium complexation. Compared with other ligand systems, the amidate ligand is easily prepared from commercially available starting materials. Electronic and steric properties of the ligand system are easily tunable to give the corresponding titanium complexes with variable reactivity.

In this thesis, the design, preparation and full characterization of a new amide proligand as well as the corresponding bis(amidate)titanium complex are described (Chapter 2). This complex was investigated as a hydroamination catalyst for both the intramolecular and intermolecular hydroamination reactions (Chapter 3). Finally,

mechanistic investigations of this complex were performed to give a proposed mechanism (Chapter 4).

1.2 Reference

1. (a) C.A. McNamara, M.J. Dixon, M. Bradley, *Chem. Rev.*, **2002**, *102*, 3275-3299; (b) S. Kobayashi, M. Sugiura, H. Kitagawa, W.W.L. Lam, *Chem. Rev.*, **2002**, *102*, 2217-2302; (c) F. Kakiuchi, S. Murai, *Acc. Chem. Res.*, **2002**, *35*, 826-834.
2. (a) V. Sridharan, *Annual Reports on the Progress of Chemistry Section B: Organic Chemistry*, **2001**, *97*, 91-112; (b) M.A. Yurovskaya, O.D. Mitikin, *Chemistry of Heterocyclic Compounds*, **1999**, *35*, 383-435.
3. (a) F. Pohlki, S. Doye, *Chem. Soc. Rev.*, **2003**, *32*, 104-114; (b) J. Seayad, A. Tillack, C.G. Hartung, M. Beller, *Adv. Synth. Catal.*, **2002**, *344*, 795-813.
4. K. S. Hayes, *Appl. Catal. A*, **2001**, *221*, 187.
5. M. B. Gasc, A. Latties, J. J. Perie, *Tetrahedron*, **1983**, *339*, 703.
6. F. J. Sardina, H. Rapoport, *Chem. Rev.*, **1996**, *96*, 1825-1872.
7. (a) M. Le Blanc, G. Santini, J. G. Riess, *Tetrahedron Lett.*, **1975**, 4151; (b) M. Le Blanc, G. Santini, J. Gallucci, J. G. Riess, *Tetrahedron*, **1977**, *33*, 1453
8. D. Steinborn, R. Taube, *Z. Chem.*, **1986**, *26*, 349.
9. (a) K. E. Harding, T. H. Tiner, B. M. Trost, I. Fleming, *Compr. Org. Synth.*, **1991**, 363; (b) E. Fernandez, M. W. Hooper, F. I. Knight, J. M. Brown, *J. Chem. Soc., Chem. Commun.*, **1997**, *2*, 173.
10. (a) R. Larock, *Angew. Chem., Int., Ed.*, **1978**, *17*, 27; (b) J. Barluenga, F. Aznar, R. Liz, R. Rodes, *J. Chem. Soc., Perkin Trans. I.*, **1980**, 2732; (c) J. Barluenga, F. Aznar, *Synthesis*, **1977**, 195.

11. (a) I. Bytschkov, S. Doye, *Eur. J. Org. Chem.*, **2003**, *6*, 935-946; (b) P. W. Roesky, T. E. Mueller, *Angew. Chem., Int. Ed.*, **2003**, *42*, 2708-2710.
12. (a) M. Nobis, B. Dries-Ben-Holscher, *Angew. Chem., Int. Ed.*, **2001**, *40*, 3983-3985; (b) M. Beller, *Med. Res. Rev.*, **1999**, *19*, 357; (c) J. Ryn, T. J. Marks, F. E. McDonald, *Org. Lett.*, **2001**, *3*, 3091-3094; (d) Y. Li, T. J. Marks, *J. Am. Chem. Soc.*, **1996**, *118*, 707-708.
13. (a) M. R. Gagne, C. L. Stern, T. J. Marks, *J. Am. Chem. Soc.*, **1992**, *114*, 275-294; (b) Y. Li, T. J. Marks, *J. Am. Chem. Soc.*, **1998**, *120*, 1757-1771; (c) V. M. Arredonodo, S. Tian, F. E. McDonald, T. J. Marks, *J. Am. Chem. Soc.*, **1999**, *121*, 3633-3639; (d) S. Hong, T. J. Marks, *J. Am. Chem. Soc.*, **2002**, *124*, 7886-7887.
14. (a) M. S. Driver, J. F. Hartwig, *J. Am. Chem. Soc.*, **1996**, *118*, 4206-4207; (b) M. Beller, H. Tranthwein, M. Eichberger, C. Breindl, J. Herwig, T. E. Miller, O. R. Thiel, *Chem. Eur. J.*, **1999**, *5*, 1306; (c) P. Diversi, L. Ermini, G. Ingrosso, A. Lucherni, C. Pinzino, L. Sagramora, *J. Organomet. Chem.*, **1995**, *494*, C1-C3.
15. M. Beller, M. Eichberger, H. Trauthwein, *Angew. Chem., Int. Ed.*, **1997**, *36*, 2225-2227.
16. (a) J. Pawlas, Y. Nakao, M. Kawatsura, J. F. Hartwig, *J. Am. Chem. Soc.*, **2002**, *124*, 3669-3679; (b) A. Ricci, *Modern Amination Methods*, Wiley-VCH, Weinheim, **2000**; (c) L. S. Hegedus, B. Akermark, K. Zetterberg, L. F. Olsson, *J. Am. Chem. Soc.*, **1984**, *106*, 7122-7126.
17. J. Kiji, S. Nishimura, S. Yoshikawa, E. Sasakawa, J. Furukawa, *Bull. Chem. Soc. Jpn.*, **1974**, *47*, 2523-2525.
18. R. Dorta, P. Egli, F. Zurcher, A. Togni, *J. Am. Chem. Soc.*, **1997**, *119*, 10857-10858.

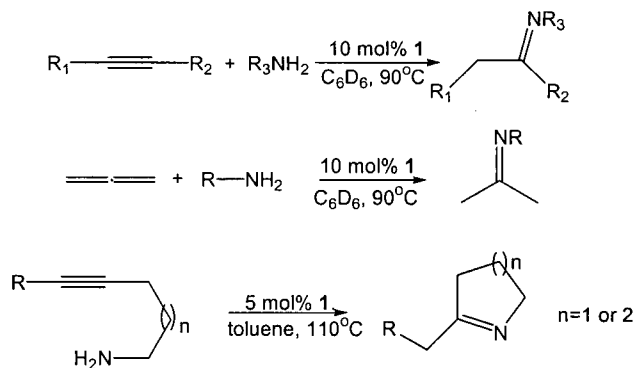
19. U. Nettekoven, J. F. Hartwig, *J. Am. Chem. Soc.*, **2002**, *124*, 1166-1167.
20. (a) Y. Li, T. J. Marks, *Organometallics*, **1996**, *15*, 3370-3372; (b) A. Tillack, I. G. Castro, C. G. Hartung, M. Beller, *Angew. Chem., Int. Ed.*, **2002**, *41*, 2541-2543; (c) I. Bytschkov, S. Doye, *Eur. J. Org. Chem.*, **2003**, 935-946; (d) P. L. McGrane, M. Tensen, T. Livinghouse, *J. Am. Chem. Soc.*, **1992**, *114*, 5459-5460; (e) P. J. Walsh, A. M. Baranger, R. G. Bergman, *J. Am. Chem. Soc.*, **1992**, *114*, 1708-1719.
21. E. Haak, I. Bytschkov, S. Doye, *Angew. Chem., Int. Ed.*, **1999**, *38*, 3389-3391.
22. C. Cao, Y. Shi and A. L. Odom, *Org. Lett.*, **2002**, *4*, 2853-2856.
23. T. Ong, G. P. Yap and D. S. Richeson, *Organometallics*, **2002**, *21*, 2839-2841.
24. L. Ackermann and R. G. Bergman, *Org. Lett.*, **2002**, *4*, 1475-1478.
25. L. Ackermann, *Organometallics*, **2003**, *ASAP*.

Chapter 2 Preparation of Amidate Ligand and Titanium Complexes

2.1 Introduction

Group 4 metal complexes are known for their extensive use as catalysts in organic chemistry. In the 1990's, a new and promising field evolved with the reports of group 4 metal complexes as catalysts for hydroamination from the Bergman and Livinghouse groups.¹ Great progress has been made by using a variety of transition and f-block metal complexes for catalytic hydroamination during the past decade.² Among them, group 4 metal complexes attract much attention because of their high reactivity, low cost and low toxicity. In particular, dimethyltitanocene (Cp_2TiMe_2 , **1**) has been shown to be a good precatalyst for both the intermolecular hydroamination of alkynes/allenes with primary amines and the intramolecular hydroamination of aminoalkynes (Scheme 2-1).³

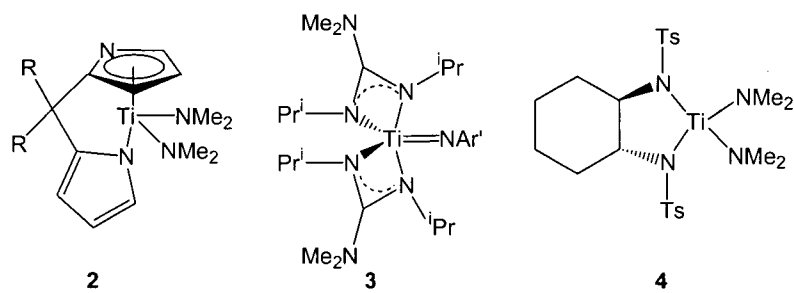
Scheme 2-1 Cp_2TiMe_2 Catalyzed Hydroamination



The catalytic scope of **1** and other Cp-based titanium complexes has been extensively investigated and reviewed.⁴ In addition, detailed hydroamination mechanistic investigations of precatalyst **1** have been carried out. However, ligand effects on the reactivity and regioselectivity for hydroamination remain unclear. Recently, much effort has been made to develop new catalyst systems to take advantage of the low cost of group 4 metals while providing enhanced and selective

reactivity. For example, titanium complexes with non-Cp containing ancillary ligands such as pyrrole ligands **2**,⁵ guanidinate ligands **3**⁶ and sulfonamidate ligands **4**⁷ have been prepared and shown to be active hydroamination precatalysts (Figure 2-1). Here we describe the application of amidates as an alternative ancillary ligand.

Figure 2-1 Titanium complexes for hydroamination



2.2 Proligand Design and Synthesis

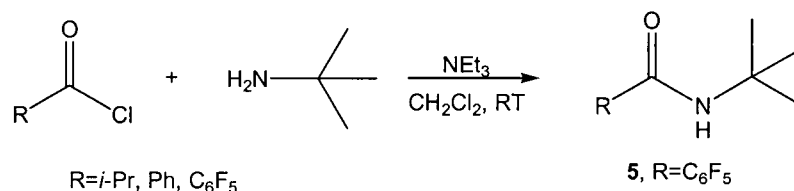
Organic amides caught our attention as being easily prepared, highly variable NO chelating proligands. Their precursors can be readily synthesized from commercially available amines and acid chlorides (Scheme 2-2). The steric and electronic properties of the resultant proligands can be tuned by using appropriate starting materials. Upon deprotonation they become monoanionic and can act as 4 or perhaps even 6-electron donors.

In contrast to the wealth of information available for the NN amidinate chelating systems, the related amidate ligands (NO chelating) are virtually unknown in transition metal chemistry.⁸ Although titanium amidates have been invoked as intermediates in numerous catalytic cycles,⁹ the number of well-defined group 4 amidate complexes remains low. Amidates have been used as bridging ligands for binuclear late transition metal complexes and more recently, there has been one example of amidates as ancillary ligands for the generation of group 4 olefin polymerization catalysts.¹⁰ One of the challenges of the amidate ligand set is the

propensity for complexes bearing these ligands to adopt multiple coordination modes, including monomeric, bridging dimeric and aggregate complexes.¹¹

We have introduced a bulky *t*-butyl group into our ligand by using *t*-butyl amine in the proligand preparation. The sterically demanding *t*-butyl group would favor the formation of monomeric complexes as well as aid in solubility and provide an NMR spectroscopic handle for complex characterization. Different acid chlorides were used to vary the electronic properties of the proligands and metal complexes. This thesis will focus on the preparation of the *N-t*-butyl(perfluorophenyl)amide **5**, in which the electron-withdrawing perfluorinated aryl group is expected to provide a highly electrophilic, reactive metal center upon complexation.

Scheme 2-2 Synthesis of the proligand



The proligand (*N-t*-butyl(perfluorophenyl)amide **5**, (*t*-Bu[NO]Ph-F₅)H, is prepared in high yield by the reaction of commercially available pentafluorobenzoyl chloride with *t*-butyl amine in the presence of triethylamine in methylene chloride (Scheme 2-2). Compound **5** is isolated as an air-stable white solid, which is further purified and dried by vacuum sublimation to give the desired product in 87% yield. This compound can also be prepared by treating pentafluorobenzoic acid with thionyl chloride to generate pentafluorobenzoyl chloride *in situ* that subsequently is treated with *t*-butyl amine to give the proligand in lower yield than via the commercial acid chloride route (74% yield).

This proligand has been fully characterized by multinuclear NMR spectroscopy, mass spectrometry and IR spectroscopy. The ¹H NMR spectrum of **5** contains two

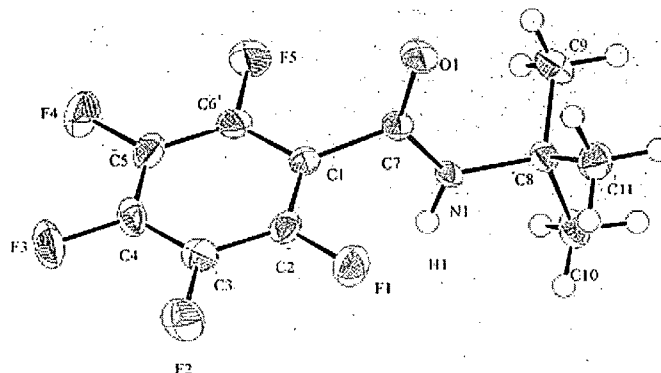
singlets at 1.40 and 5.67 ppm with an intensity ratio of 9:1. These are assigned to the methyl protons of the *t*-butyl group and the amide proton, respectively. There are 3 diagnostic carbon signals in the ^{13}C NMR spectrum: a carbonyl C signal at 156.4 ppm, and a quaternary C at 53.2 ppm and the *t*-butyl methyl C at 28.5 ppm. A complex series of signals in the aromatic region is observed between 145.6 and 135.8 ppm due to the presence of C-F coupling. The ^{19}F NMR spectrum shows three multiplets at -142.69, -153.79 and -161.29 ppm with an intensity ratio of 2:1:2, corresponding to the five F atoms on the aromatic ring. Low resolution EIMS spectrometry indicates a parent molecular ion peak at 267 m/z , consistent with the desired molecular weight. A fragment ion peak corresponding to the loss of a methyl group is found at 252 m/z . The IR spectrum of **5** indicates the presence of an N-H stretch (3259 cm^{-1}) and carbonyl functionality (1654 cm^{-1}).

Colorless crystals suitable for X-ray diffraction were obtained by cooling a saturated chloroform solution of **5** to -35°C . An ORTEP view of the molecular structure is shown in Figure 2-2. Important bond lengths and angles are given in Table 2-1. This compound shows a longer C-O bond length of 1.23 Å corresponding to a double bond while the N-C bond length is slightly shorter than a typical N-C single bond, and indicating some double bond character.

Table 2-1 Important bond lengths (Å), bond angles and dihedral angles (deg) for **5**

Compound 5		
Atom connection	Bond length(Å)	Bond angles (deg)
N(1)-C(7)	1.326(2)	-
O(1)-C(7)	1.229(2)	-
N(1)C(7)C(1)	-	114.4(1)
N(1)C(7)O(1)	-	126.1(1)
O(1)C(7)C(1)	-	119.5(1)
N(1)C(7)C(1)C(6)	-	-102.5(2)

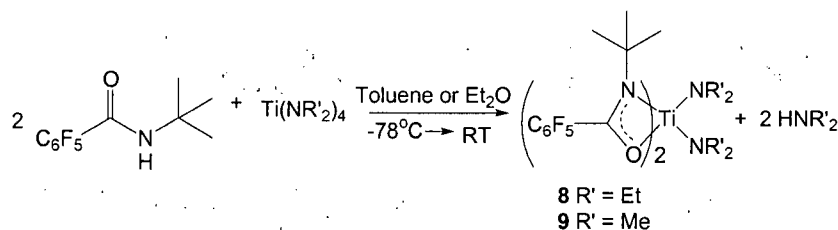
Figure 2-2. ORTEP plot of the structure of *N*-*t*-butylperfluorophenylamide **5**



2.3 Metal Complex Preparation

A protonolysis reaction was used for the preparation of the titanium metal complexes. Proligand **5** reacts with the commercially available homoleptic titanium amides $\text{Ti}(\text{NR}_2)_4$ ($\text{R}=\text{Et}$, **6** or Me , **7**) to generate the titanium complexes $[\text{NO}]_2\text{Ti}(\text{NEt}_2)_2$ **8** and $[\text{NO}]_2\text{Ti}(\text{NMe}_2)_2$ **9** (Scheme 2-3). The amine elimination reactions are carried out in toluene or diethyl ether, resulting in the formation of pentane soluble products that contain largely only one isomer, as indicated by only one methylene (4.14 ppm, $\text{R}=\text{Et}$) or methyl (3.51 ppm, $\text{R}=\text{Me}$) signal in the ^1H NMR spectrum. A dark red crystalline solid is obtained in good yield (76%, **8**; 85%, **9**) by cooling a saturated pentane solution of **8** or **9** to -35°C . Crystals of **8** suitable for X-ray crystallography can be obtained by recrystallization from dry pentane.

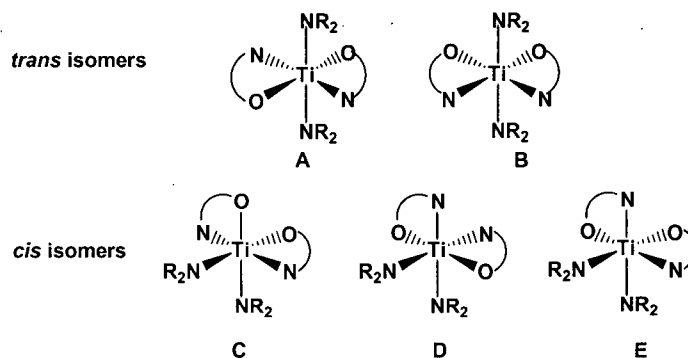
Scheme 2-3 Synthesis of Metal Complexes



The ^1H NMR spectrum of **8** shows two multiplets with a 2:15 ratio at 4.14 ppm ($\text{N}(\text{CH}_2\text{CH}_3)_2$) and 1.22 ppm ($t\text{Bu}-\text{CH}_3 + \text{N}(\text{CH}_2\text{CH}_3)_2$) respectively while in that of **9**, two singlets appear with a 2:3 ratio at 3.51 ($\text{N}(\text{CH}_3)_2$) and 1.16 ppm ($t\text{Bu}-\text{CH}_3$), respectively. This ratio is consistent with the bis(amidate)titanium-bis(amido) structure shown in Scheme 2-3. In the ^{13}C NMR spectrum, there are 11 signals for **8** and 10 for **9**, both with a carbonyl C at 160 ppm (156 ppm for free proligand **5**), a quaternary C at 53.1 ppm and a methylene (**8**) or methyl (**9**) C at 46/47 ppm. The ^{19}F NMR spectra for **8** and **9** are diagnostic of complex formation by comparing them with **5**. The peak at high field (-142 ppm for **5**) shifts to even higher field (-138 ppm for **8** and -139 ppm for **9**) upon metal complexation. Presumably, this signal corresponds to the *ortho*-F as they would be most affected by complexation to the metal. The molecular parent ion peak and fragment peaks in the EIMS of **8** and **9** are found as expected (724 and 668 m/z respectively). IR spectra of **8** and **9** indicate the presence of carbonyl group (1655 cm^{-1}) with no significant shift in vibrational frequency in comparison to free proligand **5**. This is consistent with the carbonyl binding in a dative fashion with no appreciable perturbation of the C=O bond.

Both ^1H and ^{13}C NMR spectra of **8** and **9** exhibit a single ethyl or methyl environment, indicating that there is symmetry in the molecule. Thus, of the five possible isomers as shown in Figure 2-3, E can be ruled out (C_1 symmetry). Considering the bulky substituents on N of the amidate ligand, *trans* isomers (A, C) should be favored over the *cis* isomers (B, D) which are also dominated in the case of amidinate titanium complexes. However, X-ray crystallographic study of **8** indicates that D is the preferred isomer in the solid state.

Figure 2-3 Possible isomers for titanium complex $[\text{NO}]_2\text{Ti}(\text{NR}_2)_2$

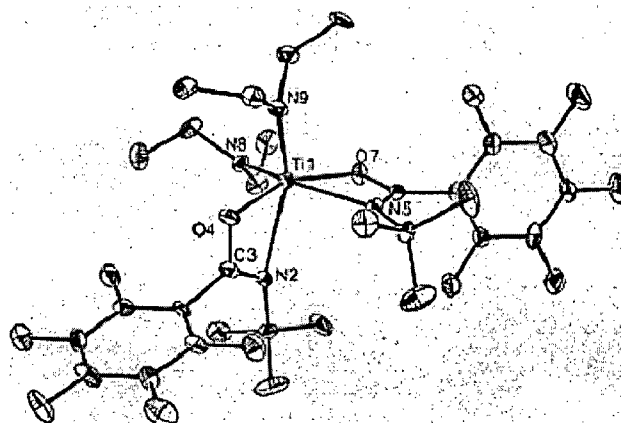


A perspective view of complex **8** which has pseudo- C_2 symmetry is shown in Figure 2-4. The titanium atom is ligated by two amidate groups and two NEt_2 units, generating a pseudo-octahedral geometry with the two NEt_2 group in a *cis*-orientation, *trans* to the N of the amidate ligands. Selected bond distances and angles are presented in Table 2-2. The $\text{Ti-N}_{\text{amidate}}$ bonds are longer than that of the $\text{Ti-N}_{\text{amido}}$ (2.36\AA vs 1.90\AA), consistent with the $\text{Ti-N}_{\text{amido}}$ bond having double bond character while the $\text{Ti-N}_{\text{amidate}}$ bond length shows single bond character. The bond lengths of $\text{C}(3)\text{-O}(4)$ and $\text{N}(2)\text{-C}(3)$ are $1.307(10)$, $1.272(11)$ respectively in **8**, while in the proligand the corresponding bond lengths are $1.229(2)$ ($\text{O}(1)\text{-C}(7)$), $1.326(2)$ ($\text{N}(1)\text{-C}(7)$). This suggests that the amidate NO backbone has delocalized multiple bond character and binds to the metal center in an asymmetric fashion with the Ti-O bond (2.04\AA) being significantly shorter than the $\text{Ti-N}_{\text{amidate}}$ bond length ($2.36/2.30\text{\AA}$). This asymmetric binding motif suggests a strong *trans*-influence upon the $\text{Ti-N}_{\text{amidate}}$ by the amido ligand.

Table 2-2 Important bond length (Å) and bond angles (deg) for 8

Titanium Complex 8			
Atom Connection	Bond Length (Å)	Atom Connection	Bond Angles (deg)
Ti(1)-N(9)	1.887(7)	O(4)C(3)N(2)	117.4(7)
Ti(1)-N(2)	2.356(7)	N(2)C(3)C(10)	131.2(8)
Ti(1)-N(5)	2.296(7)	O(4)Ti(1)N(2)	59.6(2)
Ti(1)-N(8)	1.909(7)	O(7)Ti(1)N(5)	60.7(2)
Ti(1)-O(4)	2.044(6)	N(2)C(3)C(10)C(15)	-94.2(12)
Ti(1)-O(7)	2.046(6)		
N(2)-C(3)	1.272(11)		
C(3)-O(4)	1.307(10)		

Figure 2-4. ORTEP plot of the structure of $[\text{NO}]_2\text{Ti}(\text{NR}_2)_2$ 8



Although the highly symmetric ^1H NMR spectrum is consistent with the C_2 symmetric structure observed in the solid state, variable temperature NMR spectroscopy was used to determine if in fact various isomers were interconverting quickly on the NMR time scale. Therefore, we obtained VT-NMR spectra of the titanium amidate complex 9. When the temperature was varied from -70°C to 100°C , the ^1H NMR spectrum of 9 shows no obvious change. This suggests that there is only one coordination isomer present in the solution and that this coordination geometry corresponds to a low energy conformation.

Complexes **8** and **9** are dark red crystalline solids that are air and moisture sensitive. They are easily soluble in pentane, hexanes, toluene, benzene and diethyl ether. The ^1H NMR spectrum showed no obvious change after the C_6D_6 solution of **8** was heated at 65°C for several days, indicating good thermal stability of this compound. Both **8** and **9** can be stored under nitrogen at room temperature for several months without obvious decomposition.

2.4 Conclusion

The synthesis of a new amide proligand **5** is readily accomplished in a high yielding reaction. Titanium complexes **8** and **9** are obtained in good yield via a protonolysis reaction between $\text{Ti}(\text{NR}_2)_4$ and **5**. This result establishes that the amidate ligand, which binds the metal center through an NO chelate, is a suitable ligand system for titanium. Compounds **5**, **8** and **9** were fully characterized by ^1H , ^{13}C and ^{19}F NMR spectroscopy as summarized in Table 2-3 as well as mass spectrometry, IR spectroscopy and elemental analysis. The structures of **5** and **8** were further confirmed by X-ray crystallography. VT NMR of **9** shows that only one coordination isomer is present in solution and corresponds to the C_2 symmetric structure observed in the solid state.

Table 2-3 NMR data for Compound 5, 8 and 9

	5	8	9
¹H NMR	5.67 (br, NH) 1.40 (s, <i>t</i> Bu-CH ₃)	4.14 (m, 8H, NCH ₂ CH ₃) 1.22 (m, 30H, <i>t</i> Bu-CH ₃ +CH ₂ CH ₃)	3.51 (s, 12H, NCH ₃) 1.16 (s, 18H, <i>t</i> Bu-CH ₃)
¹³C NMR	156 145 143 142 140 139 135 53 28	160 (carbonyl C) 145-125 (6 aromatic C) 53 47 30 14	160 (carbonyl C) 145-130 (6 aromatic C) 53 46 30
¹⁹F NMR	-142.7 -153.8 -161.3	-138.2 -153.4 -161.2	-139.2 -153.3 -161.1

2.5 Experimental procedures

General Materials and Methods (Apply to all chapters)

1. General Procedures

All manipulations of air- and moisture-sensitive materials were carried out with rigorous exclusion of oxygen and moisture in dry Schlenk-type glassware interfaced to a high-vacuum line or in a nitrogen-filled glovebox. Reactions were performed at r.t. unless otherwise specified.

2. Physical Techniques and Analytical Measurements

2.1 Nuclear magnetic resonance (NMR) spectroscopy

NMR spectra were recorded on Bruker AV-300 spectrometers. Chemical shifts for ¹H and ¹³C are referred to internal solvent resonance and reported relative to SiMe₄ (δ 0.00). ¹⁹F NMR chemical shifts are reported relative to external CF₃COOH.

2.2 X-ray crystallography

X-ray crystallographic analyses were performed by Dr. Brain Patrick of the UBC Chemistry Department, using a Rigaku/ADSC CCD area detector with graphite monochromated Mo-K α radiation.

2.3 Elemental analysis

Elemental analyses were conducted by Mr. Minaz Lakha of the UBC Chemistry Department, using a CARL erba Elemental Analyzer EA 1108.

2.4 Infrared (IR) spectroscopy

IR spectra were recorded on a BOMEM Michelson Series FT-IR MB-100 instrument. Samples were prepared as KBr plates (solid) or *nujol* (liquid). IR data were reported in cm^{-1} .

2.5 Mass spectrometry (MS)

Mass spectra were conducted by Mr Marshall Lapawa of the UBC Chemistry Department by using Kratos MS-50.

2.6 Gas chromatography-Mass spectrometry (GCMS)

GCMS was recorded on Agilent 6890 Series GC system with 5973 Mass Selective Detector, equipped with a 0.25 mm-0.25 μm HP-5 MS column and a H₂/air flame ionization detector (FID). He was used as the carrier gas. Temperature sequence: 50 to 300°C, 15°C/min.

3. Materials

3.1 Solvents

Reagent grade solvents were either distilled from sodium benzophenone ketyl (diethyl ether, THF) or purified by passage through activated aluminum (toluene, hexanes) under nitrogen. All deuterated solvents (CDCl₃, C₆D₆, C₇D₈) were purchased from Cambridge Isotope Laboratories. Deuterated benzene used for NMR reactions were degassed by freeze-pump-thaw methods before drying over molecular sieves.

3.2 Reagents

Reagents were purchased from commercial sources and used without further purification unless other noted. All aminoalkynes for intramolecular hydroamination were distilled under nitrogen and then dried over molecular sieves before use. All alkynes for intermolecular hydroamination were degassed by freeze-pump-thaw methods, flushed with nitrogen before storage over molecular sieves. All amines were dried by stirring over CaH_2 overnight, and then distilled under nitrogen.

3.3 Flash chromatography

Merck silica gel 60 (230-400 mesh)

Synthesis of *N*-*t*-butyl(perfluorophenyl)amide 5

Method 1 A 100 mL round-bottomed flask equipped with a stir bar was charged with 3.00 g (14.1 mmol) pentafluorobenzoic acid. The flask was cooled to 0°C and flushed under nitrogen while 20 mL dry thionyl chloride was added dropwise. The resultant mixture was warmed to room temperature, and then heated to 95 °C for 3 hours. The remaining thionyl chloride was removed by distillation. Then 20 mL methylene chloride was added to the flask and it was cooled in ice water. A solution of 30 mL methylene chloride, 2.70 mL (25.6 mmol) *t*-butyl amine, and 2.00 mL (14.5 mmol) triethylamine was loaded into an addition funnel and was added to the reaction flask dropwise. The reaction vessel was warmed to room temperature, and stirred overnight. The reaction mixture was then washed with 1M HCl (50 mL), 2M Na_2CO_3 (50 mL), H_2O (50 mL), and brine (50 mL). The organic layer was dried over anhydrous MgSO_4 and evaporated to dryness to give a white microcrystalline solid. The final product was purified and dried by sublimation yielding a white crystalline solid in 74% yield (2.80 g).

Method 2 A 250 mL round-bottomed flask equipped with stir bar was charged with 20 mL methylene chloride, 5.00 mL (47.4 mmol) *t*-butyl amine and 3.00 mL (21.7 mmol) triethylamine. This solution was cooled to 0°C and 5.00 mL (21.7 mmol) of pentafluorobenzoyl chloride was added dropwise. The resultant mixture was warmed to room temperature with stirring, resulting in a white slurry. The reaction mixture was diluted with diethyl ether (50 mL) and then washed with 1M HCl (50 mL), 1M NaOH (50 mL) and brine (50 mL). The organic layer was dried over anhydrous MgSO₄ and evaporated to dryness to give a white microcrystalline solid. The final product was purified and dried by sublimation yielding a white crystalline solid in 87% yield (5.04 g). Crystals suitable for X-ray diffraction were obtained from a CHCl₃ solution. ¹H NMR (CDCl₃, 300 MHz): δ 1.40 (9H, s, *t*-BuCH₃), 5.67 (1H, s, NH). ¹³C NMR (CDCl₃, 75 MHz): δ 156.4, 145.6, 143.6, 142.2, 140.2, 139.2, 135.8, 53.2, 28.5. ¹⁹F NMR (CDCl₃): δ -142.7 (2F), -153.8 (1F), -161.3 (2F). EIMS (*m/z*): 267(M⁺, 20), 252(M⁺-CH₃, 40), 212(20), 195(100), 167(30), 148, 117, 93, 56. IR (cm⁻¹): 3259 (w), 3066 (m), 2851 (m), 1654 (s), 1566 (m), 1506 (m). Anal. Calcd for C₁₁H₁₀ONF₅: C, 49.42; H, 3.77; N, 5.24. Found: C, 49.61; H, 3.80; N, 5.30.

Synthesis of [NO]₂Ti(NEt₂)₂ **8**

In a 50 mL Schlenk flask equipped with a stir bar, 0.561 g (1.00 mmol) of **5** in toluene was added to 0.18 mL (0.5 mmol) of Ti(NEt₂)₄ at 0°C, and then warmed to room temperature. The red solution was heated to 40 °C, and stirred overnight. The solvent was removed under vacuum, and the remaining solid was washed with dry hexanes. After filtration, the hexanes solution was evaporated to dryness to give a dark red microcrystalline product in 76% yield (0.28 g). Recrystallization from dry pentane resulted in crystals of sufficient quality for X-ray crystallography. ¹H NMR (C₆D₆, 300 MHz): δ 4.14 (m, 8H, NCH₂CH₃), 1.22 (m, 30H, *t*-Bu-CH₃ + NCH₂CH₃).

^{13}C NMR (C_6D_6 , 75 MHz): δ 160, 145-125 (aromatic C), 53.1, 47.4, 30.8, 14.2. ^{19}F NMR (C_6D_6): δ -138.2 (2F), -153.4 (1F), -161.2 (2F). EIMS (m/z): 653 (M^+ -NEt₂, 50), 580 (M^+ -2NEt₂), 458 (M^+ -C₇F₅O-NEt₂), 57 (100). IR (cm⁻¹): 3260 (w), 2978 (m), 1655 (s), 1518 (m), 1108 (s), 992 (s), 865 (s). Anal. Calcd for C₃₀H₃₈O₂N₄F₁₀Ti: C, 49.70; H, 5.24; N, 7.73. Found: C, 49.81; H, 5.56; N, 7.78.

Synthesis of [NO]₂Ti(NMe₂)₂ **9**

In a 250 mL Schlenk flask equipped with a stir bar, 0.538 g (2.015 mmol) of **5** in diethyl ether and was added to 0.224 g (1.00 mmol) of Ti(NMe₂)₄ at -78°C. The solution was warmed to room temperature and was stirred overnight. Then the solvent was removed under vacuum to give an orange powder (0.57 g, 85.3% yield). A dark red microcrystalline product was obtained by redissolving the powder in pentane and cooling the solution to -35°C. ^1H NMR (C_6D_6 , 300 MHz): δ 3.51 (s, 12H, NCH₃), 1.16 (s, 18H, *t*-Bu-CH₃). ^{13}C NMR (C_6D_6 , 75 MHz): δ 160, 145-130 (aromatic C), 53.1, 46.4, 30.6. ^{19}F NMR (C_6D_6 , 300 MHz): δ -139.2 (2F), -153.3 (1F), -161.08 (2F). EIMS (m/z): 668 (20), 625 (M^+ -NMe₂, 20), 580 (M^+ -2NMe₂, 5), 376, 252, 195, 167, 124, 57 (100). Anal. Calcd for C₂₆H₃₀O₂N₄F₁₀Ti: C, 46.72; H, 4.52; N, 8.38; Found: C, 46.52; H, 4.52; N, 7.97.

VT NMR of [NO]₂Ti(NMe₂)₂

A scalable NMR tube was charged with 6.6 mg of **9** and 0.5 mL deuterated toluene. ^1H NMR spectra were obtained at room temperature, 60, 100 and -70°C.

2.6 References

1. (a) P. J. Walsh, A. M. Baranger and R. G. Bergman, *J. Am. Chem. Soc.*, **1992**, *114*, 1708-1719; (b) P. L. McGrane, M. Jensen and T. Livinghouse, *J. Am. Chem. Soc.*, **1992**, *114*, 5459-5460.

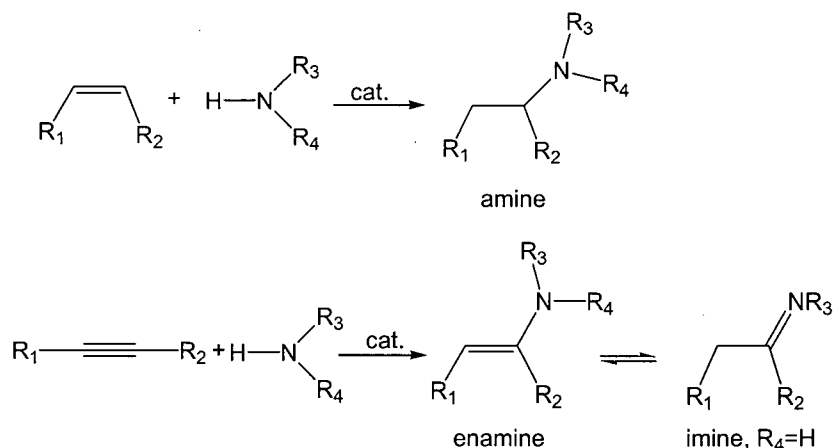
2. (a) T. E. Muller and M. Beller, *Chem. Rev.*, **1998**, *98*, 675-703; (b) U. Nettekoven and J. F. Hartwig, *J. Am. Chem. Soc.*, **2002**, *124*, 1166-1167; (c) S. Hong and T. J. Marks, *J. Am. Chem. Soc.*, **2002**, *124*, 7886-7887; (d) Y. K. Kim and T. Livinghouse, *Angew. Chem., Int. Ed.*, **2002**, *41*, 3645-3647.
3. (a) E. Haak, I. Bytschkov and S. Doye, *Angew. Chem., Int. Ed.*, **1999**, *38*, 3389-3391; (b) I. Bytschkov and S. Doye, *Tetrahedron Lett.*, **2002**, *43*, 3715-3718.
4. F. Pohlki and S. Doye, *Chem. Soc. Rev.*, **2003**, *32*, 104-114.
5. C. Cao, Y. Shi and A. L. Odom, *Org. Lett.*, **2002**, *4*, 2853-2856.
6. T. Ong, G. P. Yap and D. S. Richeson, *Organometallics*, **2002**, *21*, 2839-2841.
7. L. Ackermann and R. G. Bergman, *Org. Lett.*, **2002**, *4*, 1475-1478.
8. (a) C.-T. Chen, L.H. Rees, A.R. Cowley, M.L.H. Green, *J. Chem. Soc., Dalton Trans.*, **2001**, *11*, 1761-1767; (b) J.R. Hagadorn, J. Arnold, Reactivity of Titanium dinitrogen Complexes, *Book of Abstracts, 213 ACS National Meeting*, **1997**.
9. Patten, T. E.; Novak, B. M., *J. Am. Chem. Soc.*, **1996**, *118*, 1906-1916.
10. G. R. Giesbrecht, A. Shafir and J. Arnold, *Inorg. Chem.*, **2001**, *40*, 6069-6072.
11. B.-H. Huang, T.-L. Yu, Y.-L. Huang, B.-T. Ko and C.-C. Lin, *Inorg. Chem.*, **2002**, *41*, 2987-2994.

Chapter 3 Catalytic Hydroamination

3.1 Introduction

Hydroamination, the addition of N-H to the carbon carbon multiple bond of alkenes or alkynes, is among the most desirable transformations in organic chemistry.¹ As can be seen from Scheme 3-1, hydroamination of alkenes and alkynes converts inexpensive and readily available starting materials into amines, enamines or imines without the formation of any side products. The N-containing products are important for both research and the chemical industry. Due to the high atom efficiency of this conversion, hydroamination offers significant economical and environmental benefits in comparison with classical methods for the synthesis of amines and imines.

Scheme 3-1



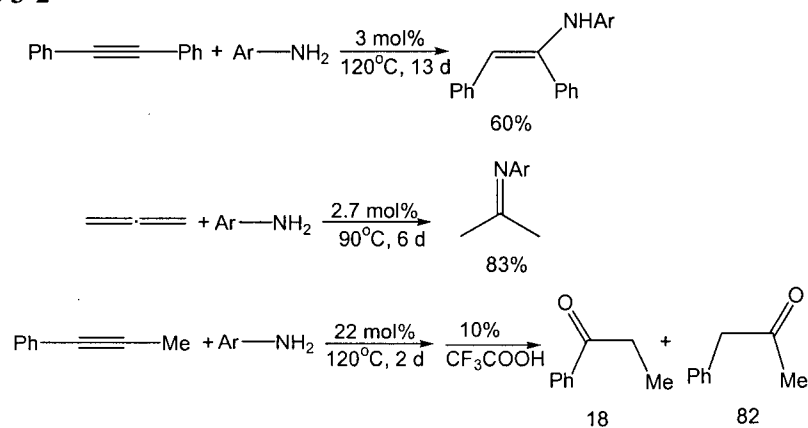
From a thermodynamic point of view, hydroamination with simple amines and alkenes/alkynes should be feasible since the corresponding reactions are slightly exothermic or almost thermoneutral.² However a high activation barrier exists for the direct addition of amines across C-C multiple bonds due to electrostatic repulsion between the lone pair of electrons at the nitrogen atom and the electron rich multiple bond. In the case of intermolecular hydroamination, the use of high temperatures to drive reactions to completion results in the hydroamination equilibrium shifting to the

starting material due to the unfavorable reaction entropy. Therefore, an alternative approach uses a catalytic procedure to shift the equilibrium to product formation.

During the last few years, great progress has been achieved on the hydroamination procedure for allenes and non-activated alkynes catalyzed by transition metal complexes,³ while in general hydroamination of alkenes remains a significant challenge.⁴ Since thermodynamics suggests that the hydroamination of alkynes can be realized more easily than that of alkenes, it is a reasonable approach to develop efficient catalysts for alkynes first and then apply the obtained knowledge to the development of new catalysts for the hydroamination of alkenes.

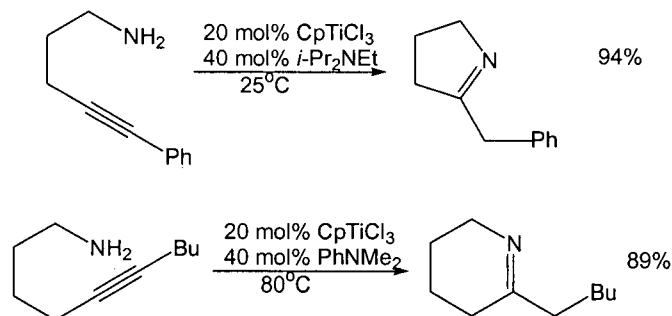
In 1992 Bergman *et al.* reported that zirconocene bisamide $\text{Cp}_2\text{Zr}(\text{NH}-2,6\text{-Me}_2\text{C}_6\text{H}_3)_2$ catalyzed the intermolecular addition of 2,6-dimethylaniline to alkynes and allenes (Scheme 3-2).⁵ These reactions were performed in the presence of 2-3 mol% catalyst at 90-120°C in benzene or toluene over days to give enamines or the tautomeric imines. Further investigation revealed that hydroamination of alkynes or allenes with sterically less demanding amines (such as aniline) did not proceed efficiently in the presence of zirconocene bisamide. Catalytic hydroamination of unsymmetrically disubstituted alkynes with the same catalyst took place with good to moderate regioselectivities. In general, the more favored product bore the smaller alkyne substituent located α to the nitrogen atom. There were no comments regarding the hydroamination reaction of terminal alkynes, however the cycloaddition product with anti-Markovnikov selectivity was observed for the stoichiometric reaction of a terminal alkyne with $\text{Cp}_2\text{Zr}=\text{NR}$ (the active species for hydroamination reaction, which will be further discussed in Chapter 4).^{5b}

Scheme 3-2

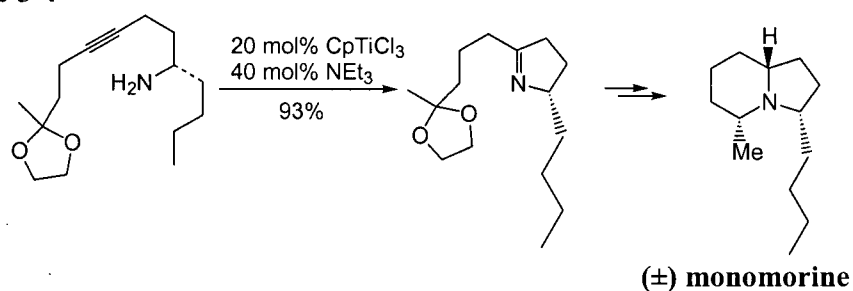


Also in 1992, Livinghouse *et al.* found that CpTiCl_3 and $\text{CpTiCl}(\text{NEt}_2)_2$ were efficient catalysts for the intramolecular hydroamination of aminoalkynes.⁶ Several five- and six-membered cyclic imines were synthesized from corresponding aminoalkynes (Scheme 3-3). The efficiency of this procedure was demonstrated by using CpTiCl_3 -catalyzed cyclization of aminoalkynes at room temperature as the key step for the total synthesis of the indolizidine alkaloid (\pm)-monomorine (Scheme 3-4).⁷ However these complexes do not catalyze intermolecular hydroamination reactions.

Scheme 3-3

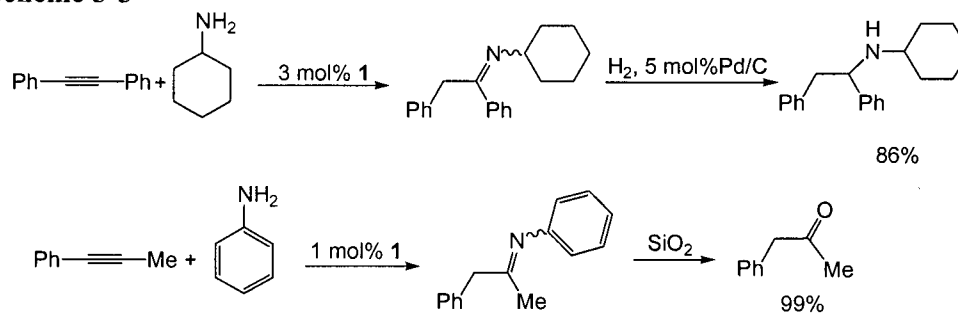


Scheme 3-4



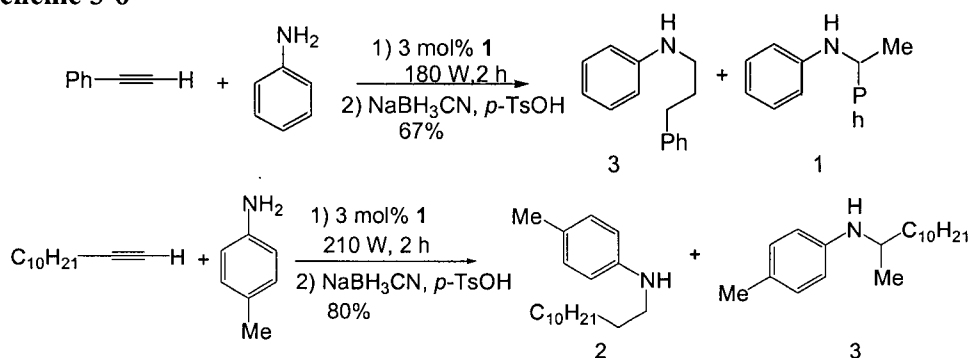
Inspired by the pioneering work of Bergman and Livinghouse, Doye *et al.* showed that the bisamide complexes of titanium such as $\text{Cp}_2\text{Ti}(\text{NHC}_6\text{H}_5)_2$ are better hydroamination catalysts than the corresponding zirconium complexes. While investigating possible general catalyst precursors, the same group found that the readily available reagent, dimethyltitanocene (Cp_2TiMe_2 , **1**), is a widely applicable, inexpensive hydroamination catalyst of low toxicity.⁸ Primary aryl and alkyl amines can be coupled to symmetrically and asymmetrically substituted internal alkynes by using Cp_2TiMe_2 as a precatalyst. In the case of asymmetrically substituted alkyl aryl alkynes, the reaction occurs with high regioselectivity. In general, the more favored product bears the smaller alkyne substituent located α to the nitrogen atom (anti-Markovnikov product). The reaction of terminal alkynes is also possible, but with lower yields in comparison to that of internal alkynes. Typical hydroamination reactions are carried out at 100 to 110°C in toluene for 40 to 72 h, while the reaction time can be dramatically shortened by using microwave heating instead of conventional heating.⁹ The initially formed imines can either be hydrolyzed to ketones or reduced to amines (Scheme 3-5). While aniline derivatives and sterically hindered alkyl amines (such as *t*-butyl amine and benzhydryl amine) react smoothly under these reaction conditions, a significant decrease in reactivity is observed for sterically less hindered *n*-alkyl and benzylamines.

Scheme 3-5



Impressively, the hydroamination of terminal alkynes can also be realized when Cp_2TiMe_2 is used as a catalyst under microwave heating.⁹ In contrast to alkyl aryl alkynes, corresponding hydroamination reactions of terminal alkynes lead to the formation of both Markovnikov and anti-Markovnikov regioisomeric products. While the formation of the internal addition product (Markovnikov) is favored in addition reactions of aniline derivatives to terminal alkyl alkynes, the terminal addition product (anti-Markovnikov) is preferred in reactions between anilines and phenylacetylene (Scheme 3-6).

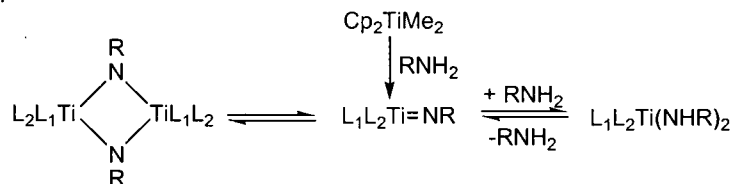
Scheme 3-6



Mechanistic investigations in the Bergman and Doye groups explain the fact that sterically demanding amines are better substrates.^{5,8} The presence of an equilibrium between the catalytically active imido complex, imido complex dimers and bisamides (Scheme 3-7) results in a preference for imido dimers or bisamide complexes in the case of less sterically hindered amines.¹⁰ This also suggests that the titanium complexes with bulky ligands should shift the equilibrium to the catalytically active imido complex and result in accelerated reactions of sterically less hindered amines. This was confirmed by using the Cp^*TiMe_2 as a hydroamination catalyst.¹¹ The hydroamination reaction between *n*-propylamine and diphenylacetylene reaches 100% conversion after 4 h with 6 mol% catalyst loading at 114°C. In comparison, an identical hydroamination reaction using Cp_2TiMe_2 as a catalyst does not reach 100%

conversion even after 48 h. For the hydroamination of less bulky amines with unsymmetrical alkynes, the observed regioselectivity is lower than that of sterically demanding amines. For the same hydroamination reaction, the regioselectivity is consistent whether Cp_2TiMe_2 or Cp^*TiMe_2 as the catalyst. This result indicates that the amine is at least partially responsible for the observed regioselectivity.

Scheme 3-7



Very recently, it was recognized that Cp_2TiMe_2 is also an efficient catalyst for the intramolecular hydroamination of aminoalkynes.¹² Both γ and δ -aminoalkynes can be converted into the corresponding five- and six-membered cyclic amines respectively by Cp_2TiMe_2 -catalyzed hydroamination and subsequent reduction (Scheme 3-8). In contrast, seven- and eight-membered rings are formed slowly under similar conditions.

Scheme 3-8

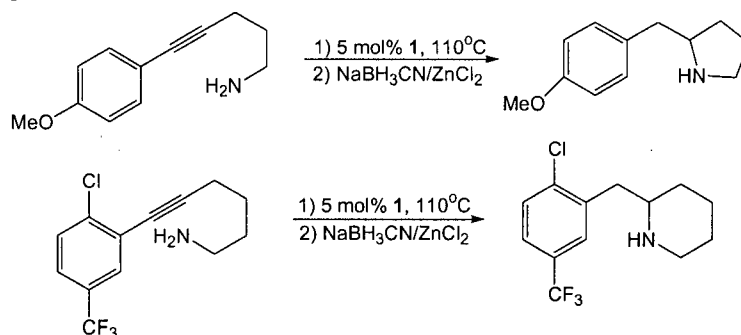
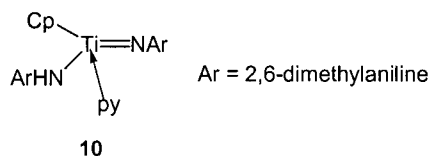


Figure 3-1 Pyridine-trapped imido complex



Bergman *et al.* have shown that the catalytically active species of the Cp_2TiMe_2 -catalyzed intermolecular hydroamination is a cyclopentadienyl(amido)titanium imido

complex, **10** (Figure 3-1), which rapidly catalyzes the addition of 2,6-dimethylaniline to diphenylacetylene and allenes.¹³ The isolated pyridine-trapped titanium imido complex exhibits substantially higher reactivity than the Cp_2TiMe_2 precursor. Doye *et al.* also reported Cp-based titanium imido complexes (Figure 3-2 **13**, **14**) as hydroamination catalysts.¹⁴

Beller *et al.* used titanocene alkyne complexes **11** and **12** as catalysts for the hydroamination of internal and terminal alkynes.¹⁵ It is noteworthy that the reactions of terminal alkynes with alkyl amines proceed with high selectivity to give the corresponding anti-Markovnikov products.

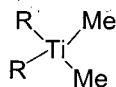
As can be seen from Figure 3-2, a wide variety of titanium complexes have been developed as hydroamination catalysts in recent years. Many are based on titanocene with one or two Cp ligands while recent developments have focused on titanium complexes with non-Cp ancillary ligands.

Recent research from the Odom group indicated that $\text{Ti}(\text{NMe}_2)_4$, **7**, another commercially available titanium complex, also demonstrates hydroamination activity.¹⁶ The reaction is fast with many substrates and selective for Markovnikov products, especially for the hydroamination of terminal alkynes with aryl amines. The results reported suggest that hydroamination with alkyl amines always gives poor yields. On the basis of these limitations, they developed titanium dipyrrolylmethane complexes as hydroamination catalysts.¹⁷ $\text{Ti}(\text{NMe}_2)_2(\text{dpma})$ (dipyrrolyl- α -methylmethylamine, **15**), can increase the regioselectivity for the hydroamination of 1-hexyne with aniline (Markovnikov:anti-Markovnikov>50:1). Many functional groups were tolerated, including halogenated anilines. Reaction rates involving electron deficient arenes are greatly decreased, indicating large electronic effects. As in the case of **7**, hydroamination reactions with alkyl amines often results in slower rates

Figure 3-2 Ti complexes for hydroamination

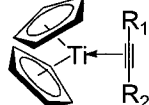


Cp_2TiMe_2 based Ti complexes



$\text{R} = \text{C}_5\text{H}_4\text{Me}, \text{C}_5\text{H}_4\text{Et}, \text{C}_5\text{H}_4\text{Pr}, \text{C}_5\text{H}_4\text{t-Bu}, \text{C}_5\text{H}_4\text{SiMe}_2\text{Nt-Bu}, \text{C}_5\text{H}_4\text{SiMe}_2\text{NPh}, \text{C}_5\text{Me}_5$

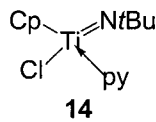
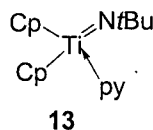
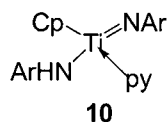
Cp_2TiR (titanocene alkyne complexes)



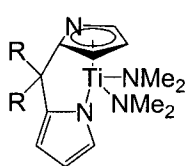
11, $\text{R}_1=\text{R}_2 = \text{SiMe}_3$

12, $\text{R}_1=\text{SiMe}_3, \text{R}_2 = \text{Ph}$

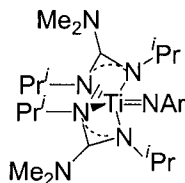
Ti imido complexes



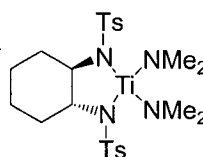
Non-Cp based Ti complexes



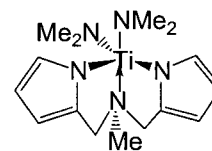
$\text{Ti}(\text{NMe}_2)_2(\text{dmpm})$, **2**



3



bis(sulfonamido) Ti, **4**



$\text{Ti}(\text{NMe}_2)_2(\text{dpma})$, **15**

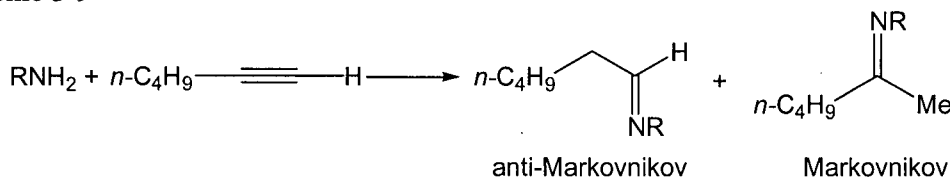
relative to that of arylamines. Benzyl amine and benzhydryl amine proceed in 70 to 90% yield respectively in 48 h with benzyl amine giving higher Markovnikov selectivity ($M/\text{anti-M} > 50:1$) than benzhydryl amine does (3:1). $\text{Ti}(\text{NMe}_2)_2(\text{dmpm})$, **2**, another derivative of **7**, gives similar results to **15** with an even faster reaction rate.¹⁸

A typical reaction for terminal alkynes can be carried out at 25°C with 5 mol% catalyst loading and go to completion within 10 min. Higher temperatures and longer times are required for the hydroamination of internal alkynes.

Richeson *et al.* reported the first Cp-free titanium imido complexes such as **3**, which contained guanidinate ancillary ligand.¹⁹ Initial results indicate that terminal alkynes are better substrates than internal alkynes. The reactivity of **3** is comparable with that of **1**.

Since the catalytic activity of each complex strongly depends on the properties of the employed substrates, especially in the case of intermolecular hydroamination, it is difficult to make a reliable prediction for the choice of catalyst for a certain reaction. For example, in the case of the hydroamination of 1-hexyne with amines, different regioselectivity can be realized by using different titanium complexes as catalyst (Scheme 3-9). Titanocene-alkyne complexes **11** or **12** can be used for selectively anti-Markovnikov addition of alkylamines to 1-hexyne.¹⁵ However, Markovnikov product is favored when employing Ti(NMe₂)₂(dpma) as a catalyst for the same reaction.¹⁷

Scheme 3-9

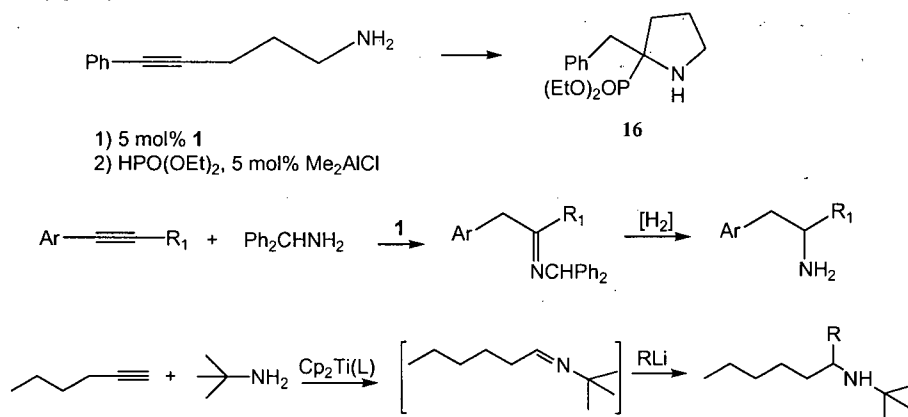


Cp₂TiMe₂ can be regarded as a general catalyst for both intermolecular and intramolecular hydroamination among the known titanium complexes so far. However, considering the relatively harsh (110°C) reaction conditions employed and long reaction times (24 h or even longer), it does not offer significant advantages over other catalysts. Furthermore, Cp₂TiMe₂ is not an ideal catalyst for the hydroamination of terminal alkynes, which usually gives a mixture of both Markovnikov and anti-Markovnikov products. This remains an important synthetic challenge as the

regioselective hydroamination of terminal alkynes offers a potential method for the preparation of terminal amine compounds important to both research and the chemical industry.

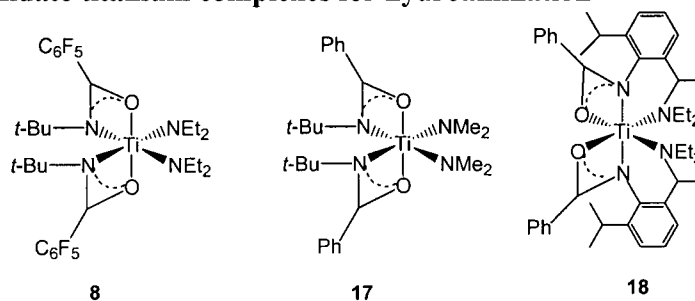
In recent years there have been reports of the application of catalytic hydroamination in the synthesis of organic molecules. The Cp_2TiMe_2 -catalyzed hydroamination of alkynes has been used as an efficient tool for the synthesis of biologically interesting compounds such as α -amino phosphonate²¹ (**16**) and 2-arylethylamine derivatives²² (Scheme 3-10). It also offers a novel procedure to convert alkynes into primary amines by using benzhydrylamine in the hydroamination step followed by hydrogenation.²³ Branched secondary aliphatic amines can be synthesized by combining titanium-catalyzed hydroamination of alkynes with the addition of organometallic reagents using a one-pot procedure.²⁴

Scheme 3-10



In this chapter, we will focus on the application of titanium amidate **8** as a precatalyst for hydroamination. Comparable results from complexes **17** and **18** are included when applicable (Figure 3-3).

Figure 3-3 Amidate titanium complexes for hydroamination



3.2 Results and Discussion: Intramolecular Hydroamination

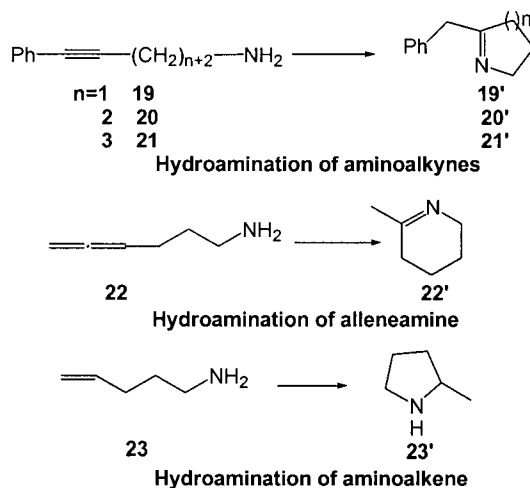
Initial investigations focused on intramolecular hydroamination catalyzed by titanium amidate complex **8**. Because of the neutral entropy ($\Delta S=0$) of the intramolecular reaction, the ΔG_0 value for the intramolecular addition of N-H bonds to C-C multiple bonds is more favorable than that of intermolecular reactions. There have been many literature reports of intramolecular hydroamination reactions catalyzed by different catalysts.^{6,12,16,20} Thus, these initial experiments allowed us to easily compare and evaluate the activity of **8** with other literature reports.

The catalytic activity of **8** can be easily tested by screening the hydroamination of aminoalkynes (**19**, **20**, **21**), alleneamine (**22**) and aminoalkene (**23**) which are easily prepared from commercially available starting materials by following literature procedures (Scheme 3-11).²⁵ The addition generates an enamine with an exocyclic double bond. A subsequent 1,3-hydrogen shift leads to isomerization of the initially formed enamine to more stable imine.

The hydroamination reaction was carried out in *d*₆-benzene on NMR tube scale and monitored by ¹H NMR spectroscopy. The initial experiments monitored by ¹H NMR spectroscopy employing the γ -aminoalkyne (5-phenyl-4-pentyn-1-amine) **19** showed that the intramolecular hydroamination/cyclization reaction in the presence of 3.0 mol% of **8** is in fact very fast at 25°C in C₆D₆. The aminoalkyne **19** was completely

consumed within 15 minutes and only the corresponding cyclic imine **19'** was observed in almost quantitative yield with a diagnostic peak at 3.80 ppm (CH_2N) in the 1H NMR spectrum (98%, NMR yield, using 1,3,5-trimethoxybenzene as internal standard). The same reaction catalyzed by **17** needed a longer time (3.5 h) to be complete. For the reaction of δ -aminoalkyne (6-phenyl-5-hexyn-1-amine) **20**, a higher reaction temperature (60°C) and a longer time (3 h) were needed for 100% conversion. No catalytic activity was observed at room temperature. In the case of 7-phenylhept-6-yn-1-amine **21**, only 15% conversion of the starting material was detected by 1H NMR spectroscopy after heating at 60°C for 6 h. No formation of any side products was detected in any case.

Scheme 3-11



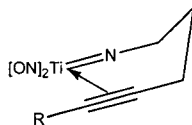
The results in Table 3-1 demonstrate that under the employed reaction conditions, γ -, δ - and ϵ - aminoalkynes can be converted regioselectively into five-, six- and seven-membered heterocycles. For the 5-membered ring hydroamination, titanium complex **8** with electron withdrawing substituent (C_6F_5) on the carbonyl moiety of the amidate ligand dramatically enhances catalytic activity compared with same reaction catalyzed by **17**, the congeneric of **8** with C_6H_5 incorporated into the ligand. The dependence of relative rates of cyclization on ring size results in the 5-membered ring

Table 3-1 Comparison of Hydroamination of aminoalkynes and alleneamines

Substrate	Catalyst	mol% catalyst	T (°C)	t (h)	Yield*
19	8	2.0	25	<0.25	98
	17	5.0	25	3.5	98
	1, Cp ₂ TiMe ₂ ¹²	5.0	110	6	90
	7, Ti(NMe ₂) ₄ ¹⁶	5.0	25	0.5	quant
	CpTiCl ₃ ⁶	20	25	0.5	94
20	8	5.0	65	3	quant
	CpTiCl ₃ ⁶	20	80	0.5	88
	1, Cp ₂ TiMe ₂ ¹²	5.0	110	6	83
21	8	5.0	60	6	15
	1 ¹²	5.0	110	72	<30
22	8	6.5	70	2.5	98
	4, Bis(sulfonamide)Ti ²⁰	5.0	25	5	quant

being formed more quickly than the 6-membered ring, which was in turn much more reactive than the 7-membered ring, consistent with what has been observed in the lanthanide-catalyzed intramolecular hydroamination of aminoalkynes.¹⁷ This is explained by the “chair-like” transition state in the case of substrate **19** (Figure 3-4).

Figure 3-4 Hydroamination transition state of 5-membered ring substrate



For the more challenging substrate, allene amine **22**, the hydroamination reaction is complete with high yield (98%, NMR) within 3 hours after heating at 70°C with 6.5 mol% catalyst loading, giving exclusively the imine product **22'** with a diagnostic peak at 3.52 ppm (CH₂N). This is comparable with the bis(sulfonamide) titanium complex recently developed by Bergman *et al.* (25°C, 5 h, quant. yield).²⁰

As can be seen from Table 3-1, compared with other published group 4 complexes, **8** is noteworthy for its low catalyst loading, mild reaction conditions and excellent yields of 5- and 6-membered heterocycles with high regioselectivity. However, the

attempted hydroamination reaction of aminoalkene (unactivated carbon carbon double bond) by using **8** as a catalyst was not successful.

3.3 Intermolecular Hydroamination of Terminal Alkynes with Primary Amines

Due to the promising preliminary results for intramolecular hydroamination catalyzed by **8**, we chose to investigate intermolecular hydroamination. In general, intermolecular hydroamination reactions are more difficult than intramolecular reactions because of the negative ΔS_0 values of the reactions. At the high temperatures necessary to initiate the reaction, the equilibrium can shift to the starting materials rather than giving hydroamination products. This problem is exacerbated when volatile small molecule starting materials are used.

Different terminal alkynes—1-hexyne **24**, cyclohexylacetylene **25**, 3,3-dimethyl-1-butyne **26**, phenylacetylene **27** and several primary amines (alkyl-amines—*t*-butyl amine **28**, *isopropyl* amine **29**, benzyl amine **30**, benzhydryl amine **31**; arylamines—aniline **32** and 2,6-dimethyl aniline **33**) were used as substrates. Initial investigations focused on substrates with different steric properties. Typical reactions were carried out at 65 °C for 24 hours (90 °C for phenylacetylene) using C₆D₆ as solvent on an NMR tube scale (Scheme 3-12).²⁷ Typical catalyst loading is 10.0 mol% and the ratio between alkyne and amine was maintained near 1:1. The NMR yield was obtained by comparison of the integration of the aryl resonances of 1,3,5-trimethoxybenzene and a well resolved signal for the product imine.

As shown in Table 3-2 (entries 1a-1f), different amines (**28-33**) reacted with 1-hexyne to give products with different regioselectivities and variable yields. Anti-Markovnikov products were preferred in cases using alkyl amines, but when arylamines (aniline and 2,6-dimethylaniline) were employed, Markovnikov products were observed. Only the anti-Markovnikov product was detected in the case of *t*-butyl

Scheme 3-12

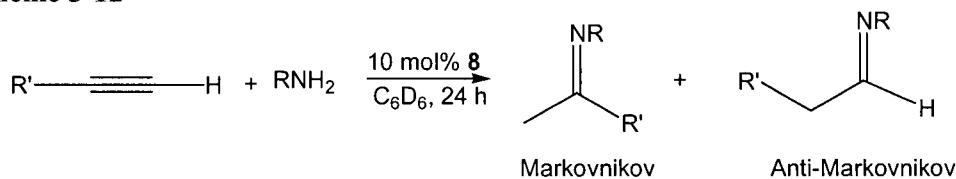


Table 3-2 Hydroamination of terminal alkynes with primary amines

Entry	Alkyne	R	T (°C)	Yield (% NMR)	Anti- M :M ^b
1a		<i>t</i> -butyl	65	93	>49:1
1b		<i>isopropyl</i>	65	78	>49:1
1c		benzyl	65	28	4:1 ^a
1d		benzhydryl	65	47	12:1
1e		aniline	65	20	1:6
1f		2,6-dimethylaniline	65	79	<1:49
2a		<i>t</i> -butyl	65	98	>49:1
2b		<i>isopropyl</i>	65	99	>49:1
2c		benzyl	65	decomposed	-
2d		benzhydryl	65	93	>49:1
2e		aniline	65	7	>49:1
2f		2,6-dimethylaniline	65	72	<1:49
3a		<i>t</i> -butyl	65	80	>49:1
3b		<i>isopropyl</i>	65	36	>49:1
3c		benzyl	65	decomposed	-
3d		benzhydryl	65	95	>49:1
3e		aniline	65	10	>49:1
3f		2,6-dimethylaniline	65	10	>49:1
4a		<i>t</i> -butyl	90	61	>49:1
4b		<i>isopropyl</i>	90	60	>49:1
4c		benzyl	90	decomposed	-
4d		benzhydryl	90	81	>49:1
4e		aniline	90	24	1:1
4f		2,6-dimethylaniline	90	75 ^c	3:1

^a. Markovnikov product was found by GCMS.^b. Ratios were confirmed by GCMS^c. Z/E = 6:1

amine and *isopropyl* amine, as indicated by the diagnostic triplet at 7.40 ppm in the ¹H NMR spectrum. While for the benzyl and benzhydryl amine, the hydroamination affords a mixture of anti-Markovnikov and Markovnikov products in 4:1 and 12:1 ratio respectively, based on both ¹H NMR spectroscopy and GCMS results. Hydroamination of 1-hexyne with 2,6-dimethylaniline gave exclusively Markovnikov product in 79% yield as observed with a diagnostic singlet at 1.30 ppm in the ¹H

NMR spectrum (same result observed when 4-chloro-2,6-dimethylaniline was employed, resulting in 60% yield), while anti-Markovnikov and Markovnikov products were detected at a 1:6 ratio (GCMS result, further confirmed by isolation of amines after LAH reduction) in the case of aniline. The different regioselectivities for different amines indicates the importance of the steric factors of the amines in the hydroamination reaction. Bulky amines result in good regioselectivity, while the less sterically demanding amines often give a mixture of both Markovnikov and anti-Markovnikov products. The yields are also affected by the steric properties of the amines. More sterically hindered amines give higher yields than less bulky amines (*t*-butyl 93% vs *isopropyl* 78%; benzhydryl 46.6% vs benzyl 27.9%; 2,6-dimethylaniline 79% vs aniline 20%). Increased steric bulk favoring product formation has been previously observed.⁸ Within the group, the reaction of 1-hexyne and benzyl amine using **18** as a precatalyst gave good yields (88%) with high regioselectivity (anti-Markovnikov exclusively). This result showed that the steric effects of the metal complexes could also improve reactivity and selectivity of the hydroamination reaction. Compared with published titanium complexes, **8**-catalyzed hydroamination of 1-hexyne with different primary amines shows comparable or better yields and regioselectivities.

For the hydroamination of cyclohexylacetylene (**25**), as the results in Table 3-2 (entries 2a-2f) indicate, the performed alkylamine addition takes place regioselectively (anti-Markovnikov addition). In the case of arylamines, aniline gives exclusively anti-Markovnikov product in very low yield (unreacted aniline and alkyne were detected by GCMS), while 2,6-dimethylaniline affords only Markovnikov product in good yield (72%). Increased yield with increased steric bulk is consistent with previous observations. The reactions with benzyl amine (entry 2c) and aniline

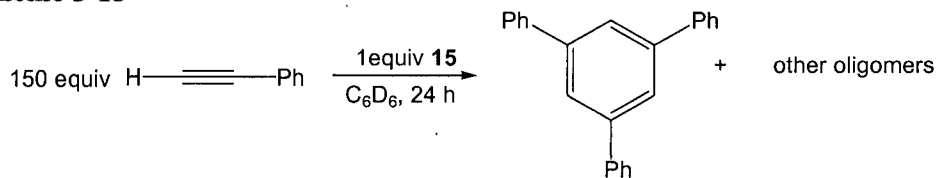
(entry 2e, the conversion was only 7% after 24 hours) do not go to complete conversion possibly due to the presence of side reactions. Again **18**-catalyzed hydroamination reaction (entry 2c) proceeds in high yield (87%) with high anti-Markovnikov selectivity under similar reaction conditions, further indicating the steric effect of the employed metal complex on the hydroamination results.

For the hydroamination of sterically demanding 3,3-dimethyl-1-butyne, as shown in Table 3-2 (entries 3a-3f), both alkyl and arylamines afford exclusively anti-Markovnikov products in varying yield except for benzylamine, for which catalyst decomposition was observed. Bulky alkylamines (*t*-butyl, benzhydrylamine) give excellent yields, while the yield for *isopropyl* amine is only 36%. In the case of aryl amine, both aniline and 2,6-dimethylaniline give anti-Markovnikov products in low yield (<10%), but no Markovnikov product was found in either case. For entries 3b and 3c, the reaction proceeds much faster when using **8** as catalyst rather than **18**, which needs 120 h to go to completion. In contrast to the result of **8**-catalyzed hydroamination of 3c, the reaction catalyzed by **18** gives 87% yield with high anti-Markovnikov selectivity. These results indicate that steric properties of both amine and alkyne have effects on the hydroamination reaction. From the perspective of alkyl alkyne substrates, sterically hindered alkynes give good results when using less bulky catalyst; while bulky catalysts are ideal for less sterically hindered alkynes.

For the hydroamination of phenylacetylene with different amines (Table 3-2, entries 4a-4f), except for benzyl amine, anti-Markovnikov products are preferred for both alkyl and aryl amines with different ratios of anti-Markovnikov to Markovnikov products. Only anti-Markovnikov products are detected by ^1H NMR spectroscopy when the amine is bulky. In the case of aniline and 2,6-dimethylaniline, the ratio of the hydroamination products (anti-M:M) is 1:1 and 3:1, respectively (hydroamination

of 4-methoxyphenylacetylene with 2,6-dimethylaniline gave anti-Markovnikov product in 80% yield at 6:1 ratio of Z/E isomers). The yields of the hydroamination are good except for those of the benzyl amine and aniline. In the ^1H NMR spectra for all hydroamination reactions, unidentified side products were detected. This is consistent with other reported Ti-catalyzed hydroamination reactions of phenylacetylene.¹⁷ Odom *et al.* suggest that oligomerization of phenylacetylene is a major side reaction (Scheme 3-13). 1,3,5-triphenylbenzene was isolated in 45% yield along with other oligomers when treating an excess of phenylacetylene (150 equivalents) with 1 equivalent of **15**.¹⁷

Scheme 3-13



Summary of hydroamination with primary amines of different terminal alkynes

For both quarternary and tertiary alkyl substituted primary amines, the hydroamination with different terminal alkynes affords exclusively anti-Markovnikov product with good to excellent yields with different alkynes. Less sterically hindered 1-hexyne and cyclohexylacetylene gave almost quantitative yields. The reduced yields of 1-hexyne versus cyclohexylacetylene are due to the higher volatility of the 1-hexyne substrate. Also, the yield decreases with bulkier alkynes, which is contrary to the steric effect of amines on hydroamination—bulky amines favor the progress of the reaction while bulky alkynes inhibit the progress of the reaction. This contrasting behavior will be discussed at length in Chapter 4. The lower yields obtained with phenylacetylene in comparison to the comparably sized cyclohexylacetylene can be attributed to electronic effects of the substrate.

Anti-Markovnikov product is favored for hydroamination of benzhydrylamine with different alkynes. More sterically demanding alkynes gave regioselectively anti-Markovnikov product with excellent yields; while less bulky 1-hexyne affords a mixture of anti-Markovnikov and Markovnikov products at 12:1 ratio with 47% yield.

In the case of 2,6-dimethylaniline, hydroamination with all alkynes gave good yields. Interestingly, there are totally different regioselectivities for different alkynes. Less bulky alkynes such as 1-hexyne and cyclohexylacetylene afford Markovnikov products while more sterically hindered alkynes favor anti-Markovnikov products.

In order to demonstrate that this hydroamination procedure is applicable to gram scale syntheses of amine-containing small molecules, larger scale hydroaminations (0.5 to 1 mmol) of selected cases with lower catalyst loading (5 mol%) followed by LAH/THF reduction were carried out (Figure 3-5). The yields are summarized in Table 3-3. All compounds were identified by ^1H and ^{13}C NMR spectroscopy, EIMS spectrometry and IR spectroscopy. New compounds were further characterized by HRMS or elemental analysis. This investigation also demonstrated that in most cases the reported NMR yields are representative of isolated yields.

Figure 3-5 Isolated amine after LAH/THF reduction

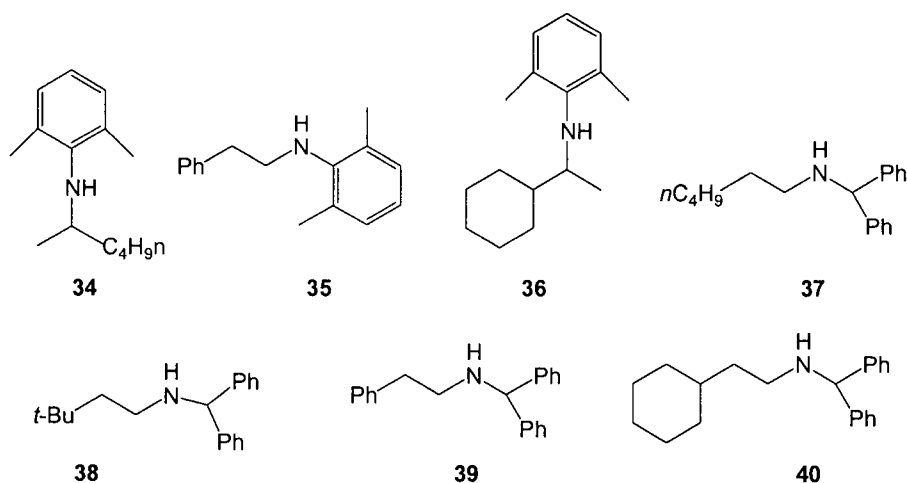


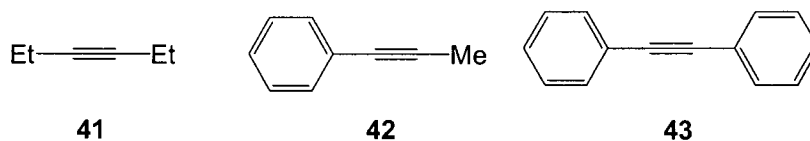
Table 3-3 Results of Hydroamination followed by LAH/THF reduction

Entry	Amine	R	Product	T (°C)	Yield (% NMR)	Yield ^a (Isolated)	Anti- M :M
5a		<i>n</i> -butyl	37	65	47	43	>12:1
5b		cyclohexyl	40	65	93	89	>49:1
5c		<i>t</i> -butyl	38	65	95	94	>49:1
5d		phenyl	39	65	81	51	>49:1
6a		<i>n</i> -butyl	34	65	79	71	<1:49
6b		cyclohexyl	36	65	72	44	<1:49
6c		<i>t</i> -butyl	-	65	10	- ^b	>49:1
6d		phenyl	35	65	75	61	>49:1

^a after LAH/THF reduction.^b Unsuccessful in isolating the amine due to low yield.

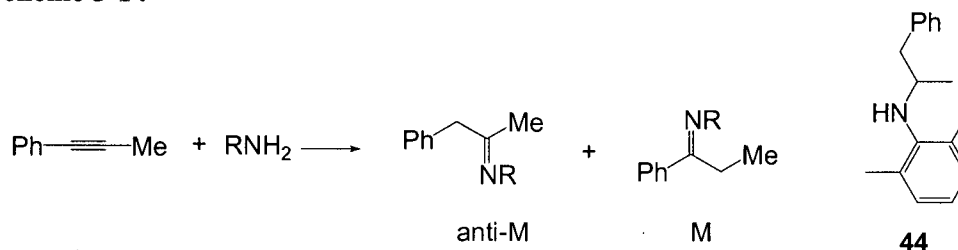
3.4 Intermolecular Hydroamination of Internal Alkynes with Primary Amines

The catalytic reactivity of **8** was further investigated by using internal alkynes (Figure 3-6) such as 3-hexyne **41**, phenylmethylacetylene **42** and diphenylacetylene **43** as substrates. Again, preliminary results were obtained using NMR tube reactions with 10 mol% catalyst loading. The reaction was monitored by ¹H NMR spectroscopy after heating at 90°C for 24 or 48 h.

Figure 3-6 Internal alkyne substrates

In most cases the hydroamination of internal alkynes was not successful. One example that worked was the addition of 2,6-dimethylaniline to phenylmethylacetylene, giving anti-Markovnikov product with 50% yield (57% conversion) after heating at 90°C for 24 h (Scheme 3-14). The yield of isolated amine **44** using improved reaction conditions after LAH/THF reduction is 71% with 5 mol% catalyst loading at the hydroamination step.

Scheme 3-14



GCMS shows a 4:1 ratio of anti-Markovnikov and Markovnikov product for the hydroamination of phenylmethylacetylene with benzhydryl amine after hydrolyzing over SiO₂. The presence of unidentified side reactions may be responsible for the low yield (<15%) of the expected hydroamination products.

Cp-based complexes such as **1**, **11** and **12** are good catalysts for hydroamination of internal alkynes with different primary amines. However these experiments are carried out at very high temperature for extended periods of time (100 to 120°C for up to 5 d). Anti-Markovnikov selectivity was observed in the case of unsymmetrically substituted alkynes. When complex **2** or **15** was employed as catalyst, the reaction is Markovnikov selective. Compared with these complexes, **8** is not an efficient catalyst for the hydroamination of internal alkynes, although higher reaction temperatures were not attempted.

3.5 Conclusion

The reactivity and scope of **8** as a hydroamination catalyst was investigated by using different substrates. In general, **8** is an efficient intramolecular hydroamination catalyst for the cyclization of δ -, γ -aminoalkynes and allene amines, which afford 5- or 6-membered heterocycles. The formation of 7-membered rings is slow. Hydroamination of terminal alkynes with bulky primary amines gives products with varying yields and regioselectivities (anti-Markovnikov product for alkylamines while Markovnikov products dominate for arylamines). Less sterically hindered amines

such as benzyl amine and aniline are not ideal substrates when using **8** as a hydroamination catalyst. The efficient synthesis of seven secondary amines was demonstrated. These amine containing small molecules may be useful building blocks suitable for further synthetic elaboration. Finally, the hydroamination of internal alkynes with primary amines was only successful for select substrate combinations at 90°C.

3.6 Experimental

Typical NMR scale hydroamination reaction

All hydroamination reactions were performed on NMR tube scale using sealable NMR tubes.

Intramolecular hydroamination: A vial was loaded with 5 mol% of **8** and internal standard 1,3,5-trimethoxybenzene dissolved in C₆D₆ and the aminoalkyne or alleneamine was added by pipette. The mixture was then transferred to a sealable NMR tube. The tube was sealed (and heated to 65 °C) and the reaction progress was monitored by ¹H NMR spectroscopy and allowed to proceed to completion.

Intermolecular hydroamination: A vial was charged with 0.01 mmol of **8** and 0.05 mmol of 1,3,5-trimethoxybenzene. These materials were dissolved in C₆D₆ before 0.1 mmol of amine and alkyne were added to the same vial separately. The resulting solution was then transferred to a sealable NMR tube. A ¹H NMR spectrum was obtained at time zero. The tube was then heated to 65 or 90 °C for 24 h before another ¹H NMR spectrum was obtained. The yield was measured by comparison of the integration of the aryl resonances of 1,3,5-trimethoxybenzene and a well-resolved signal for the imine product.

GCMS sample preparation The hydroamination product was hydrolyzed over SiO₂ in chloroform for 2 to 3 h before filtration.

Typical hydroamination/reduction procedure

A vial was charged with 0.05 mmol of **8** which was dissolved in C₆D₆ before 1.0 mmol of amine and alkyne were added to the same vial separately. The resulting solution was transferred to a sealable NMR tube. The tube was then heated to 65 or 90 °C until the starting materials were consumed, as judged by ¹H NMR spectrum. The obtained brown liquid was added to 1.0 mmol LAH/THF solution. After having stirred at room temperature over night, 0.5 mL of 2 M HCl was added and the mixture was extracted with diethyl ether (10 mL × 2 times). 2 M NaOH solution was added to the aqueous layer until it was basic, followed by diethyl ether extraction (10 mL × 2 times). The combined organic layers were washed with brine. After drying over MgSO₄ and concentrating under vacuum, the residue was purified by flash chromatography (silica gel 200-300 mesh, hexanes/diethyl ether) to give the amine product.

Preparation of 7-phenylhept-6-yn-1-amine **21**²⁵

(a) Preparation of lithium phenylacetylide **45**. A solution of 3.00 mL of phenylacetylene (27 mmol) in 150 mL THF was cooled to -78°C and treated with 20.00 mL (32 mmol) of *n*-butyllithium (1.60 M/*n*-hexane). The mixture was warmed to room temperature and stirred over night.

(b) Preparation of 7-bromo-1-phenyl-1-heptyne **46**. A solution of 5.00 mL (27 mmol) of 1-bromo-5-chloro-pentane in 100 mL of THF was treated with 170 mL (27 mmol) of lithium phenylacetylide **45** dropwise and then stirred at 0°C for 2 h. The reaction mixture was then warmed to room temperature and refluxed overnight. Then it was poured into 200 mL of distilled H₂O and the layer was separated. The aqueous layer was extracted with 50 mL of diethyl ether for three times. The combined ether extracts and organic phase were washed with 200 mL of brine, dried over MgSO₄ and

filtered, and then the ether and THF were removed from the filtrate by rotary evaporation. Distillation (95-100°C, full vacuum) of the residue gave 5.00 g (90%) of colorless Br(CH₂)₅CCPh. ¹H NMR (300 MHz, CDCl₃): δ 7.36 (m, 2H, Ph-*H*), 7.26 (m, 3H, Ph-*H*), 3.54 (t, J=6.7Hz, 2H, CH₂Br), 2.42 (t, J=6.7Hz, 2H, CH₂CC), 1.83 (m, 2H, CH₂CH₂Br), 1.60 (m, 4H, 2CH₂).

(c) Preparation of N-(7-Phenyl-6-heptynyl)phthalimide **47**. Compound **46** and 5.00 g (26.6 mmol) of potassium phthalimide were heated at 100°C in 50 mL of anhydrous DMF overnight. After cooling down, the solution was poured into a mixture of CHCl₃ (150 mL) and H₂O (150 mL). The aqueous phase was separated and extracted with 50 mL of CHCl₃ for three times. The combined CHCl₃ solution and the organic phase were washed with 100 mL of 0.2 M NaOH (to remove the unreacted phthalimide) and 200 mL of H₂O, respectively. After drying over MgSO₄ and filtrating, the CHCl₃ and DMF were removed in vacuum and the residue was triturated with 100 mL of diethyl ether. After collection by filtration, the solid residue was dried at reduced pressure to give 7.20 g (94%) of C₈H₄O₂N(CH₂)₅CCPh as a pale yellow solid. ¹H NMR (300 MHz, CDCl₃): δ 7.82 (m, 2H, Ph-*H*), 7.67 (m, 2H, Ph-*H*), 7.30 (m, 2H, Ph-*H*), 7.23 (m, 3H, Ph-*H*), 3.69 (t, J=7.2Hz, 2H, CH₂N), 2.39 (t, J=6.8Hz, CH₂CC), 1.72 (m, 2H, CH₂CH₂N), 1.64 (m, 2H, CH₂CH₂CC), 1.52 (m, 2H, CH₂).

(d) Preparation of 7-phenylhept-6-yn-1-amine **21**. Compound **47** and 2.27 g (45.4 mmol) of hydrazine monohydrate in 50 mL of CH₃OH were refluxed for 2.5 hours. The reaction mixture was then cooled to 0°C and filtered. The pale yellow solids were washed with 5.00 mL of cold CH₃OH for three times, and then the organic phase was concentrated to an oily residue by rotary evaporation. After distillation (95-100°C, full vacuum), 2.15 g (51%) of H₂N(CH₂)₅CCPh was obtained. ¹H NMR (300 MHz,

CDCl₃): δ 7.36 (m, 2H, Ph-*H*), 7.25 (m, 3H, Ph-*H*), 2.70 (t, $J=6.7\text{Hz}$, 2H, CH₂N), 2.40 (t, $J=7.0\text{Hz}$, 2H, CH₂CC), 1.62 (m, 2H, CH₂CH₂N), 1.47 (m, 4H, 2CH₂), 1.15 (brs, 2H, NH₂). ¹³C NMR (75 MHz, CDCl₃): δ 131.4, 128.0, 127.4, 123.9, 90.0, 80.6, 42.0, 33.2, 28.5, 26.1, 19.3.

5-membered heterocycle 2-benzyl-1-pyrroline 19'. This pyrrole derivative was synthesized from 0.102 mmol (16 mg) 5-phenyl-4-pentyn-1-amine **19** and 0.004 mmol (3 mg) of **8** using the procedure described under typical NMR-scale intramolecular hydroamination. The NMR data agree with the literature report.²⁵ The yield was estimated by the ¹H NMR spectrum using 1,3,5-trimethoxybenzene as internal standard. ¹H NMR (300 MHz, C₆D₆): δ 7.20-7.05 (m, 5H, Ph-*H*), 3.80 (t, 2H, CH₂N), 3.58 (s, 2H, CH₂Ph), 2.05 (t, 2H, CH₂C=N), 1.40 (m, 2H, CH₂).

6-Membered heterocycle 2-benzyl-3,4,5,6-tetrahydropyridine 20': The procedure described above was employed except that 0.007 mmol (5.0 mg) of **8** and 24.5 mg of 6-phenylhex-5-yn-1-amine **20** were used. The NMR data agree with the published data.¹⁷ The yield was estimated by ¹H NMR spectrum using 1,3,5-trimethoxybenzene as internal standard. ¹H NMR (300 MHz, C₆D₆): δ 7.51-6.97 (m, 5H, Ph-*H*), 3.60 (m, 2H, CH₂N), 3.43 (s, 2H, CH₂Ph), 1.70 (m, 2H, CH₂C=N), 1.20 (m, 4H, 2CH₂).

7-Membered heterocycle 2-benzyl-3,4,5,6-tetrahydro-2H-azepin 21'. The product described above was employed except that 0.0057 mmol (4.1 mg) of **8** and 0.08 mmol (14.9 mg) of 7-phenylhept-6-yn-1-amine **21** were used. The NMR data agree with the published data.¹⁷ The yield (15%) was estimated by ¹H NMR spectrum using 1,3,5-trimethoxybenzene as internal standard. ¹H NMR (300 MHz, C₆D₆): δ 7.3-6.9 (m, 5H, Ph-*H*), 3.55 (m, 2H, CH₂N), 3.50 (s, 2H, CH₂Ph), 2.00 (m, 2H, CH₂C=N), 1.39 (m, 4H, 2CH₂), 0.98 (m, 2H, CH₂).

Alleneamine 22' The procedure described above was employed except that 0.009 mmol (6.5 mg) of **8** and 0.139 mmol (13.5 mg) of alleneamine **22** were used. The NMR data agree with the published data.²⁰ The yield (98%) was estimated by ¹H NMR spectrum using 1,3,5-trimethoxybenzene as internal standard. ¹H NMR (300 MHz, C₆D₆): δ 3.52 (m, 2H, CH₂N), 1.77 (s, 3H, Me-H), 1.62 (m, 2H, CH₂C=N), 1.24 (m, 6H, 3CH₂).

Amine 34 The general hydroamination/reduction procedure was used to synthesize amine **34** from 1 mmol of 1-hexyne and 2,6-dimethylaniline. After reduction with LAH/THF and purification by flash chromatography (hexanes/diethyl ether), compound **34** was isolated as a yellow oil in 71% yield (146.4 mg). ¹H NMR (300 MHz, CDCl₃): δ 6.91 (d, J=7.2 Hz, 2H, Ph-H); 6.71 (t, J=7.2 Hz, 1H, Ph-H); 3.2 (m, 1H, NCH); 2.7 (b, 1H, NH); 2.2 (s, 6H, Ph-CH₃); 1.5 (m, 1H, CH₂); 1.28 to 1.32 (m, 5H, CH₂); 0.98 (d, J=6.3 Hz, 3H, CHCH₃); 0.84 (t, J=6.9 Hz, 3H, CH₂CH₃). ¹³C NMR (75 MHz, CDCl₃): δ 145.3, 128.99, 121.2, 52.5, 38.3, 28.8, 23.0, 21.5, 19.2, 14.2. IR (cm⁻¹): 3041, 3007, 1595, 1440. EIMS (*m/z*): 205 (M⁺, 15), 190 (7), 148 (100), 134 (7), 77. C₁₄H₂₃N calcd. C 81.95, H 11.22, N, 6.83. Found: C 82.17, H 11.34, N 6.77.

Amine 35²⁶ The general hydroamination/reduction procedure was used to synthesize amine **35** from 0.367 mmol of phenylacetylene and 2,6-dimethylaniline. After reduction with LAH/THF and purification by flash chromatography (hexanes/diethyl ether), compound **35** was isolated as a colorless oil in 61% yield (50 mg). ¹H NMR (300 MHz, CDCl₃): δ 7.3 (m, 2H, Ph-H), 7.28 (m, 3H, Ph-H), 6.96 (d, J=7.2 Hz, 2H, Ph-H), 6.8 (t, J=7.2 Hz, 1H, Ph-H), 3.26 (t, J=7.0 Hz, 2H, NCH₂), 3.05 (br, 1H, NH), 2.88 (t, J=7.0 Hz, 2H, Ph-CH₂), 2.14 (s, 6H, PhCH₃). ¹³C NMR (75 MHz, CDCl₃): δ 145.9, 139.5, 129.1, 128.8, 128.5, 126.4, 121.7, 49.4, 37.0, 18.4. IR (cm⁻¹): 3084, 3026, 1595, 1454. EIMS (*m/z*): 225 (M⁺, 50), 134 (100), 105, 91, 77.

Amine 36 The general hydroamination/reduction procedure was used to synthesize amine **36** from 0.459 mmol of cyclohexylacetylene and 2,6-dimethylaniline. After reduction with LAH/THF and purification by flash chromatography (hexanes/diethyl ether), compound **36** was isolated as a pale yellow oil in 44% yield (46.5 mg). ^1H NMR (300 MHz, CDCl_3): δ 6.95 (d, $J=7.2$ Hz, 2H, Ph-*H*), 6.77 (t, $J=7.2$ Hz, 1H, Ph-*H*), 3.15 (m, 1H, NCH), 2.95 (br, 1H, NH), 2.25 (s, 6H, PhCH₃), 1.65-2.0 (m, 5H, CH₂), 1.4 (m, 1H, CH₂), 1.0-1.35 (m, 5H, CH₂), 0.95 (d, $J=6.7$ Hz, 3H, CHCH₃). ^{13}C NMR (75 MHz, CDCl_3): δ 145.4, 128.9, 128.7, 120.8, 56.7, 44.2, 30.0, 28.4, 26.7, 26.6, 26.5, 19.1, 17.6. IR (cm^{-1}): 3041, 3007, 2962, 1595, 1475. EIMS (m/z): 231 (M^+ , 15), 148 (100). HRMS: calcd ($\text{C}_{16}\text{H}_{25}\text{N}$): 231.1987; Found: 231.1990.

Amine 37²⁷ The general hydroamination/reduction procedure was used to synthesize amine **37** from 1 mmol of 1-hexyne and benzhydrylamine. After reduction with LAH/THF and purification by flash chromatography (hexanes/diethyl ether), compound **7** was isolated as orange oil in 43% yield (98 mg). ^1H NMR (300 MHz, CDCl_3): δ 7.42 to 7.19 (m, 10H, Ph-*H*), 4.8 (s, 1H, Ph₂CH), 2.57 (t, $J=6.9$ Hz, 2H, NCH₂), 1.7 (br, 1H, NH), 1.65 to 1.5 (m, 2H, CH₂), 1.35 to 1.24 (m, 6H, CH₂), 0.88 (t, $J=6.7$ Hz, 3H, CH₂CH₃). ^{13}C NMR (75 MHz, CDCl_3): δ 144.3, 128.4, 127.3, 126.9, 67.7, 48.3, 31.8, 30.2, 27.0, 22.6, 14.0. IR (cm^{-1}): 3084, 3024, 2955, 1452. EIMS (m/z): 267 (M^+ , 20), 236 (5), 210 (20), 196 (15), 167 (100), 106 (5).

Amine 38 The general hydroamination/reduction procedure was used to synthesize amine **38** from 0.34 mmol of 3,3-dimethyl-1-butyne and benzhydrylamine. After reduction with LAH/THF and purification by flash chromatography (hexanes/diethyl ether), compound **38** was isolated as a pale yellow solid in 94% yield (85 mg). ^1H NMR (300 MHz, CDCl_3): δ 7.40 (d, $J=7.0$ Hz, 4H, Ph-*H*), 7.30 (m, 4H, Ph-*H*), 7.27 (m, 2H, Ph-*H*), 4.83 (s, 1H, Ph₂CH), 2.60 (m, 2H, NCH₂), 1.5 (m, 2H, CH₂), 1.4 (b,

1H, NH), 0.88 (s, 9H, *t*BuCH₃). ¹³C NMR (75 MHz, CDCl₃): δ 144.4, 128.4, 127.2, 126.9, 67.9, 44.6, 44.4, 29.9, 29.6. IR (cm⁻¹): 3084, 3026, 2967, 1454. EIMS (*m/z*): 267 (M⁺, 25), 252 (5), 236 (10), 225 (10), 167 (100), 152 (15), 106, 77. C₁₉H₂₅N: calcd: C 85.39, H 9.36, N 5.24; Found: C 85.21, H 9.53, N 5.28.

Amine 39²⁸ The general hydroamination/reduction procedure was used to synthesize amine **39** from 0.35 mmol of phenylacetylene and benzhydramine. After reduction with LAH/THF and purification by flash chromatography (hexanes/diethyl ether), compound **39** was isolated as yellow oil in 51% yield (51 mg). ¹H NMR (300 MHz, CDCl₃): δ 7.39-7.2 (m, 15H, Ph-*H*), 4.85 (s, 1H, Ph₂CH), 2.86 (s, 4H, CH₂), 1.17 (s, 1H, NH). ¹³C NMR (75 MHz, CDCl₃): δ 144.1, 140.1, 128.7, 128.4, 127.2, 126.9, 126.1, 67.3, 49.3, 36.5. IR (cm⁻¹): 3084, 3024, 1493, 1452. EIMS (*m/z*): 287 (M⁺, 10), 196 (40), 167 (100), 152, 105, 91.

Amine 40 The general hydroamination/reduction procedure was used to synthesize amine **40** from 0.574 mmol of cyclohexylacetylene and benzhydramine. After reduction with LAH/THF and purification by flash chromatography (hexanes/diethyl ether), compound **40** was isolated as colorless oil in 89% yield (150 mg). ¹H NMR (300 MHz, CDCl₃): δ 7.37 to 7.14 (m, 10H, Ph-*H*), 4.76 (s, 1H, Ph₂CH), 2.54 (t, J=7.2 Hz, 2H, NCH₂), 1.62 (m, 5H, CH+CH₂), 1.39 (m, 3H, NH+CH₂), 1.23 to 1.10 (m, 4H, CH₂), 0.88 to 0.81 (m, 2H, CH₂). ¹³C NMR (75 MHz, CDCl₃): δ 144.4, 128.4, 127.2, 126.8, 67.7, 45.9, 38.0, 35.6, 33.4, 26.6, 26.3. IR (cm⁻¹): 3084, 3024, 2918, 1599. EIMS (*m/z*): 293 (M⁺, 20), 262 (5), 216 (20), 196 (10), 182 (30), 167 (100), 152, 91, 55. HRMS: calcd (C₂₁H₂₇N): 293.2144; Found: 293.2143.

Amine 44 The general hydroamination/reduction procedure was used to synthesize amine **44** from 1.069 mmol of phenylmethylacetylene and 2,6-dimethylaniline. After reduction with LAH/THF and purification by flash chromatography (hexanes/diethyl

ether), compound **44** was isolated as yellow oil in 71% yield (180 mg). ^1H NMR (300 MHz, CDCl_3): δ 7.33 to 6.86 (m, 8H, Ph-*H*), 3.6 (m, 1H, NCH), 3.0 (dd, 2H, PhCH₂), 2.65 (m, 1H, NH), 2.01 (s, 6H, PhCH₃), 1.11 (d, $J=6.0$ Hz, 3H, CHCH₃). ^{13}C NMR (75 MHz, CDCl_3): δ 144.8, 139.4, 129.4, 129.2, 128.9, 128.2, 126.1, 121.4, 54.0, 44.4, 20.8, 19.0. IR (cm^{-1}): 3084, 3026, 1595, 1494. EIMS (m/z): 239 (M^+ , 50), 224 (10), 208 (5), 148 (100), 105, 91, 77. HRMS: calcd ($\text{C}_{17}\text{H}_{21}\text{N}$): 239.1674; Found: 239.1675.

3.7 References

1. T. E. Muller and M. Beller, *Chem. Rev.*, **1998**, *98*, 675-703.
2. D. Steinborn and R. Taube, *Z. Chem.*, **1986**, *26*, 349.
3. a) I. Bytshkov, S. Doye, *Eur. J. Org. Chem.*, **2003**, 935-946; b) F. Pohlki, S. Doye, *Chem. Soc. Rev.*, **2003**, *32*, 104-114.
4. P. W. Roesky, T. E. Muller, *Angew. Chem., Int. Ed.*, **2003**, *42*, 2708-2710.
5. a) P.J. Walsh, A. M. Baranger and R. G. Bergman, *J. Am. Chem. Soc.*, **1992**, *114*, 1708-1719; b) P. J. Walsh, F. J. Hollander and R. G. Bergman, *Organometallics*, **1993**, *12*, 3705-3723.
6. a) P. L. McGrane, M. Jensen and T. Livinghouse, *J. Am. Chem. Soc.*, **1992**, *114*, 5459-5460; b) P. L. McGrane and T. Livinghouse, *J. Am. Chem. Soc.*, **1993**, *115*, 11485-11489.
7. P. L. McGrane and T. Livinghouse, *J. Org. Chem.*, **1992**, *57*, 1323-1324.
8. E. Haak, I. Bytshkov and S. Doye, *Angew. Chem., Int. Ed.*, **1999**, *38*, 3389-3391.
9. I. Bytschkov and S. Doye, *Eur. J. Org. Chem.*, **2001**, 4411-4418.
10. F. Pohlki and S. Doye, *Angew. Chem., Int. Ed.*, **2001**, *40*, 2305-2308.
11. A. Heutling and S. Doye, *J. Org. Chem.*, **2002**, *67*, 1961-1964.
12. I. Bytschkov and S. Doye, *Tetrahedron Lett.*, **2002**, *43*, 3715-3718.

13. J. S. Johnson and R. G. Bergman, *J. Am. Chem. Soc.*, **2001**, *123*, 2923-2924.
14. F. Pohlki, A. Heutling, I. Bytschkov, T. Hotopp and S. Doye, *Synlett*, **2002**, 799.
15. A. Tillack, I. Garcia Castro, C. G. Hartung, M. Beller, *Angew. Chem., Int. Ed.*, **2002**, *41*, 2541-2543.
16. Y. Shi, J. T. Ciszewski and A. L. Odom, *Organometallics*, **2001**, *20*, 3967-3969.
17. C. Cao, J. T. Ciszewski and A. L. Odom, *Organometallics*, **2001**, *20*, 5011-5013.
18. Y. Shi, C. Hall, J. T. Ciszewski, C. Cao and A. L. Odom, *Chem. Comm.*, **2003**, 586-587.
19. T. G. Ong, G. P. A. Yap and D. S. Richeson, *Organometallics*, **2002**, *21*, 2839-2841.
20. L. Ackermann and R. G. Bergman, *Org. Lett.*, **2002**, *4*, 1475-1478.
21. E. Haak, I. Bytschkov and S. Doye, *Eur. J. Org. Chem.*, **2002**, 457-463.
22. H. Siebeneicher and S. Doye, *Eur. J. Org. Chem.*, **2002**, 1213.
23. E. Haak, H. Siebeneicher and S. Doye, *Org. Lett.*, **2000**, *2*, 1935-1937.
24. I. G. Castro, A. Tillack, C. G. Hartung and M. Beller, *Tetrahedron. Lett.*, **2003**, *44*, 3217-3221.
25. Y. Li and T. J. Marks, *J. Am. Chem. Soc.*, **1996**, *118*, 9295-9306.
26. H. Mammen, M. Wind, H. Luthardt, C. Fieseler, W. Steinke, U. Thust, K. Naumann, W. Kramer, E. Schiewarld, *Fungicide for Controlling Phytophthora infestans.*, Ger (East) **1985**.
27. P. V. Ramachandran, M. P. Jennings and H. C. Brown, *Org. Lett.*, **1999**, *1*, 1395-1397.
28. C.H. Yoon, A. Nagle, C. Chen, D. Gandhi, K.W. Jung, *Org. Lett.*, **2003**, *5*, 2259-2262.

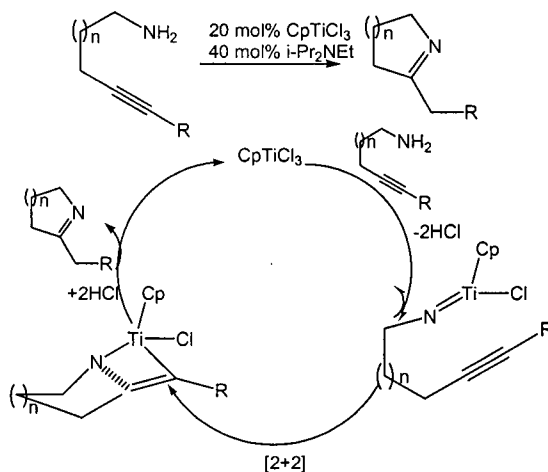
Chapter 4 Mechanistic Investigations

4.1 Introduction

In addition to the first report of an early transition metal complex (zirconocene bisamide) that could be used for catalytic hydroamination, Bergman *et al.* also reported extensive mechanistic investigations of this process.¹ These investigations provided the basis for subsequent investigations into the titanium catalyzed processes.

For the CpTiCl_3 -catalyzed intramolecular hydroamination of aminoalkynes, Livinghouse proposed that the active catalyst is in fact the titanium imido monomers which were generated from CpTiCl_3 and the amine part of the aminoalkyne substrates by losing two equivalents of HCl .² The *in situ* formed imido complex then undergoes an intramolecular [2+2] cycloaddition with the carbon carbon triple bonds to form titanazacyclobutene, which can be protonated by HCl to give the anticipated cycloaddition imine product and regenerate the CpTiCl_3 complex to continue the catalytic cycle (Scheme 4-1).

Scheme 4-1

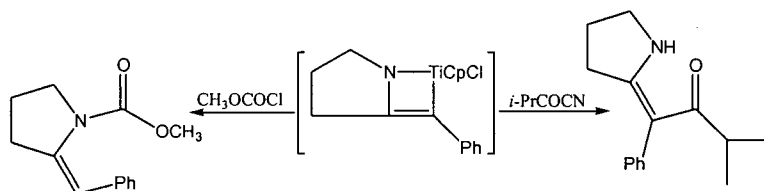


The present ring-size dependence of cyclization rates for the intramolecular hydroamination of aminoalkynes is $5 > 6 \gg 7$, consistent with classical stereoelectronically controlled cyclization processes. This can be explained by a preference for a

pseudo-chair seven-membered transition state, as T. J. Marks proposed for the lanthanide-catalyzed hydroamination of aminoalkynes.³

Even though attempts to isolate and characterize bicyclic titanaazacyclobutenes were frustrated by the high reactivity of these species, the formation of these intermediates in stoichiometric cyclization was achieved.² These complexes could then be selectively functionalized on carbon or nitrogen by the use of appropriate carbon centered electrophiles.² For example, treatment of titanaazacyclobutene with acyl cyanides or nitriles affords exclusive functionalization at carbon, while acylation of azametallabutene with acyl chlorides led to selective functionalization at nitrogen (Scheme 4-2).

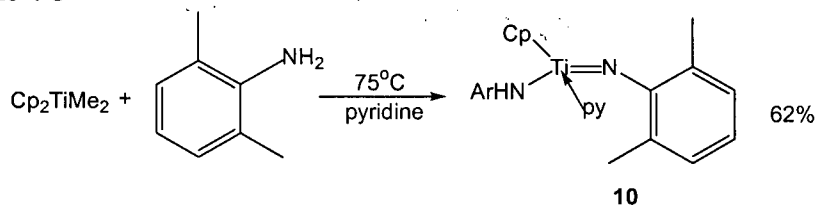
Scheme 4-2



Since Doye *et al.* discovered that Cp_2TiMe_2 is an efficient catalyst for intermolecular hydroamination of alkynes,⁴ both the Doye and Bergman groups have investigated the intermolecular hydroamination mechanism of this complex.

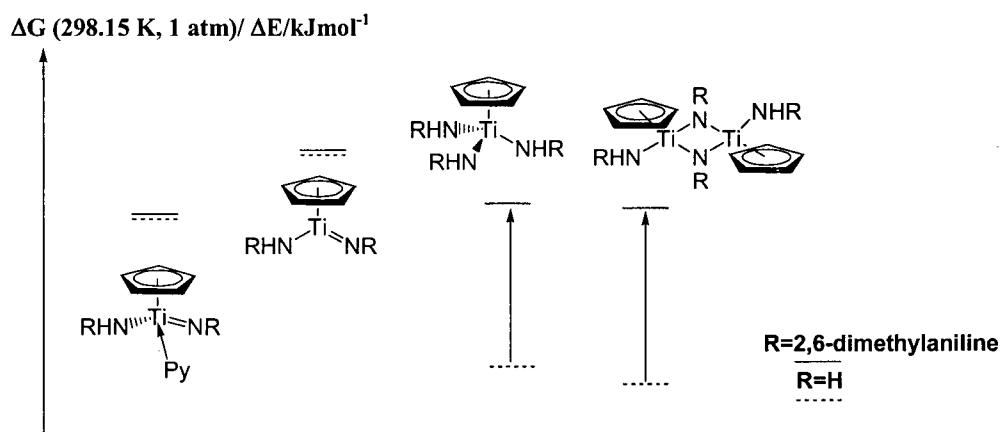
A mechanistic investigation from the Bergman group established that an unexpected ligand exchange reaction of Cp_2TiMe_2 **1** with amine results in the loss of a cyclopentadienyl ligand to generate a highly active monocyclopentadienyl titanium imido complex **10**.⁵ After heating a mixture of Cp_2TiMe_2 , 2,6-dimethylaniline and pyridine to 75°C for 24 h, the corresponding pyridine stabilized intermediate was isolated in 62% yield (Scheme 4-3). The same mono-Cp complex is assumed to be formed in Cp_2TiMe_2 -catalyzed hydroamination as free CpH was observed under catalytic conditions.

Scheme 4-3



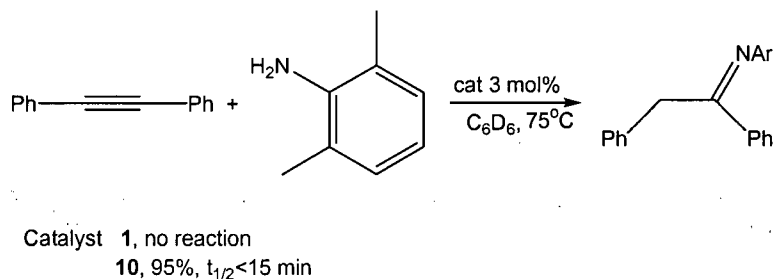
To further understand the hydroamination mechanism, Bergman *et al.* studied the relative energies of potential catalyst resting states via DFT calculations.⁶ The preference for pyridine ligation in the presence of 2,6-dimethylaniline toward the formation of species such as $\text{CpTi}(\text{NHR})_3$, dinuclear complexes and free pyridine is due to steric constraints, as shown by the DFT calculations. Although the computed strength of pyridine coordination to the simplified imido complex ($\text{R}=\text{H}$) is weaker than the driving force for formation of the trisamide and imido dimer, the steric congestion of three 2,6-dimethylaniline ligands at the metal center inverts the relative stabilities (Figure 4-1).⁶

Figure 4-1 Influence of the substituents on the relative stabilities of CpTi complexes



The isolated imido complex **10** shows higher hydroamination activity than that of Cp_2TiMe_2 . As can be seen from Scheme 4-4, the hydroamination of diphenylacetylene with 2,6-dimethylaniline can proceed at 75°C to give 95% yield when using the monocyclopentadienyl titanium imido complex as catalyst, while no reaction happens when Cp_2TiMe_2 is employed.⁵

Scheme 4-4



Kinetic investigations in the Doye group of the reaction between an internal alkyne and 4-methylaniline shows that the rate of hydroamination depends on the concentration of Cp_2TiMe_2 and 4-methylaniline.⁷ They proposed the existence of preequilibria that interconvert the active imido species with both titanium amides and dinuclear titanium complexes, which are responsible for the low reaction rates of sterically less hindered amines. This interpretation is strongly supported by the DFT calculation of the steric influence of amine substituents for the stabilities of imido, imido dimer and trisamide titanium complexes reported by Bergman *et al.*⁶

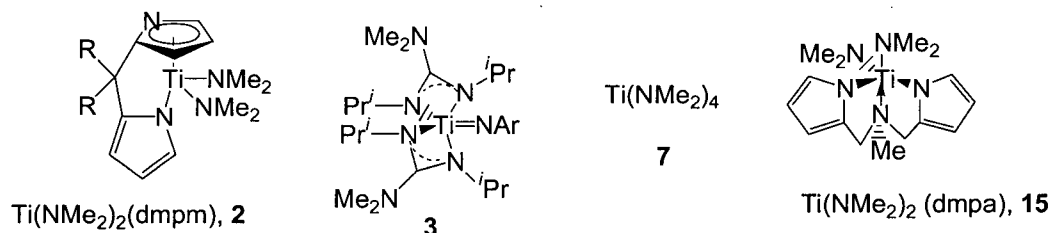
Titanaazacyclobutenes are proposed as intermediates in the catalytic cycle, analogous to the $\text{Cp}_2\text{Zr}(\text{NHR})_2$ -catalyzed hydroamination of alkynes¹ or the stoichiometric reaction of allenes with zirconium and titanium pyridine imido derivatives.⁸ The proposed catalytic cycle is outlined in Scheme 4-5. The hydroamination of alkyne takes place by a reversible [2+2] cycloaddition with the imido complex followed by amine protonation of the formed titanaazacyclobutene and a final α -elimination of enamide amide complex to give the corresponding enamine and regenerate the imido complex.

So far there are no reports regarding the mechanism of hydroamination reactions catalyzed by 2, 3, 7 or 15 (Figure 4-2).⁹ Complex 7 has been shown to produce isolable bridging imido complexes on reaction with primary amines.¹⁰ Excess of

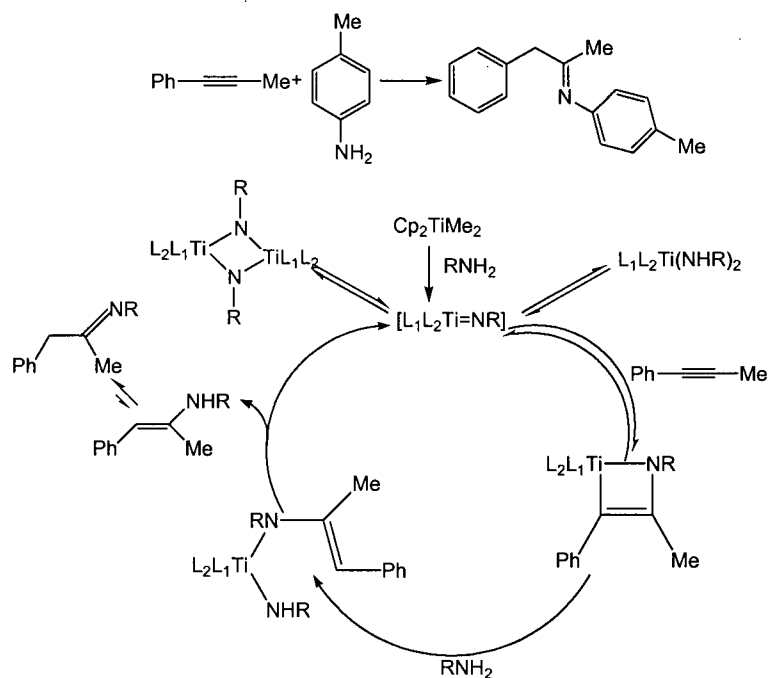
amine present under catalytic conditions may support monomeric species for reaction with alkynes.

Figure 4-2

Non-Cp based Ti complexes



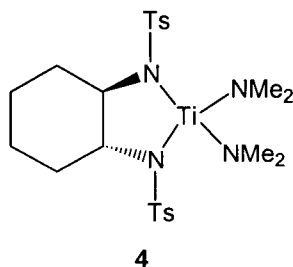
Scheme 4-5



Very recently, Bergman *et al.* reported the mechanistic investigations of the hydroamination of allene amine catalyzed by **4** and analogues (Figure 4-3).¹¹ The ¹H NMR spectrum of the stoichiometric reaction between the bis(sulfonamide) titanium complex and 2,6-dimethylaniline reveals the formation of the imido complex accompanied by liberation of amine. Isolated pyridine-stabilized titanium imido

complex showed comparable activity to that of observed by using the bis(sulfonamide) precatalyst.

Figure 4-3 Bis(sulfonamide) titanium complex



4.2 Hydroamination Mechanistic Investigations of Titanium Amidate Complexes as Hydroamination Catalysts

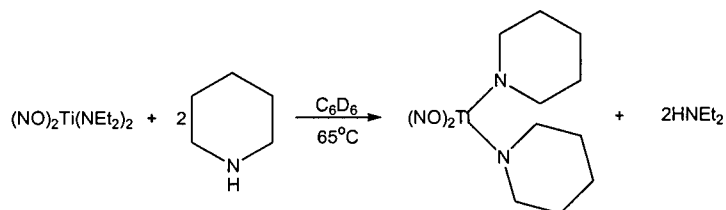
4.2.1 Proposed Mechanism

As shown in Chapter 3, titanium amidate **8** is an efficient catalyst for the hydroamination of terminal alkynes with bulky amines. When monitoring this reaction by ^1H NMR spectroscopy, the spectrum only shows starting materials, products (imine), free diethyl amine (and oligomers of alkyne in the case of phenylacetylene) under most catalytic conditions. There is no evidence of free ligand formation during the reaction. This is easily monitored by ^{19}F NMR spectroscopy due to the diagnostic shifts of the *ortho*-fluorines between the bound and free ligand. Hydroamination of terminal alkynes with less bulky primary amines such as aniline and benzyl amine always gives low yields. Although rigorous kinetic experiments were not performed, it was noted that higher catalyst loading increased the rate of product formation.

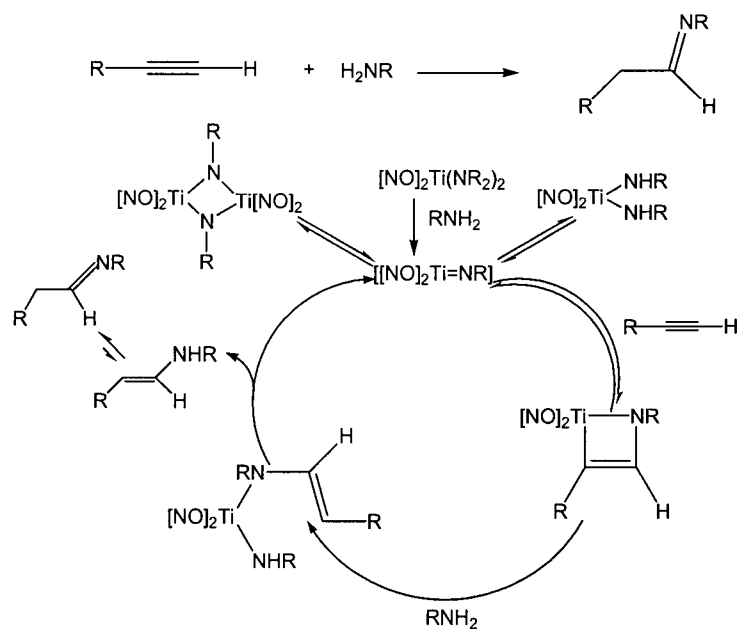
All reported titanium complex-catalyzed hydroaminations involve primary amines, thereby suggesting a titanium imido complex as the catalytic species. To verify this point, we carried out the titanium amidate catalyzed hydroamination reaction of a

terminal alkyne with a secondary amine, which would be incapable of forming an imido intermediate. The reaction of 1-hexyne with piperidine was carried out on NMR tube scale using 1,3,5-trimethoxybenzene as internal standard. The ^1H NMR spectrum revealed the formation of free diethyl amine, but no hydroamination product was detected even after heating at 65°C for several days. A stoichiometric reaction between **8** and pyridine was then investigated on NMR tube scale. The ^1H NMR spectrum showed that the ratio of formed amine to consumed **8** was 2:1, indicating the substitution of the amido groups by secondary amine to form a new bisamide complex (Scheme 4-6).

Scheme 4-6



Scheme 4-7



Based on literature reports,^{1,2,5,11} and our results of hydroamination reactions catalyzed by titanium amidates **8** and **9**, we proposed the hydroamination reaction

mechanism as shown in Scheme 4-7. In the presence of primary amine, the amidate complex will generate the titanium imido complex, which will be in equilibrium with its dimer and bisamide titanium complex. The coordinatively unsaturated imido complex can then coordinate the electron rich terminal alkyne regioselectively. This regioselective coordination is usually sterically controlled where the steric bulk of the imido substituent dictates anti-Markovnikov selectivity. This species then undergoes cycloaddition to form titanaazacyclobutene. Protonation at the Ti-C bond by primary amine gives an enamide amide complex, which undergoes α -elimination to give the hydroamination product and regenerate the catalytically active imido complex.

4.2.2 Reaction between Titanium Complex 8 or 9 with Hindered Primary Amines

In an attempt to verify the formation of catalytically active titanium imido complexes, stoichiometric reactions of bulky aryl and alkyl amines with **8** or **9** were carried out on NMR tube scale using 1,3,5-trimethoxybenzene as internal standard. All reactions were performed at ambient temperature.

For the reaction of 2,6-dimethylaniline with **8** (Scheme 4-8), the ^1H NMR spectrum is quite informative (Figure 4-4). Multiplets at 2.47 and 0.98 ppm with 2:3 ratios show the formation of free diethyl amine. A second set of multiplets of comparable ratio at 3.55 and 2.90 ppm are interpreted to be diethyl amines dynamically coordinated to the titanium center. The methyl signal of 2,6-dimethylaniline shifts from δ 1.90 ppm in free dimethylaniline to δ 2.89 ppm, which indicates the formation of titanium imido bond. This is comparable to that of other 2,6-dimethyl phenyl titanium imido complexes previously reported by Bergman (2.30 ppm)³ and Richeson¹² (*vide infra*). Furthermore, the ratio of integration of the *t*-butyl singlet at 1.13 ppm to that of the methyl singlet of 2,6-dimethylaniline at 2.89 ppm is consistent with two amidate ligands for per imido species formed.

Scheme 4-8

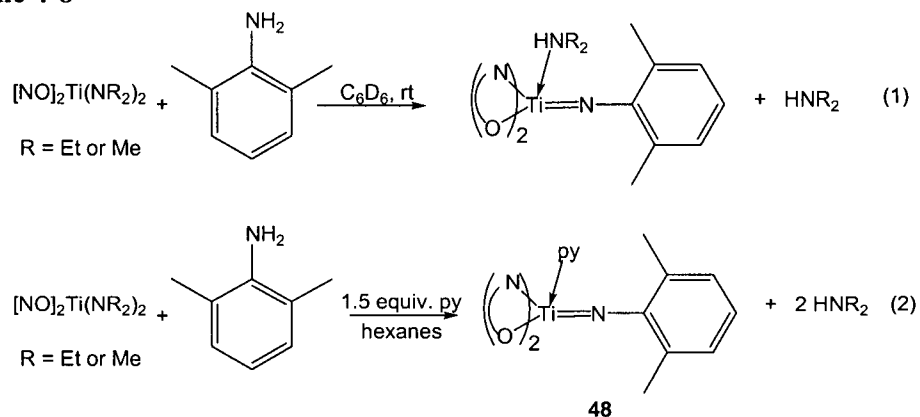
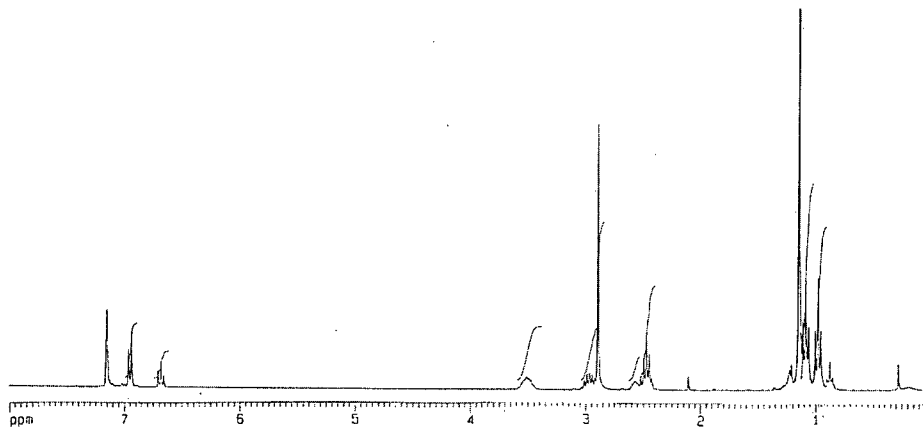


Figure 4-4

¹H NMR Spectrum of the Stoichiometric Reaction between 8 and 2,6-Dimethylaniline



Similar results can be obtained from the reaction of 2,6-dimethylaniline with 9, in which both the ¹H NMR and ¹³C NMR spectra indicate the presence of the desired imido complex. The ¹³C NMR spectrum is particularly diagnostic with the C attached to the imido N being at δ 159.9 ppm in comparison with δ 143.5 ppm in free 2,6-dimethylaniline. The reaction reaches completion within minutes at room temperature. In both cases, the yield of imido complex is above 85% by using an internal standard. The pyridine trapped imido complex **48** can be isolated as dark red microcrystals in 60% yield by carrying out the reaction in presence of pyridine. This compound has been fully characterized by ¹H, ¹³C, and ¹⁹F NMR spectroscopy as well

as LRMS and HRMS. Mass spectrometry was used to confirm the formation of monomeric species in which both LRMS and HRMS gave molecular ion peak at 699, consistent with the molecular weight of pyridine-trapped imido complex **48** losing the coordinated pyridine.

Figure 4-5 Pyridine stabilized Ti imido complex

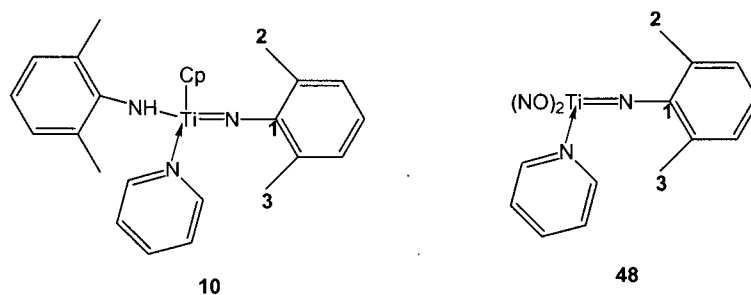


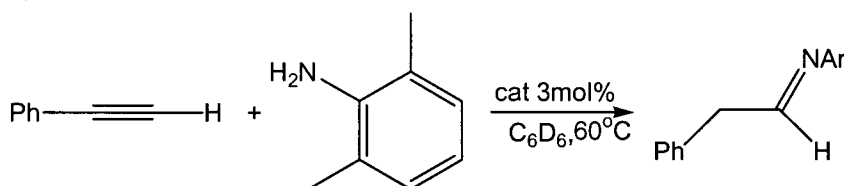
Table 4-1 Summary of NMR spectroscopic data for 10 and 48

	10	48
¹H NMR	8.73 (d, 2H, Py-H) 6.69 (t, 1H, Py-H) 6.32 (t, 2H, Py-H) 2.30 (s, 6H, Me-H)	9.36 (d, 2H, Py-H) 6.80 (t, 1H, Py-H) 6.60 (m, 3H, Py-H+Ph-H) 2.83 (s, 6H, Me-H)
¹³C NMR		
1	159.6	159.9
2	20.5	19.34

In order to verify that the isolated titanium imido complex **48** is a competent catalyst, the hydroamination reaction of phenylacetylene with 2,6-dimethylaniline was carried out using similar reaction conditions with complex **9** and **48** as catalyst, respectively (Scheme 4-9). The reaction catalyzed by imido complex was observed to proceed with a $t_{1/2} < 3$ h, while the reaction catalyzed by **9** had a $t_{1/2}$ of 4.5 h. These results ensure that the imido complex can indeed be used as an efficient catalyst. There is a small change observed in reactivity between the two species; however this change is not as dramatic as the results obtained from a similar investigation with the Bergman system (**10**) when contrasted with the Doye system (**1**) (Scheme 4-4). This suggests the ready formation of the bis(amidate) titanium imido complex from

complex **8** or **9** in the presence of bulky primary amine. Experimentally, this is consistent with the observation that the formation of the desired titanium imido species was immediate at room temperature, as was observed during its preparation, while higher temperature and longer reaction times were necessary for the formation of the imido species in the Bergman case. Also, both amidate ligands remain coordinated as shown by ^1H NMR spectroscopy. The strongly electron withdrawing amidate ligands generate a highly electrophilic titanium metal center that results in good catalyst activity.

Scheme 4-9



Catalyst **3**, $([\text{NO}]_2\text{Ti}(\text{NMe}_2)_2)$, 50%, 4.5 h
48, $([\text{NO}]_2\text{TiNCHPh}_2(\text{py}))$, 70%, 3 h

For the reaction of benzhydryl amine with **9** (Scheme 4-10), the NMR tube scale reaction shows the formation of dimethyl amine, both free and coordinated to the titanium metal center with the appearance of two broad peaks between 2.60 and 2.20 ppm (HNMe_2). After removing the solvent and redissolving in C_6D_6 , the ^1H NMR spectrum of the residue shows a doublet at 2.37 ppm with 6:1 ratio to the singlet at 5.75 ppm, the methine proton of the benzhydryl amine. These diagnostic signals indicate the presence of the desired titanium imido complex coordinated by a molecule of dimethyl amine. The NMR yield of the formed imido complex is over 90% based on internal standard. Again, the imido complex of benzhydryl amine can be trapped as a pyridine adduct. Yellow crystals of **49** were obtained in 40% yield by cooling a pentane solution of the crude product to -35°C . This complex has been

characterized by ^1H , ^{13}C , and ^{19}F NMR spectroscopy as well as EIMS and X-ray structure which was shown in Figure 4-6.¹³

Scheme 4-10

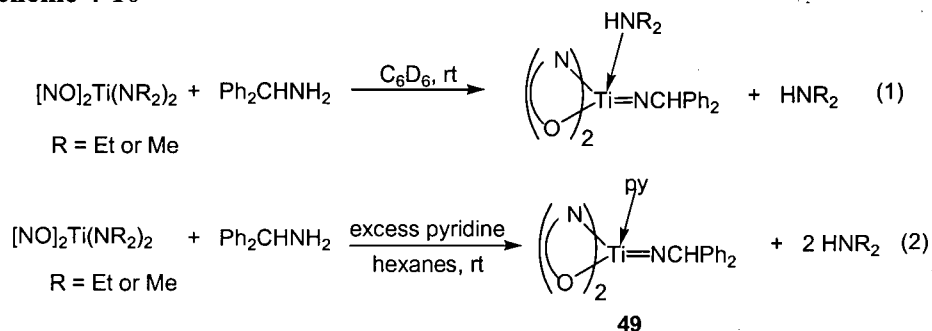
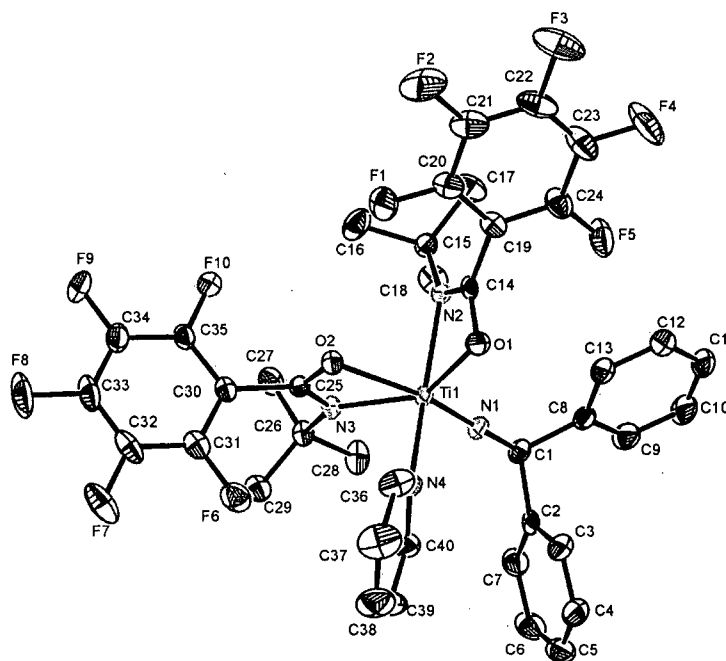


Figure 4-6 ORTEP plot of the structure of Ti imido complex 49



The stoichiometric reaction of **9** and *t*-butyl amine (Scheme 4-11) on an NMR tube scale also shows the formation of amine, both free and coordinated to the titanium center. Yellow crystals of **50** were obtained by cooling the crude product solution to -35°C (Scheme 4-11, eq 1). The pyridine trapped imido complex **51** was obtained by carrying out the reaction in the presence of excess pyridine, to afford yellow

crystalline solids after cooling the crude solution to -35°C (Scheme 4-11, eq 2). Both compounds were characterized by ^1H , ^{13}C , and ^{19}F NMR spectroscopy and EIMS spectrometry. HRMS of **50** shows molecular weight corresponding to **50** losing the coordinating dimethyl amine, similar to the case of **48**.

Scheme 4-11

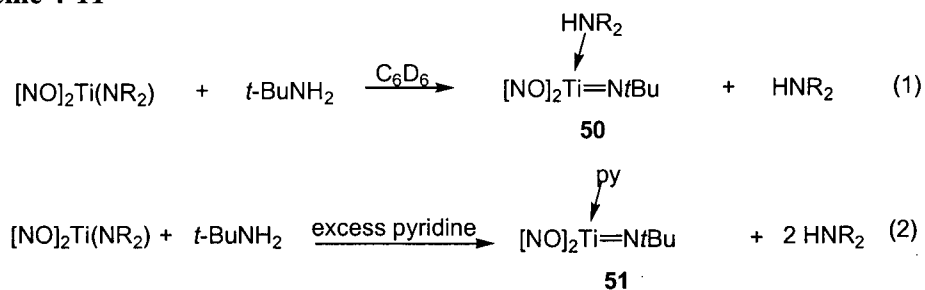


Figure 4-7 Structures of **48**, **49**, **50**, **51**

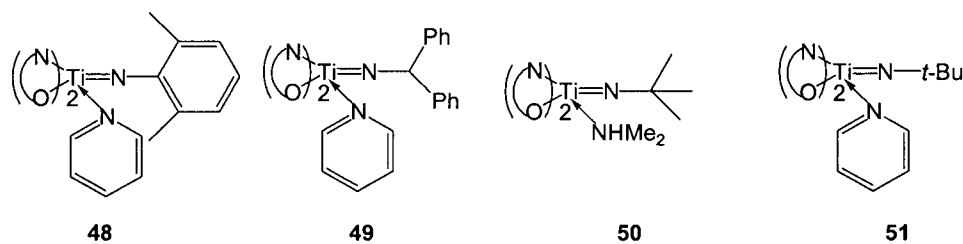


Table 4-2 Summary of NMR Spectroscopic data of **48**, **49**, **50**, **51**

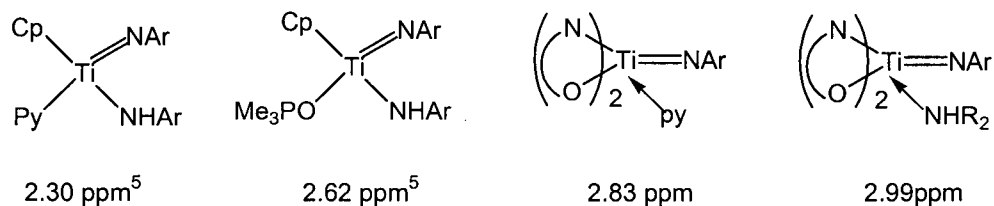
NMR	48	49	50	51
^1H	9.30 (d, 2H) 6.86 (d, 2H) 6.80 (t, 1H) 6.60 (m, 3H) 2.83 (s, 6H) 1.13 (s, 18H)	8.95 (d, 2H) 7.55 (d, 2H) 7.13 (m, 3H) 6.99 (m, 3H) 6.80 (t, 1H) 6.53 (t, 2H) 5.77 (s, 1H) 1.24 (s, 18H)	2.65(s, 6H) 1.26 (s, 18H) 1.22 (s, 9H)	9.30 (br, 2H) 6.90 (m, 1H) 6.68 (t, 2H) 1.20 (s, 18H) 1.18 (s, 9H)
^{19}F	-139.1 -153.4 -161.3	-139.8 -153.9 -161.3	-139.6 -153.8 -161.3	-139.6 -154.2 -161.3

The impact of various ancillary ligands can be evaluated by comparing the methyl chemical shift of the 2,6-dimethylpyridine derived imido complexes (Figure 4-8). The

electron withdrawing N, O ligand causes a significant downfield shift in this diagnostic signal.

Figure 4-8

Chemical shift for methyl group of the 2,6-dimethylaniline moiety (imido)



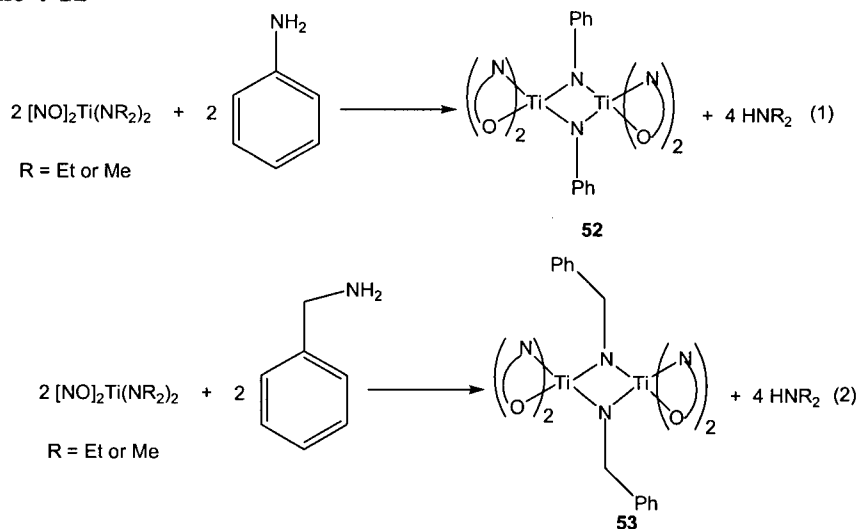
4.2.3 Reaction of Titanium Complex 8 or 9 with Less Sterically Hindered Amines

From the preliminary results in Chapter 3, it is clearly indicated that less sterically hindered primary amines (such as aniline and benzyl amine) always give low yields in the intermolecular hydroamination with terminal alkynes. This is consistent with the result from Doye's group when they use Cp_2TiMe_2 as catalyst.¹⁴ This is due to the preequilibrium between the catalytically active imido complex, the imido complex dimer and the bisamide complex.⁷ It is reasonable to propose that this equilibrium is also present in the titanium amidate **8** catalyzed hydroamination reactions.

The proposed mechanism based on qualitative observations was further probed using a series of stoichiometric reactions with non-bulky amines. First the stoichiometric reaction of **8** with aniline was carried out on an NMR tube scale using 1,3,5-trimethoxybenzene as internal standard in C_6D_6 . Within 30 minutes, insoluble red powder had precipitated from the solution. The ^1H NMR spectrum shows multiplets at 2.47 and 0.98 ppm with 2:3 ratio, consistent with the formation of free diethyl amine. By using the internal standard, the ratio of formed amine to the reacted titanium complex was established as being 2:1. This suggests that all reacted titanium complex gave two equivalents of free amine and insoluble red precipitate.

In attempt to characterize the identity of this precipitate, a larger scale reaction of aniline with **9** was carried out in hexanes (Scheme 4-12, eq 1). Filtration of the obtained orange slurry gave a red powdery solid, **52**. The mass spectrum of the powder gives a clear molecular ion peak at 1342 m/z , which is consistent with that of the titanium imido complex dimer.

Scheme 4-12



These results give support for the formation of the desired imido complex that quickly forms and the undesired imido dimer in the presence of less bulky amines, as previously proposed by Doye (Scheme 4-12). Furthermore, a comparable zirconium analogue has been structurally characterized and was described as an insoluble compound by Bergman *et al.*¹⁵

A further investigation was done with the less sterically hindered alkylamine—benzyl amine, which had been noted to give low yields in hydroamination reactions catalyzed by the titanium amidate complex. The stoichiometric reaction of **9** with benzyl amine gave a qualitatively similar result, although here the formed precipitate is a yellow powder. The ratio of formed amine to the consumed titanium amidate complex was 2:1 as determined using an internal standard. Further characterization of the yellow powder **53** was attempted using mass spectrometry. In this case the

expected molecular ion peak (1370 m/z) was missing, however an ion peak (1103 m/z) corresponding to the fragment due to lose of one amidate ligand was detected. This mass spectrometric fragmentation pattern has been consistently observed in the analysis of other amidate complexes.¹⁶

Further attempts to obtain NMR spectroscopic data for both titanium imido bridging dimers were unsuccessful due to their very low solubility.

4.2.4 Cycloaddition of Titanium Imido Complexes to Alkynes

Since the first report of structurally characterized titanium imido complexes in 1990, the titanium imido literature appears to be very polarized. Many examples have been isolated but are characterized as unreactive, or highly reactive species that can be generated *in situ*, but are rarely isolable.¹⁷ The later complexes demonstrate high chemical reactivity such as C-H bond activation and N-C bond-forming reactions with unsaturated substrates.^{12,18}

For the hydroamination reaction catalyzed by titanium amidate complexes **8** or **9**, the observed titanium imido species are proposed to react via a cycloaddition type reaction to form a titanaazacyclobutene. The regioselectivity observed in different reactions originates from this key step. In order to get more knowledge of this step, efforts have been made to isolate the metallacyclobutene intermediate. Stoichiometric reactions between the imido complex generated from **8** or **9** and terminal alkynes resulted in solutions with a deeper color. However, the resultant complex ¹H NMR spectra were not helpful in yielding further information regarding the progress of the reaction. Efforts to obtain crystals from the reaction mixture were unsuccessful.

4.3 Conclusion

Based on the stoichiometric reactions of bulky and less bulky primary amines with **8** or **9**, experimental results were obtained to support the proposed mechanism of titanium amidate catalyzed hydroamination as shown in Scheme 4-7.

The titanium amidate complexes react with primary amines to give the corresponding imido complexes, which have been observed spectroscopically and presumably undergo a subsequent cycloaddition reaction with the alkynes. The formed azametallacyclobutene affords hydroamination products upon protonolysis and regenerates the catalytically active imido species. The poor reactivity with less sterically hindered primary amine can be explained by the formation of insoluble imido bridging dimers that are not catalytically active.

It is very interesting to note that titanium amidate complexes **8** and **9** are active hydroamination catalysts for terminal alkynes, while limited activity was observed in the case of internal alkynes which can be efficiently catalyzed by Cp_2TiMe_2 . Even though the reaction that was carried out at a comparable high temperature and long time (90°C , 72 h), no hydroamination products were detected. Since the mechanistic investigation indicates that the titanium imido complexes are the active species for both precatalysts, the different ancillary ligands are responsible for the different observed activity.

4.4 Experimental.

Reaction of 2,6-dimethyl aniline with **9**

NMR scale: A vial was charged with 14.1 mg (0.0211 mmol) of **9** and 2.8 mg (0.0167 mmol) of 1,3,5-trimethoxybenzene dissolved in C_6D_6 . 2.6 mg (0.0215 mmol) of 2,6-dimethyl aniline was added by pipette. The mixture was then transferred to an

NMR tube. A ^1H NMR spectrum was obtained 1 h after the sample was prepared. The yield of the titanium imido complex was over 85% based on the internal standard.

Py-trapped titanium imido complex 48: A vial was charged with 67.0 mg (0.100 mmol) of **9** dissolved in hexanes. 12.3 mg (0.102 mmol) of 2,6-dimethylaniline and 16.4 mg (0.208 mmol) of pyridine were added by pipette. The mixture was then transferred to a Schlenk tube charged with a stir bar and stirred overnight at room temperature. The solvent was removed under vacuum, and the resulting dark orange residue was dissolved in pentane. Dark red microcrystalline solid was obtained in 60% yield (46.0 mg) after cooling the pentane solution to -35°C . ^1H NMR (300 MHz, C_6D_6): δ 9.30 (d, 2H, Py-*H*), 6.86 (d, 2H, Ph-*H*), 6.80 (t, 1H, Py-*H*), 6.60 (m, 3H, 2 Py-*H* + 1Ph-*H*), 2.83 (s, 6H, Ph- CH_3), 1.13 (s, 18H, CH_3). ^{13}C NMR (75 MHz, C_6D_6): δ 159.9, 159.0, 148.6, 138.7, 134.6, 129.3, 127.3, 125.7, 124.5, 121.3, 53.3, 31.9, 30.6, 28.5, 23.0, 19.3, 14.2 (missing C signals are due to the weak multiplets for C that are coupled with F and overlapped with solvent peaks). ^{19}F NMR (C_6D_6): δ -139.1 (br, 2F), -153.4 (t, 1F), -161.3 (m, 2F). EIMS (m/z): 779 (M^+ , 5), 724 (20), 699 (40), 450, 252, 195, 120, 91, 57 (100). EA for $\text{C}_{35}\text{H}_{32}\text{N}_4\text{O}_2\text{F}_{10}\text{Ti}$ Calcd: C 54.00, H 4.14, N 7.20. Found: C 52.71, H 4.33, N 7.09. HRMS for $\text{C}_{30}\text{H}_{27}\text{N}_3\text{O}_2\text{F}_{10}\text{Ti}$ (M^+ - Pyridine) Calcd.: 699.1423; Found: 699.1421.

Reaction of benzhydryl amine with 9

NMR scale: A vial was charged with 13.5 mg (0.0202 mmol) of **9** and 1.9 mg (0.0113 mmol) of 1,3,5-trimethoxybenzene dissolved in C_6D_6 . 3.2 mg (0.0175 mmol) of benzhydryl amine was added by pipette. The resulting solution was then transferred to a NMR tube. A ^1H NMR spectrum was obtained 1 h after the sample was prepared. The yield of the titanium imido complex (94%) was calculated based on the internal

standard. ^1H NMR (300 MHz, C_6D_6): δ 7.59 (d, 4H, Ph-*H*), 7.23 (t, 4H, Ph-*H*), 7.07 (t, 2H, Ph-*H*), 5.75 (s, 1H, Ph_2CH), 2.37 (d, 6H, $\text{N}(\text{CH}_3)_2$), 1.19 (s, 18H, $\text{C}(\text{CH}_3)_3$).

Pyridine-trapped titanium imido complex 49: A vial was charged with 67.2 mg (0.101 mmol) of **9** dissolved in hexanes. 18.8 mg (0.103 mmol) of benzhydryl amine and 12.3 mg (0.156 mmol) of pyridine were added to the vial separately. The resulting solution was then transferred to a Schlenk tube charged with a stir bar and stirred over night. Yellow residues were obtained after removing the solvent under vacuum. Cooling the pentane solution of the residue gave yellow crystals of **49** in 40% yield (34 mg). ^1H NMR (300 MHz, C_6D_6): δ 8.95 (d, 2H, Py-*H*), 7.55 (d, 4H, Ph-*H*), 7.13 (m, 3H, Ph-*H*), 6.99 (m, 3H, Ph-*H*), 6.80 (t, 1H, Py-*H*), 6.53 (t, 2H, Py-*H*), 5.77 (s, 1H, Ph_2CH), 1.24 (s, 18H, $\text{C}(\text{CH}_3)_3$). ^{13}C NMR (75 MHz, C_6D_6): δ 149.9, 146.3, 138.6, 129.5, 129.3, 128.3, 126.4, 125.6, 123.8, 82.0, 53.4, 52.7, 31.9, 31.2, 28.5, 23.0, 14.3. ^{19}F NMR (C_6D_6): δ -139.8 (br, 4F), -153.9 (m, 2F), -161.3 (m, 4F). EIMS (m/z): 839 (M^+ , 15), 267 (18), 252 (30), 195 (100), 106 (60).

Reaction of *t*-butyl amine with 9 A vial was charged with 66.7 mg (0.10 mmol) of **9** dissolved in hexanes, 40 mL of *t*-butyl amine was added by pipette. The mixture was then transferred to a 50 mL Schlenk tube charged with a stir bar and stirred for 4 h at room temperature. Solvent was removed under vacuum. The resulting yellow residue was redissolved in hexanes. After filtration, yellow crystals of **50** were obtained by cooling the solution to -35°C in 47% (33 mg). ^1H NMR (300 MHz, C_6D_6): δ 2.65 (s, 6H), 1.26 (s, 18H), 1.22 (s, 9H). ^{13}C NMR (75 MHz, C_6D_6): δ 140 to 125 (aromatic C), 68.0, 52.5, 52.0, 40.4, 32.2, 31.9, 31.3, 28.5, 23.0, 14.3. ^{19}F NMR (C_6D_6): δ -139.6 (br, 4F), -153.8 (m, 2F), -161.3 (m, 4F). EIMS (m/z): 651 (M^+ -2HNMe₂, 7), 636 (90), 387 (80), 346, 267, 252, 195 (100). HRMS: Calcd. for $\text{C}_{26}\text{H}_{27}\text{O}_2\text{N}_3\text{F}_{10}\text{Ti}$ (M^+ -2HNMe₂): 651.1423. Found: 651.1422.

Pyridine-trapped imido complex 51 A vial was charged with 65.5 mg (0.098 mmol) of **9** dissolved in hexanes, 14 mg (0.19 mmol) of *t*-butyl amine and 22 mg (0.28 mmol) of pyridine were added by pipette. The mixture was then transferred to a 50 mL Schlenk tube charged with a stir bar and stirred for 4 h at room temperature. Solvent was removed under vacuum. The resulting yellow residue was redissolved in hexanes and filtrated. Cooling the obtained solution to -35°C afforded yellow crystals of **51** in 60% yield (44 mg). ¹H NMR (300 MHz, C₆D₆): δ 9.30 (br, 2H, py-*H*), 6.90 (m, 1H, py-*H*), 6.68 (t, 2H, py-*H*), 1.20 (s, H, Me-*H*), 1.18 (s, H, Me-*H*). ¹³C NMR (75 MHz, C₆D₆): δ 160.0, 149.4, 138.6, 125.6, 68.5, 52.6, 31.9, 31.6, 31.1, 28.5, 23.0, 14.3 (missing aromatic C signals are due to overlapped by solvent peaks). ¹⁹F NMR (C₆D₆): δ -139.6 (br, 4F), -154.2 (m, 2F), -161.3 (m, 4F).

Reaction of aniline with 8 A vial was charged with 41.4 mg (0.057 mmol) of **8** and 4.8 mg (0.0286 mmol) of 1,3,5-trimethoxybenzene dissolved in C₆D₆. 5.2 mg (0.056 mmol) of aniline was added to the vial by pipette. The mixture was then transferred to a NMR tube. Red powdery precipitate appeared in 30 minutes. A ¹H NMR spectrum was obtained after 1 h the sample was prepared. ¹H NMR (300 MHz, C₆D₆): δ 6.24 (s, 3H, Ph-*H*), 3.31 (s, 9H, Ph-OCH₃), 2.47 (m, 4H, HNCH₂CH₃), 0.98 (t, 6H, CH₂CH₃).

Reaction of aniline with 9 A vial was charged with 73.0 mg (0.109 mmol) of **9** dissolved in hexanes. 10.2 mg (0.110 mmol) of aniline was added by pipette. The mixture was then transferred to a 50 mL round bottomed flask charged with a stir bar and stirred 2 hours at room temperature. The resulting slurry was then filtrated to give a red powdery solid of **52**. No NMR spectra were obtained due to the low solubility of this compound in most solvents. EIMS (*m/z*): 1342 (M⁺, 7), 1001 (25), 826 (3), 746 (25), 671 (25), 422, 366, 267, 252, 212, 195 (95), 57 (100).

Reaction of benzylamine with 9 A vial was charged with 13.9 mg (0.0208 mmol) of **9** and 3.9 mg (0.0232 mmol) of 1,3,5-trimethoxybenzene dissolved in C₆D₆. 2.1 mg (0.0196 mmol) of benzyl amine was added by pipette. The mixture was then transferred to a NMR tube. Pale yellow powdery precipitate of **53** appeared within 30 min. A ¹H NMR spectrum was obtained 1 h after the sample was prepared. The supernatant was then removed by pipette and the precipitate was transferred to a vial after being washed with pentane for 3 to 4 times. The remaining solvent was removed under vacuum. ¹H NMR (300 MHz, C₆D₆): δ 6.24 (s, 3H, Ph-*H*), 3.31 (s, 9H, Ph-*CH*₃), 2.55 (s, 1H, *NH*), 2.2 (br, 6H, *NCH*₃). EIMS (m/z): 1370 (missing), 1130 (M⁺-C₆F₅CO - NC(CH₃)₃, 25), 853, 748, 267, 252, 195 (100). EA for C₅₈H₅₀N₆O₄F₂₀Ti₂ Calcd: C 50.82, H 3.68, N 6.13; Found: C 47.30, H 3.76, N 6.20.

4.5 References

1. P.J. Walsh, A. M. Baranger and R. G. Bergman, *J. Am. Chem. Soc.*, **1992**, *114*, 1708-1719.
2. P. L. McGrane, M. Jensen and T. Livinghouse, *J. Am. Chem. Soc.*, **1992**, *114*, 5459-5460.
3. Y. Li and T. J. Marks, *J. Am. Chem. Soc.*, **1996**, *118*, 9295-9306.
4. E. Haak, I. Bytshkov and S. Doye, *Angew. Chem., Int. Ed.*, **1999**, *38*, 3389-3391.
5. J. S. Johnson and R. G. Bergman, *J. Am. Chem. Soc.*, **2001**, *123*, 2923-2924.
6. B. F. Straub and R. G. Bergman, *Angew. Chem., Int. Ed.*, **2001**, *40*, 4632-4635.
7. F. Pohlki and S. Doye, *Angew. Chem., Int. Ed.*, **2001**, *40*, 2305-2308.
8. (a). A. M. Baranger, P. J. Walsh and R. G. Bergman, *J. Am. Chem. Soc.*, **1993**, *115*, 2753. (b). A. Bashall, M. McPartlin, P. E. Collier, P. Mountford, L. H. Grade, D. J. M. Troesch, *Chem. Commun.*, **1998**, 2555. (c). D. J. M. Troesch,

- P.E. Collier, A. Bashall, L. H. Gade, M. McPartlin, P. Mountford, S. Radojeric, *Organometallics*, **2001**, *20*, 3308.
9. (a) Y. Shi, J. T. Ciszewski and A. L. Odom, *Organometallics*, **2001**, *20*, 3967-3969; (b) C. Cao, J. T. Ciszewski and A. L. Odom, *Organometallics* **2001**, *20*, 5011-5013; (c) Y. Shi, C. Hall, J. T. Ciszewski, C. Cao and A. L. Odom, *Chem. Comm.*, **2003**, 586-587.
 10. D. L. Thorn, W. A. Nugent, R. L. Harlow, *J. Am. Chem. Soc.*, **1981**, *103*, 357-363.
 11. L. Ackermann, R. G. Bergman, R. N. Loy, *J. Am. Chem. Soc.*, ASAP.
 12. T. G. Ong, G. P. A. Yap and D. S. Richeson, *Organometallics*, **2002**, *21*, 2839-2841.
 13. Crystal structure data were unavailable when the thesis was finished.
 14. E. Haak, I. Bytshkov and S. Doye, *Angew. Chem., Int. Ed.*, **1999**, *38*, 3389-3391.
 15. P. J. Walsh, F. J. Hollander and R. G. Bergman, *Organometallics*, **1993**, *12*, 3705-3723.
 16. Unpublished results.
 17. P. Mountford, *Chem. Commun.*, **1997**, 2127-2134.
 18. (a) T.R. Cundari, T.R. Klinckman, P.T. Wolczanski, *J. Am. Chem. Soc.*, **2002**, *124*, 1481-1487; (b) J.L. Polse, R.A. Anderson, R.G. Bergman, *J. Am. Chem. Soc.*, **1998**, *120*, 13405-13414.

Chapter 5 Summary

This thesis focuses on the exploration of new titanium amidate complexes as hydroamination catalysts, including ligand and metal complex design and preparation; catalytic hydroamination scope investigations and hydroamination mechanistic investigations. Based on recent significant progress and the increasing interest in developing novel transition metal complexes for hydroamination of alkynes/alkenes, titanium complexes **8** and **9** from the N, O amide proligand **5** were designed, prepared and characterized by multinuclear NMR spectroscopy, mass spectrometry, IR spectroscopy and X-ray crystallography. NMR scale reactions were then carried out and monitored by ^1H NMR spectroscopy to obtain preliminary results of the **8**-catalyzed hydroamination reaction.

Intramolecular hydroamination reactions were first investigated by using aminoalkyne, aminoallene and aminoalkene as substrates. Titanium complex **8** has proven to be a component catalyst for the formation of 5- or 6-membered azacycles via intramolecular hydroamination reaction with a typical 5 mol% catalyst loading. Compared with other reported titanium complexes, **8** is noteworthy for its low catalyst loading, mild reaction conditions and high regioselectivity. Hydroamination of aminoalkenes has been so far unsuccessful with these complexes.

The more challenging intermolecular hydroamination reaction was further investigated by using different alkynes and primary amines as substrates. In general, hydroamination of terminal alkynes with bulky primary amines proceeded smoothly at 65°C with 10 mol% catalyst loading. The hydroamination reaction is anti-Markovnikov selective for bulky alkyl primary amines, while only Markovnikov product was detected for the hydroamination of 1-hexyne with bulky aryl primary amine (2,6-dimethyl aniline). Neither alkyl nor aryl primary amines that are less

sterically demanding are suitable substrate for the hydroamination reaction catalyzed by **8**. Hydroamination of internal alkynes with different primary amines was unsuccessful in most cases, except for the hydroamination of phenylmethylacetylene with 2,6-dimethyl aniline.

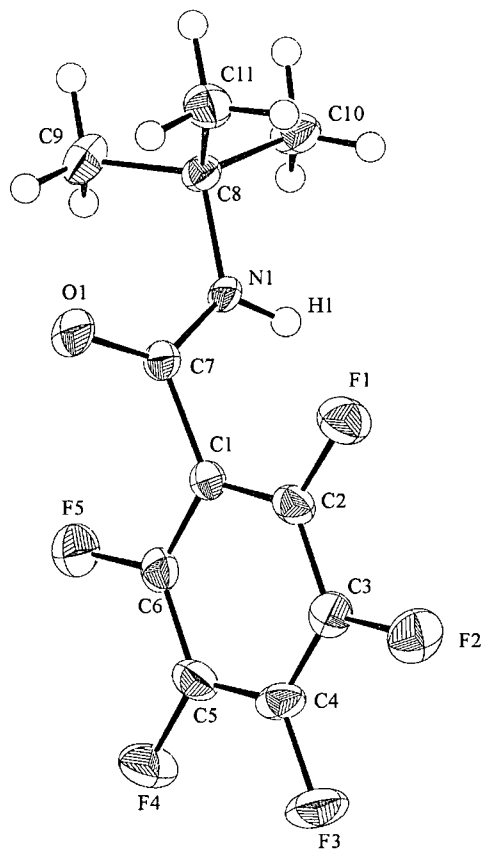
Larger scale hydroamination reactions were carried out for certain substrates with lower catalyst loading and then subjected by LAH/THF reduction to give isolable amines with yields comparable to that obtained from NMR tube scale reactions. No hydroamination products were detected for the reaction between terminal alkyne and secondary amines.

In the mechanistic investigations, the ^1H NMR spectrum of stoichiometric reaction between 2,6-dimethyl aniline and titanium amidate **8** indicated formation of the titanium imido complex, which was further proved by the isolation of the pyridine-trapped imido compound. The obtained imido complex demonstrated higher catalytic activity than titanium amidate, suggesting the titanium imido complex is the real catalyst for the hydroamination reaction. Titanium imido complexes were also detected in the NMR tube scale stoichiometric reaction between titanium amidate **9** and *t*-butyl amine or benzhydryl amine. In both cases, pyridine-trapped imido complexes were obtained and characterized by multinuclear NMR spectroscopy and mass spectrometry. The stoichiometric reaction between **9** and less sterically demanding primary amines such as benzyl amine and aniline gives insoluble precipitates, which were identified as titanium imido dimers by mass spectrometry, indicating the presence of a preequilibrium of the imido complex, and the imido dimer, as was first proposed by Doye for the Cp_2TiMe_2 system. The preference for formation of imido dimer in the case of less sterically demanding primary amines explains the low yield for relevant hydroamination reactions.

A mechanism was proposed based on literature reports and relevant stoichiometric reactions. Further investigations on the mechanism such as the attempted formation of the azametallocycle or amide enamide titanium complex were unsuccessful.

It has been shown that for most known hydroamination catalysts, the regioselectivity of products is significantly affected by the electronic and steric properties of both employed catalysts and substrates, and there is still no general hydroamination catalyst. Further investigations regarding the mechanism are therefore important for not only understanding the reaction itself, but also the design of a new generation of catalyst.

Appendix I: EXPERIMENTAL DETAILS FOR PROLIGAND 5



A. Crystal Data

Empirical Formula	$C_{11}H_{10}NOF_5$
Formula Weight	267.20
Crystal Color, Habit	clear, chip
Crystal Dimensions	0.12×0.12×0.05 mm
Crystal System	monoclinic
Lattice Type	Primitive
Lattice Parameters	$a = 6.1018(7) \text{ \AA}$ $b = 21.018(2) \text{ \AA}$ $c = 9.711(1) \text{ \AA}$ $\beta = 109.224(4)^\circ$ $V = 1175.9(2) \text{ \AA}^3$
Space Group	$P2_1/n$ (#14)
Z value	4
D_{calc}	1.509 g/cm^3
F_{000}	544.00
$\mu(\text{MoK}\alpha)$	1.50 cm^{-1}

B. Intensity Measurements

Diffractometer	Rigaku/ADSC CCD
Radiation	MoK α ($\lambda = 0.71069 \text{ \AA}$) graphite monochromated
Detector Aperture	94 mm \times 94 mm
Data Images	460 exposures @ 82.0 seconds
ϕ oscillation Range ($\chi=-90.0$)	0.0 – 190.0 $^\circ$
ω oscillation Range ($\chi=-90.0$)	-17.0 – 23.0
Detector Position	38.78 mm
Detector Swing Angle	-5.53 $^\circ$
$2\theta_{\max}$	55.7 $^\circ$
No. of Reflection Measured	Total: 10504 Unique: 2697 ($R_{\text{int}} = 0.045$)
Corrections	Lorentz-polarization Absorption / scaling/decay (corr. factors: 0.8315 – 1.0000)

C. Structure Solution and Refinement

Structure Solution	Direct Methods (SIR97)
Refinement	Full-matrix least-squares
Function Minimized	$\Sigma\omega(F_o^2 - F_c^2)^2$
Least Squares Weights	$\omega = 1/\sigma^2(F_o^2) = [\sigma_c^2(F_o^2) + p^2F_o^2/4]^{-1}$
p-factor	0.0410
Anomalous Dispersion	All non-hydrogen atoms
No. Observations ($I > 0.00\sigma(I)$)	2620
No. Variables	167
Reflection/Parameter Ratio	15.69
Residuals (refined on F ² , all data): R, Rw	0.061; 0.092
Goodness of Fit Indicator	0.93
Max Shift/Error in Final Cycle	0.00
No. Observations ($I > 3\sigma(I)$)	1616
Residuals (refined on F, $I > 3\sigma(I)$): R; Rw	0.033; 0.040
Maximum peak in Final Diff. Map	0.31 e $^-$ / \AA^3
Minimum peak in Final Diff. Map	-0.34 e $^-$ / \AA^3

Table1. Atomic coordinates and B_{iso}/B_{eq}

atom	x	y	z	B_{eq}
F(1)	0.1285(2)	0.17683(4)	0.2277(1)	3.10(2)
F(2)	0.2413(2)	0.05394(4)	0.2978(1)	3.44(2)
F(3)	0.5704(2)	-0.00329(4)	0.2093(1)	3.65(2)
F(4)	0.7868(2)	0.06198(4)	0.0508(1)	3.60(2)
F(5)	0.6712(2)	0.18502(4)	-0.0217(1)	3.22(2)
O(1)	0.1913(2)	0.26114(5)	-0.0722(1)	2.91(2)
N(1)	0.4133(2)	0.29529(5)	0.1532(1)	1.64(2)
C(1)	0.3966(2)	0.18388(6)	0.1008(1)	1.78(3)
C(2)	0.2909(3)	0.14939(6)	0.1821(2)	2.05(3)
C(3)	0.3458(3)	0.08636(6)	0.2179(2)	2.30(3)
C(4)	0.5119(3)	0.05744(6)	0.1728(2)	2.40(3)
C(5)	0.6244(3)	0.09055(7)	0.0928(2)	2.38(3)
C(6)	0.5635(3)	0.15337(6)	0.0573(2)	2.12(3)
C(7)	0.3233(2)	0.25139(6)	0.0522(2)	1.84(3)
C(8)	0.3598(2)	0.36417(6)	0.1354(1)	1.72(3)
C(9)	0.4299(3)	0.39085(7)	0.0100(2)	2.65(3)
C(10)	0.5041(3)	0.39518(6)	0.2784(2)	2.57(3)
C(11)	0.1019(3)	0.37421(7)	0.1095(2)	2.55(3)
H(1)	0.495(3)	0.2823(7)	0.236(2)	2.3(3)
H(9A)	0.5964	0.3840	0.0299	3.1319
H(9B)	0.3964	0.4366	0.0003	3.1319
H(9C)	0.3421	0.3692	-0.0807	3.1319
H(10C)	0.6694	0.3884	0.2935	3.0308
H(10A)	0.4645	0.3760	0.3591	3.0308
H(10B)	0.4713	0.4409	0.2743	3.0308
H(11B)	0.0660	0.4197	0.0981	3.0028
H(11C)	0.0627	0.3577	0.1928	3.0028
H(11A)	0.0110	0.3516	0.0207	3.0028

Table 2. Bond Lengths (Å)

atom	atom	distance	atom	atom	distance
F(1)	C(2)	1.342(2)	F(2)	C(3)	1.341(2)
F(3)	C(4)	1.341(2)	F(4)	C(5)	1.343(2)
F(5)	C(6)	1.340(2)	O(1)	C(7)	1.229(2)
N(1)	C(7)	1.326(2)	N(1)	C(8)	1.481(2)
C(1)	C(2)	1.379(2)	C(1)	C(6)	1.382(2)
C(1)	C(7)	1.515(2)	C(2)	C(3)	1.383(2)
C(3)	C(4)	1.372(2)	C(4)	C(5)	1.374(2)
C(5)	C(6)	1.382(2)	C(8)	C(9)	1.525(2)
C(8)	C(10)	1.524(2)	C(8)	C(11)	1.525(2)
N(1)	H(1)	0.84(2)	C(9)	H(9A)	0.98
C(9)	H(9B)	0.98	C(9)	H(9C)	0.98
C(10)	H(10C)	0.98	C(10)	H(10A)	0.98
C(10)	H(10B)	0.98	C(11)	H(11B)	0.98
C(11)	H(11C)	0.98	C(11)	H(11A)	0.98

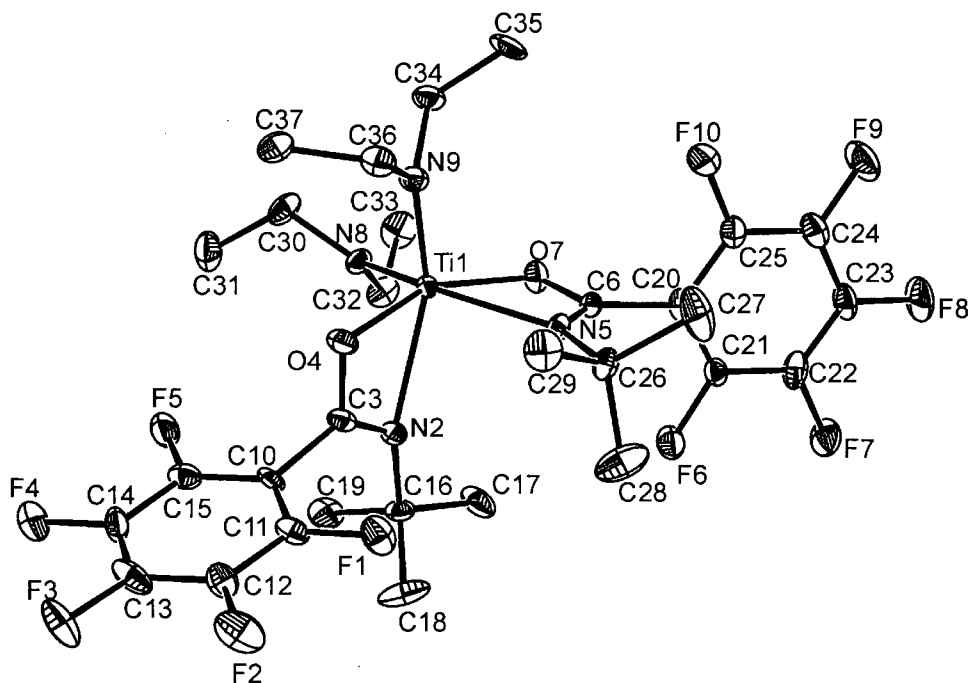
Table 3. Bond Angles(°)

atom	atom	atom	angle	atom	atom	atom	angle
C(7)	N(1)	C(8)	124.9(1)	C(2)	C(1)	C(6)	117.5(1)
C(2)	C(1)	C(7)	121.6(1)	C(6)	C(1)	C(7)	120.7(1)
F(1)	C(2)	C(1)	119.9(1)	F(1)	C(2)	C(3)	118.2(1)
C(1)	C(2)	C(3)	121.8(1)	F(2)	C(3)	C(2)	120.7(1)
F(2)	C(3)	C(4)	120.1(1)	C(2)	C(3)	C(4)	119.2(1)
F(3)	C(4)	C(3)	119.8(1)	F(3)	C(4)	C(5)	119.6(1)
C(3)	C(4)	C(5)	120.5(1)	F(4)	C(5)	C(4)	120.0(1)
F(4)	C(5)	C(6)	120.7(1)	C(4)	C(5)	C(6)	119.3(1)
F(5)	C(6)	C(1)	119.6(1)	F(5)	C(6)	C(5)	118.7(1)
C(1)	C(6)	C(5)	121.7(1)	O(1)	C(7)	N(1)	126.1(1)
O(1)	C(7)	C(1)	119.5(1)	N(1)	C(7)	C(1)	114.4(1)
N(1)	C(8)	C(9)	110.1(1)	N(1)	C(8)	C(10)	105.8(1)
N(1)	C(8)	C(11)	109.3(1)	C(9)	C(8)	C(10)	109.9(1)
C(9)	C(8)	C(11)	111.3(1)	C(10)	C(8)	C(11)	110.3(1)
C(7)	N(1)	H(1)	117(1)	C(8)	N(1)	H(1)	118(1)
C(8)	C(9)	H(9A)	109.4	C(8)	C(9)	H(9B)	109.4
C(8)	C(9)	H(9C)	109.5	H(9A)	C(9)	H(9B)	109.4
H(9A)	C(9)	H(9C)	109.6	H(9B)	C(9)	H(9C)	109.5
C(8)	C(10)	H(10C)	109.4	C(8)	C(10)	H(10A)	109.4
C(8)	C(10)	H(10B)	109.5	H(10C)	C(10)	H(10A)	109.5
H(10C)	C(10)	H(10B)	109.5	H(10A)	C(10)	H(10B)	109.6
C(8)	C(11)	H(11B)	109.5	C(8)	C(11)	H(11C)	109.5
C(8)	C(11)	H(11A)	109.4	H(11B)	C(11)	H(11C)	109.5
H(11B)	C(11)	H(11A)	109.4	H(11C)	C(11)	H(11A)	109.5

Table 4. Torsion Angles(°)

atom	atom	atom	atom	angle	atom	atom	atom	atom	angle
F(1)	C(2)	C(1)	C(6)	179.6(1)	F(1)	C(2)	C(1)	C(7)	-4.1(2)
F(1)	C(2)	C(3)	F(2)	-0.8(2)	F(1)	C(2)	C(3)	C(4)	-179.8(1)
F(2)	C(3)	C(2)	C(1)	179.6(1)	F(2)	C(3)	C(4)	F(3)	-0.3(2)
F(2)	C(3)	C(4)	C(5)	-179.0(1)	F(3)	C(4)	C(3)	C(2)	178.6(1)
F(3)	C(4)	C(5)	F(4)	0.4(2)	F(3)	C(4)	C(5)	C(6)	-179.1(1)
F(4)	C(5)	C(4)	C(3)	179.1(1)	F(4)	C(5)	C(6)	F(5)	1.0(2)
F(4)	C(5)	C(6)	C(1)	-179.3(1)	F(5)	C(6)	C(1)	C(2)	-179.9(1)
F(5)	C(6)	C(1)	C(7)	3.8(2)	F(5)	C(6)	C(5)	C(4)	-179.5(1)
O(1)	C(7)	N(1)	C(8)	3.3(2)	O(1)	C(7)	C(1)	C(2)	-98.8(2)
O(1)	C(7)	C(1)	C(6)	77.3(2)	N(1)	C(7)	C(1)	C(2)	81.3(2)
N(1)	C(7)	C(1)	C(6)	-102.5(2)	C(1)	C(2)	C(3)	C(4)	0.7(2)
C(1)	C(6)	C(5)	C(4)	0.2(2)	C(1)	C(7)	N(1)	C(8)	-176.9(1)
C(2)	C(1)	C(6)	C(5)	0.4(2)	C(2)	C(3)	C(4)	C(5)	-0.1(2)
C(3)	C(2)	C(1)	C(6)	-0.9(2)	C(3)	C(2)	C(1)	C(7)	175.4(1)
C(3)	C(4)	C(5)	C(6)	-0.4(2)	C(5)	C(6)	C(1)	C(7)	-175.9(1)
C(7)	N(1)	C(8)	C(9)	-60.9(2)	C(7)	N(1)	C(8)	C(10)	-179.6(1)
C(7)	N(1)	C(8)	C(11)	61.6(2)					

Appendix II: EXPERIMENTAL DETAILS FOR TITANIUM COMPLEX 8



A. Crystal Data

Empirical Formula	$C_{30}H_{38}N_4O_2F_{10}Ti$
Formula Weight	724.54
Crystal Color, Habit	red, chip
Crystal Dimensions	0.20×0.20×0.10 mm
Crystal System	monoclinic
Lattice Type	Primitive
Lattice Parameters	$a = 10.510(1) \text{ \AA}$ $b = 20.104(2) \text{ \AA}$ $c = 15.820(1) \text{ \AA}$ $\beta = 90.990(4)^\circ$ $V = 3342.1(5) \text{ \AA}^3$
Space Group	$P2_1/a$ (#14)
Z value	4
D_{calc}	1.440 g/cm ³
F_{000}	1496.00
$\mu(\text{MoK}\alpha)$	0.35 cm ⁻¹

B. Intensity Measurements

Diffractionmeter	Rigaku/ADSC CCD
Radiation	MoK α ($\lambda = 0.71069 \text{ \AA}$) graphite monochromated
Detector Aperture	94 mm \times 94 mm
Data Images	460 exposures @ 59.0 seconds
ϕ oscillation Range ($\chi=-90.0$)	0.0 – 190.0 $^\circ$
ω oscillation Range ($\chi=-90.0$)	-17.0 – 23.0
Detector Position	38.79 mm
Detector Swing Angle	-5.60 $^\circ$
$2\theta_{\max}$	50.1 $^\circ$
No. of Reflection Measured	Total: 19695 Unique: 4988 ($R_{\text{int}} = 0.072$)
Corrections	Lorentz-polarization Absorption / scaling/decay (corr. factors: 0.4803 – 1.0000)

C. Structure Solution and Refinement

Structure Solution	Direct Methods
Refinement	Full-matrix least-squares
Function Minimized	$\Sigma\omega(F_o^2 - F_c^2)^2$
Least Squares Weights	$\omega = 1/\sigma^2(F_o^2) + (0.0636.P)^2 + 39.47.P$ where $P = (\text{Max}(F_o^2, 0) + 2F_c^2)/3$
Anomalous Dispersion	All non-hydrogen atoms
No. Observations ($I > 0.00\sigma(I)$)	4988
No. Variables	447
Residuals (refined on F^2 , all data): R, Rw	0.140; 0.276
Goodness of Fit Indicator	1.11
Max Shift/Error in Final Cycle	0.00
No. Observations ($I > 2\sigma(I)$)	3414
Residuals (refined on F, $I > 2\sigma(I)$): R; Rw	0.104; 0.259
Maximum peak in Final Diff. Map	0.52 e $^-/\text{\AA}^3$
Minimum peak in Final Diff. Map	-0.56 e $^-/\text{\AA}^3$

Table 1. Atomic coordinates and equivalent isotropic displacement parameter

Atom	x	y	z	U(eq)
C(3)	4720(8)	972(4)	2005(6)	25(2)
C(6)	4478(8)	-1050(4)	2969(6)	25(2)
C(10)	5213(8)	1575(4)	1531(5)	25(2)
C(11)	6207(9)	1492(4)	968(5)	29(2)
C(12)	6566(10)	2017(5)	446(6)	33(2)
C(13)	5948(11)	2620(5)	490(6)	43(3)
C(14)	4982(10)	2698(4)	1060(6)	38(2)
C(15)	4609(9)	2173(5)	1544(6)	33(2)
C(16)	5911(7)	1038(3)	3362(5)	28(2)
C(17)	6129(12)	520(5)	4044(7)	58(5)
C(18)	7181(9)	1224(7)	2993(8)	60(5)
C(19)	5327(11)	1649(5)	3754(7)	42(3)
C(20)	4941(9)	-1660(4)	3414(5)	29(2)
C(21)	5938(8)	-1652(4)	3969(6)	27(2)
C(22)	6327(10)	-2210(5)	4411(6)	38(2)
C(23)	5731(10)	-2804(4)	4315(6)	38(2)
C(24)	4695(10)	-2843(5)	3759(6)	38(2)
C(25)	4307(9)	-2275(4)	3328(6)	33(2)
C(26)	5798(8)	-1040(4)	1671(5)	27(2)
C(27)	5763(14)	-1808(5)	1571(8)	60(4)
C(28)	7100(10)	-813(8)	1985(7)	65(4)
C(29)	5509(11)	-733(5)	826(6)	44(3)
C(30)	1009(9)	824(5)	2895(6)	39(2)
C(31)	970(11)	1559(5)	3114(8)	53(3)
C(32)	2408(9)	519(5)	4099(5)	34(2)
C(33)	1385(11)	236(6)	4600(7)	52(3)
C(34)	903(9)	-668(4)	2032(6)	33(2)
C(35)	852(10)	-1397(5)	1835(8)	46(3)
C(36)	2012(10)	-231(5)	793(6)	36(2)
C(37)	1272(10)	384(5)	524(7)	44(3)
N(2)	4991(7)	747(3)	2737(5)	26(2)
N(5)	4815(7)	-798(3)	2260(4)	24(2)
N(8)	2172(7)	489(4)	3182(5)	27(2)
N(9)	2061(7)	-330(3)	1708(5)	27(2)
O(4)	3834(6)	663(3)	1568(4)	30(1)
O(7)	3570(6)	-728(3)	3363(4)	31(1)
F(1)	6814(6)	920(3)	910(4)	42(1)
F(2)	7467(6)	1938(3)	-121(4)	56(2)
F(3)	6269(7)	3114(3)	-34(4)	65(2)
F(4)	4374(6)	3285(3)	1122(5)	57(2)
F(5)	3642(6)	2272(3)	2076(4)	46(2)
F(6)	6582(6)	-1078(3)	4111(4)	42(1)
F(7)	7350(6)	-2177(3)	4963(4)	52(2)
F(8)	6086(7)	-3342(3)	4740(4)	59(2)
F(9)	4096(7)	-3416(3)	3646(4)	60(2)
F(10)	3315(6)	-2328(3)	2791(4)	52(2)
Ti(1)	3297(1)	3(1)	2477(1)	20(1)
C(17B)	5540(70)	770(30)	4220(20)	58(5)

C(18B)	7210(30)	770(40)	3150(50)	60(5)
C(19B)	5980(80)	1788(5)	3410(40)	42(3)

Table 2. Bond Lengths [Å]

C(3)-N(2)	1.272(11)	C(3)-O(4)	1.307(10)
C(3)-C(10)	1.522(11)	C(3)-Ti(1)	2.575(8)
C(6)-N(5)	1.286(11)	C(6)-O(7)	1.319(10)
C(6)-C(20)	1.491(12)	C(6)-Ti(1)	2.567(8)
C(10)-C(15)	1.359(13)	C(10)-C(11)	1.394(12)
C(11)-F(1)	1.319(10)	C(11)-C(12)	1.396(12)
C(12)-F(2)	1.325(11)	C(12)-C(13)	1.379(14)
C(13)-F(3)	1.339(11)	C(13)-C(14)	1.378(14)
C(14)-F(4)	1.348(11)	C(14)-C(15)	1.366(13)
C(15)-F(5)	1.345(10)	C(16)-N(2)	1.491(11)
C(16)-C(17B)	1.512(8)	C(16)-C(19)	1.511(7)
C(16)-C(19B)	1.512(8)	C(16)-C(17)	1.513(7)
C(16)-C(18B)	1.512(8)	C(16)-C(18)	1.514(7)
C(17)-H(17A)	0.9800	C(17)-H(17B)	0.9800
C(17)-H(17C)	0.9800	C(18)-H(18A)	0.9800
C(18)-H(18B)	0.9800	C(18)-H(18C)	0.9800
C(19)-H(19A)	0.9800	C(19)-H(19B)	0.9800
C(19)-H(19C)	0.9800	C(20)-C(21)	1.356(13)
C(20)-C(25)	1.410(13)	C(21)-F(6)	1.355(10)
C(21)-C(22)	1.380(12)	C(22)-C(23)	1.355(14)
C(22)-F(7)	1.375(11)	C(23)-F(8)	1.325(10)
C(23)-C(24)	1.389(15)	C(24)-F(9)	1.324(11)
C(24)-C(25)	1.387(13)	C(25)-F(10)	1.338(11)
C(26)-N(5)	1.486(10)	C(26)-C(29)	1.499(13)
C(26)-C(28)	1.517(15)	C(26)-C(27)	1.553(13)
C(27)-H(27A)	0.9800	C(27)-H(27B)	0.9800
C(27)-H(27C)	0.9800	C(28)-H(28A)	0.9800
C(28)-H(28B)	0.9800	C(28)-H(28C)	0.9800
C(29)-H(29A)	0.9800	C(29)-H(29B)	0.9800
C(29)-H(29C)	0.9800	C(30)-N(8)	1.462(11)
C(30)-C(31)	1.518(14)	C(30)-H(30A)	0.9900
C(30)-H(30B)	0.9900	C(31)-H(31A)	0.9800
C(31)-H(31B)	0.9800	C(31)-H(31C)	0.9800
C(32)-C(33)	1.462(13)	C(32)-N(8)	1.469(11)
C(32)-H(32A)	0.9900	C(32)-H(32B)	0.9900
C(33)-H(33A)	0.9800	C(33)-H(33B)	0.9800
C(33)-H(33C)	0.9800	C(34)-N(9)	1.493(11)
C(34)-C(35)	1.500(13)	C(34)-H(34A)	0.9900
C(34)-H(34B)	0.9900	C(35)-H(35A)	0.9800
C(35)-H(35B)	0.9800	C(35)-H(35C)	0.9800
C(36)-N(9)	1.460(11)	C(36)-C(37)	1.519(14)
C(36)-H(36A)	0.9900	C(36)-H(36B)	0.9900
C(37)-H(37A)	0.9800	C(37)-H(37B)	0.9800
C(37)-H(37C)	0.9800	N(2)-Ti(1)	2.356(7)
N(5)-Ti(1)	2.296(7)	N(8)-Ti(1)	1.909(7)

N(9)-Ti(1)	1.887(7)	O(4)-Ti(1)	2.044(6)
O(7)-Ti(1)	2.046(6)	C(17B)-H(17D)	0.9800
C(17B)-H(17E)	0.9800	C(17B)-H(17F)	0.9800
C(18B)-H(18D)	0.9800	C(18B)-H(18E)	0.9800
C(18B)-H(18F)	0.9800	C(19B)-H(19D)	0.9800
C(19B)-H(19E)	0.9800	C(19B)-H(19F)	0.9800

Table 3. Bond Angles(°)

N(2)-C(3)-O(4)	117.4(7)	N(2)-C(3)-C(10)	131.2(8)
N(2)-C(3)-C(10)	111.4(7)	N(2)-C(3)-Ti(1)	65.7(5)
O(4)-C(3)-Ti(1)	51.8(4)	C(10)-C(3)-Ti(1)	162.0(6)
N(5)-C(6)-O(7)	115.5(7)	N(5)-C(6)-C(20)	130.0(7)
O(7)-C(6)-C(20)	114.4(7)	N(5)-C(6)-Ti(1)	63.2(4)
O(7)-C(6)-Ti(1)	52.3(4)	C(20)-C(6)-Ti(1)	166.6(6)
C(15)-C(10)-C(11)	118.1(8)	C(15)-C(10)-C(3)	122.2(8)
C(11)-C(10)-C(3)	119.0(7)	F(1)-C(11)-C(10)	121.2(7)
F(1)-C(11)-C(12)	118.7(8)	C(10)-C(11)-C(12)	120.0(8)
F(2)-C(12)-C(13)	118.8(8)	F(2)-C(12)-C(11)	120.9(8)
C(13)-C(12)-C(11)	120.2(9)	F(3)-C(13)-C(14)	121.2(10)
F(3)-C(13)-C(12)	119.8(9)	C(14)-C(13)-C(12)	119.0(8)
F(4)-C(14)-C(15)	119.7(10)	F(4)-C(14)-C(13)	120.2(9)
C(15)-C(14)-C(13)	120.1(9)	F(5)-C(15)-C(10)	119.9(8)
F(5)-C(15)-C(14)	117.6(9)	C(10)-C(15)-C(14)	122.4(9)
N(2)-C(16)-C(17B)	106(3)	N(2)-C(16)-C(19)	109.1(7)
C(17B)-C(16)-C(19)	79(3)	N(2)-C(16)-C(19B)	117(3)
C(17B)-C(16)-C(19B)	108.9(6)	C(19)-C(16)-C(19B)	36(3)
N(2)-C(16)-C(17)	107.0(7)	C(17B)-C(16)-C(17)	33(3)
C(19)-C(16)-C(17)	108.9(5)	C(19B)-C(16)-C(17)	130(3)
N(2)-C(16)-C(18B)	107(3)	C(17B)-C(16)-C(18B)	108.9(6)
C(19)-C(16)-C(18B)	139(3)	C(19B)-C(16)-C(18B)	108.9(6)
C(17)-C(16)-C(18B)	78(3)	N(2)-C(16)-C(18)	114.0(7)
C(17B)-C(16)-C(18)	133(3)	C(19)-C(16)-C(18)	109.0(5)
C(19B)-C(16)-C(18)	74(3)	C(17)-C(16)-C(18)	108.8(5)
C(18B)-C(16)-C(18)	37(3)	C(21)-C(20)-C(25)	115.6(8)
C(21)-C(20)-C(6)	122.6(8)	C(25)-C(20)-C(6)	121.7(8)
F(6)-C(21)-C(20)	119.7(8)	F(6)-C(21)-C(22)	117.8(8)
C(20)-C(21)-C(22)	122.5(9)	C(23)-C(22)-F(7)	118.0(8)
C(23)-C(22)-C(21)	121.8(9)	F(7)-C(22)-C(21)	120.2(9)
F(8)-C(23)-C(22)	122.5(10)	F(8)-C(23)-C(24)	119.1(9)
C(22)-C(23)-C(24)	118.5(8)	F(9)-C(24)-C(25)	120.9(10)
F(9)-C(24)-C(23)	120.0(8)	C(25)-C(24)-C(23)	119.0(9)
F(10)-C(25)-C(24)	117.8(8)	F(10)-C(25)-C(20)	119.6(8)
C(24)-C(25)-C(20)	122.6(9)	N(5)-C(26)-C(29)	107.0(7)
N(5)-C(26)-C(28)	109.2(7)	C(29)-C(26)-C(28)	109.6(9)
N(5)-C(26)-C(27)	112.0(8)	C(29)-C(26)-C(27)	108.3(8)
C(28)-C(26)-C(27)	110.6(10)	N(8)-C(30)-C(31)	113.8(9)
N(8)-C(30)-H(30A)	108.8	C(31)-C(30)-H(30A)	108.8
N(8)-C(30)-H(30B)	108.8	C(31)-C(30)-H(30B)	108.8
H(30A)-C(30)-H(30B)	107.7	C(33)-C(32)-N(8)	113.9(8)
C(33)-C(32)-H(32A)	108.8	N(8)-C(32)-H(32A)	108.8

C(33)-C(32)-H(32B)	108.8	N(8)-C(32)-H(32B)	108.8
H(32A)-C(32)-H(32B)	107.7	N(9)-C(34)-C(35)	113.5(8)
N(9)-C(34)-H(34A)	108.9	C(35)-C(34)-H(34A)	108.9
N(9)-C(34)-H(34B)	108.9	C(35)-C(34)-H(34B)	108.9
H(34A)-C(34)-H(34B)	107.7	N(9)-C(36)-C(37)	113.4(8)
N(9)-C(36)-H(36A)	108.9	C(37)-C(36)-H(36A)	108.9
N(9)-C(36)-H(36B)	108.9	C(37)-C(36)-H(36B)	108.9
H(36A)-C(36)-H(36B)	107.7	C(3)-N(2)-C(16)	126.7(7)
C(3)-N(2)-Ti(1)	84.8(5)	C(16)-N(2)-Ti(1)	147.6(5)
C(6)-N(5)-C(26)	128.5(7)	C(6)-N(5)-Ti(1)	86.8(5)
C(26)-N(5)-Ti(1)	144.7(5)	C(30)-N(8)-C(32)	114.4(7)
C(30)-N(8)-Ti(1)	125.3(6)	C(32)-N(8)-Ti(1)	120.2(5)
C(36)-N(9)-C(34)	112.8(7)	C(36)-N(9)-Ti(1)	127.1(6)
C(34)-N(9)-Ti(1)	119.7(6)	C(3)-O(4)-Ti(1)	98.0(5)
C(6)-O(7)-Ti(1)	97.0(5)	N(9)-Ti(1)-N(8)	97.6(3)
N(9)-Ti(1)-O(4)	88.4(3)	N(8)-Ti(1)-O(4)	105.1(3)
N(9)-Ti(1)-O(7)	105.9(3)	N(8)-Ti(1)-O(7)	92.7(3)
O(4)-Ti(1)-O(7)	155.6(3)	N99)-Ti(1)-N(5)	97.3(3)
N(8)-Ti(1)-N(5)	152.3(3)	O(4)-Ti(1)-N(5)	98.5(3)
O(7)-Ti(1)-N(5)	60.7(2)	N(9)-Ti(1)-N(2)	147.9(3)
N(8)-Ti(1)-N(2)	92.7(3)	O(4)-Ti(1)-N(2)	59.6(2)
O(7)-Ti(1)-N(2)	103.9(3)	N(5)-Ti(1)-N(2)	86.9(2)
N(9)-Ti(1)-C(6)	103.1(3)	N(8)-Ti(1)-C(6)	123.1(3)
O(4)-Ti(1)-C(6)	127.6(3)	O(7)-Ti(1)-C(6)	30.7(3)
N(5)-Ti(1)-C(6)	30.0(3)	N(2)-Ti(1)-C(6)	96.3(3)
N(9)-Ti(1)-C(3)	118.5(3)	N(8)-Ti(1)-C(3)	98.7(3)
O(4)-Ti(1)-C(3)	30.2(3)	O(7)-Ti(1)-C(3)	131.8(3)
N(5)-Ti(1)-C(3)	94.5(3)	N(2)-Ti(1)-C(3)	29.5(3)
C(6)-Ti(1)-C(3)	115.6(3)	H(17D)-C(17B)-H(17E)	109.5
H(17D)-C(17B)-H(17F)	109.5	H(17E)-C(17B)-H(17F)	109.5
H(18D)-C(18B)-H(18E)	109.5	H(18D)-C(18B)-H(18F)	109.5
H(18E)-C(18B)-H(18F)	109.5	H(19D)-C(19B)-H(19E)	109.5
H(19D)-C(19B)-H(19F)	109.5	H(19E)-C(19B)-H(19F)	109.5

Table 4. Torsion Angles (°)

N(2)-C(3)-C(10)-C(15)	-94.2(12)	O(4)-C(3)-C(10)-C(15)	83.1(10)
Ti(1)-C(3)-C(10)-C(15)	63(2)	N(2)-C(3)-C(10)-C(11)	95.3(11)
O(4)-C(3)-C(10)-C(11)	-84.7(10)	Ti(1)-C(3)-C(10)-C(11)	-107.0(19)
C(15)-C(10)-C(11)-F(1)	-178.4(8)	C(3)-C(10)-C(11)-F(1)	-7.5(12)
C(15)-C(10)-C(11)-C(12)	0.8(13)	C(3)-C(10)-C(11)-C(12)	171.7(8)
F(1)-C(11)-C(12)-F(2)	2.5(14)	C(10)-C(11)-C(12)-F(2)	-176.7(8)
F(1)-C(11)-C(12)-C(13)	179.8(9)	C(10)-C(11)-C(12)-C(13)	0.6(14)
F(2)-C(12)-C(13)-F(3)	-0.3(15)	C(11)-C(12)-C(13)-F(3)	-177.7(9)
F(2)-C(12)-C(13)-C(14)	177.9(9)	C(11)-C(12)-C(13)-C(14)	0.5(15)
F(3)-C(13)-C(14)-F(4)	-2.6(15)	C(12)-C(13)-C(14)-F(4)	179.2(9)
F(3)-C(13)-C(14)-C(15)	175.2(9)	C(12)-C(13)-C(14)-C(15)	-3.0(15)
C(11)-C(10)-C(15)-F(5)	179.8(8)	C(3)-C(10)-C(15)-F(5)	9.2(13)
C(11)-C(10)-C(15)-C(14)	-3.3(14)	C(3)-C(10)-C(15)-C(14)	-173.9(9)
F(4)-C(14)-C(15)-F(5)	-0.7(14)	C(13)-C(14)-C(15)-F(5)	-178.5(9)
F(4)-C(14)-C(15)-C(10)	-177.7(9)	C(13)-C(14)-C(15)-C(10)	4.5(15)

N(5)-C(6)-C(20)-C(21)	89.3(12)	O(7)-C(6)-C(20)-C(21)	-91.8(10)
Ti(1)-C(6)-C(20)-C(21)	-98(3)	N(5)-C(6)-C(20)-C(25)	-95.3(12)
O(7)-C(6)-C(20)-C(25)	83.6(10)	Ti(1)-C(6)-C(20)-C(25)	77(3)
C(25)-C(20)-C(21)-F(6)	-178.1(8)	C(6)-C(20)-C(21)-F(6)	-2.4(13)
C(25)-C(20)-C(21)-C(22)	1.1(13)	C(6)-C(20)-C(21)-C(22)	176.7(9)
F(6)-C(21)-C(22)-C(23)	179.4(9)	C(20)-C(21)-C(22)-C(23)	0.2(15)
F(6)-C(21)-C(22)-F(7)	-1.2(13)	C(20)-C(21)-C(22)-F(7)	179.6(8)
F(7)-C(22)-C(23)-F(8)	1.2(14)	C(21)-C(22)-C(23)-F(8)	-179.4(9)
F(7)-C(22)-C(23)-C(24)	180.0(9)	C(21)-C(22)-C(23)-C(24)	-0.6(15)
F(8)-C(23)-C(24)-F(9)	-1.6(14)	C(22)-C(23)-C(24)-F(9)	179.6(9)
F(8)-C(23)-C(24)-C(25)	178.6(9)	C(22)-C(23)-C(24)-C(25)	-0.2(14)
F(9)-C(24)-C(25)-F(10)	-0.4(14)	C(23)-C(24)-C(25)-F(10)	179.4(9)
F(9)-C(24)-C(25)-C(20)	-178.2(9)	C(23)-C(24)-C(25)-C(20)	1.5(15)
C(21)-C(20)-C(25)-F(10)	-179.7(8)	C(6)-C(20)-C(25)-F(10)	4.6(13)
C(21)-C(20)-C(25)-C(24)	-1.9(13)	C(6)-C(20)-C(25)-C(24)	-177.6(9)
O(4)-C(3)-N(2)-C(16)	-176.5(7)	C(10)-C(3)-N(2)-C(16)	0.7(15)
Ti(1)-C(93)-N(2)-C(16)	-171.9(8)	O(4)-C(3)-N(2)-Ti(1)	-4.6(7)
C(10)-C(3)-N(2)-Ti(1)	172.6(9)	C(17B)-C(16)-N(2)-C(3)	158(3)
C(19)-C(16)-N(2)-C(3)	74.9(10)	C(19B)-C(16)-N(2)-C(3)	37(3)
C(17)-C(16)-N(2)-C(3)	-167.5(9)	C(18B)-C(16)-N(2)-C(3)	-86(3)
C(18)-C(16)-N(2)-C(3)	-47.2(11)	C(17B)-C(16)-N(2)-Ti(1)	-6(3)
C(19)-C(16)-N(2)-Ti(1)	-90.0(10)	C(19B)-C(16)-N(2)-Ti(1)	-128(3)
C(17)-C(16)-N(2)-Ti(1)	27.7(11)	C(18B)-C(16)-N(2)-Ti(1)	110(3)
C(18)-C(16)-N(2)-Ti(1)	148.0(9)	O(7)-C(6)-N(5)-C(26)	-180.0(8)
C(20)-C(6)-N(5)-C(26)	-1.0(15)	Ti(1)-C(6)-N(5)-C(26)	-179.1(9)
O(7)-C(6)-N(5)-Ti(1)	-0.9(7)	C(20)-C(6)-N(5)-Ti(1)	178.1(9)
C(29)-C(26)-N(5)-C(6)	160.1(9)	C(28)-C(26)-N(5)-C(6)	-81.4(12)
C(27)-C(26)-N(5)-C(6)	41.5(13)	C(29)-C(26)-N(5)-Ti(1)	-18.4(13)
C(28)-C(26)-N(5)-Ti(1)	100.2(11)	C(27)-C(26)-N(5)-Ti(1)	-136.9(9)
C(31)-C(30)-N(8)-C(32)	59.1(11)	C(31)-C(30)-N(8)-Ti(1)	-124.0(8)
C(33)-C(32)-N(8)-C(30)	58.2(11)	C(33)-C(32)-N(8)-Ti(1)	-118.9(8)
C(37)-C(36)-N(9)-C(34)	82.9(10)	C(37)-C(36)-N(9)-Ti(1)	-89.7(9)
C(35)-C(34)-N(9)-C(36)	74.3(10)	C(35)-C(34)-N(9)-Ti(1)	-112.5(8)
N(2)-C(3)-O(4)-Ti(1)	5.3(8)	C(10)-C(3)-O(4)-Ti(1)	-172.4(6)
N(5)-C(6)-O(7)-Ti(1)	1.0(8)	C(20)-C(6)-O(7)-Ti(1)	-178.2(6)
C(36)-N(9)-Ti(1)-N(8)	122.0(7)	C(34)-N(9)-Ti(1)-N(8)	-50.2(7)
C(36)-N(9)-Ti(1)-O(4)	17.0(7)	C(34)-N(9)-Ti(1)-O(4)	-155.3(6)
C(36)-N(9)-Ti(1)-O(7)	-143.0(7)	C(34)-N(9)-Ti(1)-O(7)	44.8(7)
C(36)-N(9)-Ti(1)-N(5)	-81.5(7)	C(34)-N(9)-Ti(1)-N(5)	106.3(6)
C(36)-N(9)-Ti(1)-N(2)	14.5(10)	C(34)-N(9)-Ti(1)-N(2)	-157.7(6)
C(36)-N(9)-Ti(1)-C(6)	-111.4(7)	C(34)-N(9)-Ti(1)-C(6)	76.4(7)
C(36)-N(9)-Ti(1)-C(3)	17.8(8)	C(34)-N(9)-Ti(1)-C(3)	-154.4(6)
C(30)-N(8)-Ti(1)-N(9)	-33.3(8)	C(32)-N(8)-Ti(1)-N(9)	143.4(6)
C(30)-N(8)-Ti(1)-O(4)	57.0(8)	C(32)-N(8)-Ti(1)-O(4)	-126.2(6)
C(30)-N(8)-Ti(1)-O(7)	-139.8(7)	C(32)-N(8)-Ti(1)-O(7)	37.0(7)
C(30)-N(8)-Ti(1)-N(5)	-155.3(7)	C(32)-N(8)-Ti(1)-N(5)	21.4(10)
C(30)-N(8)-Ti(1)-N(2)	116.2(7)	C(32)-N(8)-Ti(1)-N(2)	-67.1(7)
C(30)-N(8)-Ti(1)-C(6)	-144.4(7)	C(32)-N(8)-Ti(1)-C(6)	32.3(8)
C(30)-N(8)-Ti(1)-C(3)	87.2(8)	C(32)-N(8)-Ti(1)-C(3)	-96.1(7)
C(3)-O(4)-Ti(1)-N(9)	178.6(5)	C(3)-O(4)-Ti(1)-N(8)	81.2(5)

C(3)-O(4)-Ti(1)-O(7)	-54.4(8)	C(3)-O(4)-Ti(1)-N(5)	-84.2(5)
C(3)-O(4)-Ti(1)-N(2)	-2.9(5)	C(3)-O(4)-Ti(1)-C(6)	-76.0(6)
C(6)-O(7)-Ti(1)-N(9)	89.0(5)	C(6)-C(7)-Ti(1)-N(8)	-172.3(5)
C(6)-O(7)-Ti(1)-O(4)	-34.9(9)	C(6)-O(7)-Ti(1)-N(5)	-0.6(5)
C(6)-O(7)-Ti(1)-N(2)	-78.9(5)	C(6)-O(7)-Ti(1)-C(3)	-68.1(6)
C(6)-N(5)-Ti(1)-N(9)	-103.6(5)	C(26)-N(5)-Ti(1)-N(9)	75.2(10)
C(6)-N(5)-Ti(1)-N(8)	18.5(9)	C(26)-N(5)-Ti(1)-N(8)	-162.7(9)
C(6)-N(5)-Ti(1)-O(4)	167.0(5)	C(26)-N(5)-Ti(1)-O(4)	-14.3(10)
C(6)-N(5)-Ti(1)-O(7)	0.6(5)	C(26)-N(5)-Ti(1)-O(7)	179.4(10)
C(6)-N(5)-Ti(1)-N(2)	108.4(5)	C(26)-N(5)-Ti(1)-N(2)	-72.8(10)
C(26)-N(5)-Ti(1)-C(6)	178.8(13)	C(6)-N(5)-Ti(1)-C(3)	136.9(5)
C(26)-N(5)-Ti(1)-C(3)	-44.4(10)	C(3)-N(2)-Ti(1)-N(9)	5.9(8)
C(16)-N(2)-Ti(1)-N(9)	173.8(8)	C(3)-N(2)-Ti(1)-N(8)	-102.9(5)
C(16)-N(2)-Ti(1)-N(8)	64.9(9)	C(3)-N(2)-Ti(1)-O(4)	3.0(5)
C(16)-N(2)-Ti(1)-O(4)	170.9(10)	C(3)-N(2)-Ti(1)-O(7)	163.6(5)
C(16)-N(2)-Ti(1)-O(7)	-28.6(10)	C(3)-N(2)-Ti(1)-N(5)	104.8(5)
C(16)-N(2)-Ti(1)-N(5)	-87.3(9)	C(3)-N(2)-Ti(1)-C(6)	133.3(5)
C(16)-N(2)-Ti(1)-C(6)	-58.8(9)	C(16)-N(2)-Ti(1)-C(3)	167.9(12)
N(5)-C(6)-Ti(1)-N(9)	81.8(5)	O(7)-C(6)-Ti(1)-N(9)	-99.1(5)
C(20)-C(6)-Ti(1)-N(9)	-92(3)	N(5)-C(6)-Ti(1)-N(8)	-169.9(5)
O(7)-C(6)-Ti(1)-N(8)	9.2(6)	C(20)-C(6)-Ti(1)-N(8)	16(3)
N(5)-C(6)-Ti(1)-O(4)	-16.4(6)	O(7)-C(6)-Ti(1)-O(4)	162.7(5)
C(20)-C(6)-Ti(1)-O(4)	170(3)	N(5)-C(6)-Ti(1)-O(7)	-179.0(8)
C(20)-C(6)-Ti(1)-O(7)	7(2)	O(7)-C(6)-Ti(1)-N(5)	179.0(8)
C(20)-C(6)-Ti(1)-N(5)	-174(3)	N(5)-C(6)-Ti(1)-N(2)	-72.5(5)
O(7)-C(6)-Ti(1)-N(2)	106.6(5)	C(20)-C(6)-Ti(1)-N(2)	114(3)
N(5)-C(6)-Ti(1)-C(3)	-49.1(6)	O(7)-C(6)-Ti(1)-C(3)	129.9(5)
C(20)-C(6)-Ti(1)-C(3)	137(3)	N(2)-C(3)-Ti(1)-N(9)	-176.4(5)
O(4)-C(3)-Ti(1)-N(9)	-1.6(6)	C(10)-C(3)-Ti(1)-N(9)	22(2)
N(2)-C(3)-Ti(1)-N(8)	80.0(5)	O(4)-C(3)-Ti(1)-N(8)	-105.2(5)
C(10)-C(3)-Ti(1)-N(8)	-81.8(19)	N(2)-C(3)-Ti(1)-O(4)	-174.8(8)
C(10)-C(3)-Ti(1)-O(4)	23.4(17)	N(2)-C(3)-Ti(1)-O(7)	-21.6(6)
O(4)-C(3)-Ti(1)-O(7)	153.2(5)	C(10)-C(3)-Ti(1)-O(7)	176.6(18)
N(2)-C(3)-Ti(1)-N(5)	-75.6(5)	O(4)-C(3)-Ti(1)-N(5)	99.3(5)
C(10)-C(3)-Ti(1)-N(5)	122.7(19)	O(4)-C(3)-Ti(1)-N(2)	174.8(8)
C(10)-C(3)-Ti(1)-N(2)	-162(2)	N(2)-C(3)-Ti(1)-C(6)	-53.3(6)
O(4)-C(3)-Ti(1)-C(6)	121.6(5)	C(10)-C(3)-Ti(1)-C(6)	145.0(18)